A Meier-Gorlin syndrome mutation in *ORC4* leads to locus specific chromosome breakage and a ribosome deficiency in *Saccharomyces cerevisiae*

Joseph C. Sanchez

A dissertation submitted in partial fulfillment of the requirements

for the degree of

Doctor of Philosophy

University of Washington

2017

Reading Committee:

Bonita J. Brewer, Chair

M.K. Raghuraman, Co-Chair

Takato Imaizumi

Toshio Tsukiyama

Program Authorized to Offer Degree:

Molecular and Cellular Biology

©Copyright 2017

Joseph C. Sanchez

University of Washington

Abstract

A Meier-Gorlin syndrome mutation in *ORC4* leads to locus specific chromosome breakage and a ribosome deficiency in *Saccharomyces cerevisiae*

Joseph C. Sanchez

Chair of the Supervisory Committee:

Professor Bonita J. Brewer

Molecular and Cellular Biology Program

Department of Genome Sciences

A form of dwarfism known as Meier-Gorlin syndrome (MGS) is caused by recessive mutations in one of six different genes (*ORC1, ORC4, ORC6, CDC6, CDT1,* and *MCM5*). These genes encode components of the pre-replication complex that assembles at origins of replication prior to S phase. Also, variants in two additional replication initiation genes have joined the list of causative mutations for MGS (Geminin and *CDC45*). The identity of the causative MGS genes strongly suggests that some aspect of replication is amiss in MGS patients; however, no evidence has yet been obtained regarding what aspect of replication is faulty nor is there a specific hypothesis for how a problem with replication might produce the specific phenotypes of MGS patients. This dissertation aims to characterize the cellular and molecular phenotype of MGS mutations to better understand how they might

give rise to the developmental phenotypes observed in humans with this condition. Since the site of one of the missense mutations in the human *ORC4* alleles is conserved between humans and yeast, I sought to determine in what way this single amino acid change affects the process of chromosome replication, by introducing the comparable mutation into yeast (*orc4*^{Y232C}). I found that *orc4*^{Y232C} yeast cells have a prolonged S phase due to compromised replication initiation at the ribosomal DNA (rDNA) locus located on chromosome XII. The inability to initiate replication at the rDNA locus results in chromosome breakage and a severely reduced rDNA copy number in the survivors, presumably helping to ensure complete replication of chromosome XII. Although reducing rDNA copy number may help ensure complete chromosome replication, *orc4*^{Y232C} cells struggle to meet the high demand for ribosomes. This finding provides evidence linking two pathways that are not typically thought of as being connected, DNA replication and ribosome biogenesis. Furthermore, it raises the possibility that the phenotypes observed in humans with MGS are a result of defects in a totally unexpected pathway—ribosome biogenesis.

TABLE OF CONTENTS

Section ..... page

List of figures iii

Acknowledgements v

Dedication vii

Chapter 1: Eukaryotic DNA replication and disease 1

1.1: Origin initiation in *S. cerevisiae* and Humans 1

1.2: Dysfunction of replication initiation and disease 4

1.3: Research goals 7

1.4: Chapter layout 7

Chapter 2: Investigating the growth, cell cycle, and replication initiation phenotypes of *orc4*^{Y232C} yeast cells 10

2.1: Introduction 10

2.2: Results 11

2.3: Discussion 14

2.4: Materials and Methods 15

Chapter 3: The *orc4*^{Y232C} allele results in reduced copy number and origin activity at the rDNA locus 27

3.1: Introduction 27

3.2: Results 28

3.3: Discussion 38

3.4: Materials and Methods 42

Chapter 4: The severe loss of rDNA repeats in *orc4*^{Y232C} cells leads to a reduction in ribosome production and translational capacity 71

4.1: Introduction 71

4.2: Results 72

4.3: Discussion 75

4.4: Materials and Methods 77

Chapter 5: Concluding Remarks and Future Directions 85

Table 1: List of strains and plasmids used in this study 97

List of References 98

Vita 110

LIST OF FIGURES

Figure Number: ..... Page

Figure 1.1: Structural comparison of the Human and *S. cerevisiae* ORC subunits. 9

Figure 2.1: Position of the Human Orc4-Tyr174 and *S. cerevisiae* Orc4-Tyr232 18

Figure 2.2: The *orc4*^{Y232C} allele confers a slow growth phenotype in budding yeast. 19

Figure 2.3: Completion of S-phase is delayed in *orc4*^{Y232C} cells 20

Figure 2.4: The early replication pattern is altered in *orc4*^{Y232C} cells. 21

Figure 2.5: Comparison of ssDNA profiles for *ORC4* and *orc4*^{Y232C} chromosomes. 22

Figure 2.6: Sensitivity of *orc4*^{Y232C} cells to hydroxyurea (HU). 24

Figure 2.7: Origins proximal to centromeres are less active in *orc4*^{Y232C} cells. 25

Figure 3.1: The relative DNA content of *orc4*^{Y232C} cells is less than *ORC4* cells. 46

Figure 3.2: Quantitative Southern blot analysis of repetitive DNA sequences. 47

Figure 3.3: Cartoon depiction of the yeast rDNA locus. 48

Figure 3.4: CHEF gel analysis of Chr XII size in *ORC4* and *orc4*^{Y232C} cells. 49

Figure 3.5: CHEF gel analysis of variation in rDNA copy number in six additional isolates (a-f) of *orc4*^{Y232C}. 50

Figure 3.6: The rDNA copy number in *orc4*^{Y232C} cells stabilizes at ~30 copies. 51

Figure 3.7: Long-term growth of isolate "e" shows rDNA copy number stabilizes at ~30 copies. 52

Figure 3.8: Superimposition of the Human and *S. cerevisiae* Cdc45 proteins 53

Figure 3.9: CHEF gel analysis of variation in rDNA copy number of five isolates (a-e) of *cdc45*^{P542L}. 54

Figure 3.10: CHEF gel analysis of variation in rDNA copy number of five isolates (a-e) of *orc6*^{Y418S}. 55

Figure 3.11: Origin initiation at the rDNA locus is reduced in orc4^{Y232C} cells. 56

Figure 3.12: The *orc4*^{Y232C} rDNA copy number phenotype is not rescued by an additional copy of *orc4*^{Y232C}. 57

Figure 3.13: Sequence comparison of the ACS of BY4741 and RM11-1a rDNA origin, *rARS* 58

Figure 3.14: The slow growth phenotype is exacerbated in *ORC4-rDNA*^{RM} cells 59

Figure 3.15: *orc4*^{Y232C}-*rDNA*^{RM} cells are unable to grow at 37^{o} C. 60

Figure 3.16: Outline of strategy used to release intact rDNA array from Chr XII by restriction enzyme digest with *BamHI*. 61

Figure 3.17: Only ~10 rDNA repeats remain in *orc4*^{Y232C}-*rDNA*^{RM} cells. 62

Figure 3.18: Origin activity is not detectable at the rDNA locus in *orc4*^{Y232C}-*rDNA*^{RM} cells.. 63

Figure 3.19: CHEF gel analysis of variation in rDNA copy number in six additional isolates (a-f) of *orc4*^{Y232C}- *rDNA*^{RM}. 64

Figure 3.20: Cell-cycle defects are exacerbated in *orc4*^{Y232C}- *rDNA*^{RM} cells. 65

Figure 3.21: Comparison of ssDNA profiles for *ORC4-rDNA*^{RM} and *orc4*^{Y232C}-*rDNA*^{RM} chromosomes. 66

Figure 3.22: Pairwise comparisons of the relative area under the peak at each origin measured in ssDNA profiles. 68

Figure 3.23: Cartoon illustration of Chr XII (containing 10 copies of rDNA (rDNA$_{10}$)) and Chr IV 69

Figure 3.24: Chromosome breakage is specific to Chr XII in *orc4*^{Y232C}-*rDNA*^{RM} cells. 70

Figure 4.1: Polysome profiles from *ORC4* and *orc4*^{Y232C} yeast cells. 79

Figure 4.2: The total nucleic acid content of cells is resolved by gel electrophoresis. 80

Figure 4.3: Quantitative hybrid Southern/Northern blot analysis ribosomal RNA 81

Figure 4.4: Relative fluorescence of *ORC4-rDNA*^{RM} and *orc4*^{Y232C}-*rDNA*^{RM} harboring Rpl10-GFP 82

Figure 4.5: Relative fluorescence of *ORC4-rDNA*^{BY} and *orc4*^{Y232C}-*rDNA*^{BY} harboring Rpl10-GFP 83

Figure 4.6: Sensitivity of *orc4*^{Y232C}-*rDNA*^{RM} cells to cycloheximide 84

Figure 5.1: CHEF gel analysis of variation in rDNA copy in segregants from an *ORC4/orc4*^{Y232C} *RAD52/rad52Δ::KanMX* heterozygous diploid 93

Figure 5.2: CHEF gel analysis of variation in rDNA copy in segregants from an *ORC4/orc4*^{Y232C} *FOB1/fob1Δ::KanMX* heterozygous diploid 94

Figure 5.3: Slow growth phenotype of *rARSΔ* candidates (1-7) 95

Figure 5.4: CHEF gel analysis of Chr XII size in *rARSΔ* candidates (1-7) 96

ACKNOWLEDGEMENTS

There are several people whom I would like to thank for providing support throughout my academic career up to this point. I would like to thank Dr. Veronica Evans, for encouraging me to pursue undergraduate research and for helping to connect me with the Initiative for Maximizing Student Development Program (IMSD) at the University of New Mexico (UNM). The UNM IMSD program led by Dr. Maggie Werner-Washburne, Dr. Steve Phillips, and Lupe Atencio was instrumental in solidifying my decision to pursue a career as a scientist. I would like to thank all members of the IMSD program, especially Maggie, for their past and continual support and guidance. The UNM IMSD program also provided me with my first research experience in the lab of Dr. Mary Ann Osley, where I worked under the guidance of Dr. Toyoko Tsukuda. I am thankful for everything Mary Ann and Toyoko taught me and for challenging me to think about my research project critically.

I have truly enjoyed my experience during graduate school and I credit this largely to having such great mentors. It has been a pleasure to have Bonny and Raghu as my thesis advisors and they have gone above and beyond their duty as mentors. In addition to providing excellent mentorship over the years, Bonny and Raghu have grown to become close friends of mine and I will sincerely miss interacting with them daily. Along with Bonny and Raghu, I wish to thank other members of the Brewer/Raghuraman lab including Kelsey Lynch, Rebecca Martin, Madison Miller, Elizabeth Kwan, and Gina Alvino for their support and helpful discussions. I extend my gratitude to former Brewer/Raghuraman lab members Thomas Pohl, Haley Amemiya, Mackenzie Croy, Shanti Neff-Baro, and Alex Mason who have worked on various aspects of this project not included in this dissertation. I

would also like to thank all members of my thesis committee (Dr. Maitreya Dunham, Dr. Raymond Monnat, Dr. Takato Imaizumi, and Dr. Toshio Tsukiyama) for the support, guidance, and advice that they have provided on my thesis research.

Outside of academics, I would like to thank my friends and family for their support and encouragement during my pursuit of a doctoral degree. My friends in New Mexico and in Seattle have always been there to provide a helping hand, listening ear, or shoulder to lean on and I am grateful for each of them. I would like to thank my family: Joseph P. Sanchez (Father), Irene Sanchez (Mother), and Valerie Trask (Sister) along with all her family—the support and encouragement you all have provided has been invaluable. Finally, I would like to thank my beautiful wife Monica Sanchez. Since we met as undergraduates, you have always been by my side. I am lucky to have shared the experience of graduate school with such talented and driven scientist and it is a privilege to have you as a colleague, my wife, and a best friend.

DEDICATION

This dissertation is dedicated to

Andres Maestas Jr., (August 31st, 1922 – December 2nd, 2015)

Carolina C. Maestas, (January 11th, 1932 – December 9th, 2016)

Frank A. Sanchez, (June 3rd, 1922 – October 15th, 1997)

Dell C. Sanchez, (June 16th, 1926 – June 27th, 2002)

Chapter 1

Eukaryotic DNA Replication and Disease

1.1: Origin initiation in *S. cerevisiae* and *H. sapiens*

The faithful and timely duplication of a cell's genome is required every round of division. During eukaryotic S phase, DNA replication initiates at multiple sites along each chromosome called origins of replication. Eukaryotic replication initiation has been best characterized in the budding yeast *Saccharomyces cerevisiae*, where chromosomal origins were first identified by their ability to maintain recombinant plasmids after transformation into yeast (Stinchcomb et al. 1979). The majority of these Autonomous Replication Sequences or ARS elements correspond to the ~300 chromosomal origins of replication scattered across the genome and share a core consensus sequence called the ACS (ARS consensus sequence) (Liachko et al. 2013). The ACS is an 11-17 bp AT-rich core consensus sequence called the ARS Consensus Sequence (ACS), which is necessary but not sufficient for origin activation. Additionally, most origins in *S. cerevisiae* contain 1-3 B-elements (B1, B2, and B3) that are located 3' to the ACS (Dhar et al. 2012). Unlike the ACS, no single B-element is essential for origin activation; however, the presence of B-elements has been shown to increase origin activity (Dhar et al. 2012).

Unlike in budding yeast, origins of replication in higher eukaryotes do not seem to share a core consensus sequence. Attempts to isolate specific DNA sequences that are capable of replicating episomal DNA in mammalian cells have been unsuccessful (Krysan et al. 1989; Heinzel et al. 1991); however, origin activity has been mapped to handful of specific chromosomal locations, such as the human lamin B2 locus and human β-globin locus (Wang et al. 2004; Kitsberg et al. 1993; Paixão et al. 2004). Although specific sequences necessary for the origin activity of these loci have been identified, they do not appear to share a core consensus sequence. Additionally, origin initiation has been observed across a broader range, such as in the case in the ribosomal (rDNA locus), where multiple replication initiation events have been mapped to the 31 kb non-transcribed spacer present in each rDNA repeat (Little et al. 1993).

Features that define origins in higher eukaryotes differ significantly from yeast ARSs, but the proteins that carry out origin recognition and initiation are strikingly conserved in sequence and structure across eukaryotes (10–13; Fig 1.1). Biochemical and genetic work in yeast identified many of the essential genes for replication initiation (Bell and Stillman 1992; Liang et al. 1995; Tanaka and Diffley 2002). In budding yeast, a six-membered protein complex called the Origin Recognition Complex (Orc1-6) binds ARSs throughout the cell cycle (Liang and Stillman 1997). To become competent (or licensed) for initiation, additional proteins are recruited by ORC during the M and G1 phases (Fragkos et al. 2015). The first licensing factor to bind is Cdc6, which facilitates the recruitment of the Mcm2-7 helicase component through an interaction with Cdt1 (Randell et al. 2006; Cocker et al. 1996; Diffley et al. 1994; Speck et al. 2005; Chen et al. 2007; Yuan et al. 2017). Collectively, this protein complex is known as the Pre-Replication Complex

(Pre-RC) and, once assembled on an origin, licenses it to initiate DNA replication or "fire" in the subsequent S phase. During the onset of S phase CDK- and DDK-dependent phosphorylation events complete assembly of the replisomes, including two helicase complexes, allowing replication to proceed bi-directionally from the origin of replication (Sclafani and Holzen 2007; Stillman 2005; Ilves et al. 2010).

It is crucial that a sufficient number of origins are activated to fire during S phase to ensure complete replication of the genome; however, this process also must be tightly regulated to prevent re-replication of the genome. If unregulated it can result in genome instability or possibly cell death. In eukaryotes, different mechanisms exist to help ensure that any given origin fires only once during S phase. In budding yeast, CDK levels increase as cells enter S phase, not only allowing origin activation but also preventing re-formation of the Pre-RC through nuclear export of Mcm2-7 and degradation of the initiation factors Cdc6 and Cdt1. In higher eukaryotes, origin initiation is regulated by CDK activity and the initiation inhibiting protein Geminin. During S phase, different events that help regulate Pre-RC assembly are mediated by CDK activity including removal of ORC from DNA, the destruction of both Cdt1 and ORC, and export of Cdc6 from the nucleus. Geminin is present during S, G2, and M phases of the cell cycle and is targeted for destruction by the anaphase-promoting complex at the end of mitosis. During S phase, Geminin interacts with Cdt1 to prevent loading of Mcm2-7 onto origins of replication. Cells have evolved various mechanisms to tightly regulate origin initiation during S phase; however, these mechanisms are not always failsafe. What might be the consequences at both the cellular and organismal level when origin initiation is not properly regulated?

1.2: Dysfunction of replication initiation and disease

As chromosome replication is essential for cell division, there has been a tacit assumption that mutations that impair the function of proteins involved in replication initiation would be incompatible with metazoan life. Yet, a handful of diseases have been shown to be caused by mutations in proteins necessary for replication initiation (Jackson et al. 2014). One might predict that mutations in proteins involved in the same process, such as replication initiation, would result in similar phenotypes; however, different diseases associated with mutations in proteins necessary for origin initiation result in different phenotypes including cancer, adrenal failure, and dwarfism (Jackson et al. 2014).

Cancer is often associated with increased genome instability; therefore, it should not come as a surprise that mutations in proteins required for genome replication have been associated with different cancers (Jackson et al. 2014). For example, MCM2-7 dysfunction is known to result in the development of cancer in mice (Shima et al. 2007; Pruitt et al. 2007). A hypomorphic allele of *MCM4* known as c*haos3* (*chromosome aberrations occurring spontaneously*) is associated with genome instability and breast adenocarcinomas in female mice, (Shima et al. 2007) although male mice homozygous for this mutation do not suffer from elevated rates of cancer occurrence. The specific variant identified in the $Mcm4^{Chaos3/Chaos3}$ allele results in a nonsynonymous mutation (F345I) and biochemical work has shown that this mutation results in destabilization of the Mcm4 protein (Shima et al. 2007). In addition, mice deficient for MCM2 develop lymphomas and exhibit elevated levels of genome instability (Pruitt et al. 2007). To date, mutations in MCM2-7 have not been shown to be causative for cancer in humans; however, a specific mutation in human

MCM4 (G486D) has been identified in several skin cancers and this mutation has been shown to result in destabilization of the MCM2-7 complex (Tatsumi and Ishimi 2017). Although mutations in the MCM2-7 complex have not yet been shown to be causative for cancer in humans, mutations in this complex have been shown to causative for other human diseases.

A variant in *MCM4* has been identified in humans who suffer from adrenal failure, short stature, and a natural killer cell deficiency (Hughes et al. 2012). The specific variant identified results in a frameshift mutation and truncated protein product (Hughes et al. 2012). Unlike $Mcm4^{Chaos3/Chaos3}$ mice, humans carrying this frame-shift mutation in *MCM4* do not have elevated incidences of cancer (Hughes et al. 2012). Although only one variant in *MCM4* has been shown to be causative for this disorder in humans, several mutations in other proteins required for replication initiation have been identified in a different human condition whose phenotypes also include short stature.

In 2011 researchers reported that amino acid substitutions in proteins involved in the initiation of DNA replication are responsible for a form of proportionate dwarfism called Meier-Gorlin syndrome (MGS) (Bicknell et al. 2011a; Guernsey et al. 2011). Individuals with MGS have phenotypes that include short stature, small external ears and missing or underdeveloped kneecaps (Gorlin et al. 1975; Meier et al. 1959)—phenotypes not obviously associated with chromosome replication defects. The specific genetic variants found in patients with MGS include homozygous or compound heterozygous alterations in six different Pre-RC genes (*ORC1*, *ORC4*, *ORC6*, *CDT1*, *CDC6*, and *MCM5*) (Bicknell et al. 2011a; Guernsey et al. 2011; Vetro et al. 2017). Recent work has identified

de novo autosomal dominant mutations in Geminin (encoded by GMNN), an inhibitor of DNA replication that is unique to higher eukaryotes (Burrage et al. 2015). Additionally, biallelic mutations in *CDC45*, which is required for both origin initiation and elongation during S phase, have been found to be causative for some cases of MGS (Fenwick et al. 2016). Considering the known roles of these proteins in origin initiation, a reasonable hypothesis is that these mutations are adversely affecting DNA replication and thus reducing cell proliferation so that individuals harboring these variants are uncommonly small. Consistent with this hypothesis, previous work has found that cells derived from MGS patients are diminished in their ability to initiate replication; however, defects in replication initiation are not correlated with the rate of progression through S phase in MGS cells (Stiff et al. 2013; Bicknell et al. 2011b). Additionally, MGS mutations have been shown to affect aspects of cell biology other than DNA replication, such as centrosome duplication and cilia formation (Stiff et al. 2013; Hossain and Stillman 2012). The defective cilia formation phenotype observed in MGS cells is thought to contribute to some of the developmental abnormalities associated with this condition (Stiff et al. 2013).

Although the proteins linked with MGS have been studied extensively in yeast and other eukaryotes, it is not clear how MGS mutations might affect chromosome replication to give rise to the phenotypes observed in humans. Therefore, understanding how MGS mutations affect chromosome replication is crucial to further our understanding of how they contribute to the phenotypes in humans.

1.3: Research Goals

The goals of this dissertation are to characterize the molecular and cellular phenotypes associated with MGS mutations to gain a better understanding of how defects in replication initiation might lead to the phenotypes observed in humans with this condition. Specifically, this work addresses the following questions regarding MGS mutations in the model organism *S. cerevisiae*: (1) How do MGS mutations affect chromosome replication? (2) Are certain regions of the yeast genome more sensitive to changes in chromosome replication caused by MGS mutations? (3) Do MGS mutations affect aspects of cellular biology other than DNA replication? My work in addressing these questions reveals that in yeast, MGS mutations alter the dynamics of chromosome replication and indirectly affect cell growth and division by restricting ribosome production.

1.4: Chapter Layout

In this dissertation, I utilize the budding yeast *S. cerevisiae* as a model organism to the study how mutations associated with MGS affect cellular well-being. In Chapter 2, I replace the genomic copy of the budding yeast *ORC4* with a mutated version (*orc4*^{Y232C}) bearing a tyrosine-to-cysteine change that is orthologous to the Tyr174Cys mutation reported in human patients (Guernsey *et al*, 2011). I show that yeast cells bearing this *orc4*^{Y232C} allele have a longer cell cycle time that is mostly accounted for by a lengthened S phase. Additionally, I find that in *orc4*^{Y232C} cells ~15% of the earliest firing origins are altered in their time and/or efficiency of initiation. In Chapter 3, I show that the ribosomal

DNA locus is a part of the yeast genome that is particularly sensitive to the changes in origin initiation observed in *orc4*^{Y232C} cells. I find that in *orc4*^{Y232C} cells, the origins present in each copy of the ribosomal DNA (rDNA) are severely compromised in their ability to fire and that the number of copies of the rDNA repeat drops from ~150 to as few as 10. My findings reveal that the mechanism for rDNA copy number loss is chromosome XII breakage as a consequence of the "random replication gap" problem. In Chapter 4, I show that the reduction in rDNA copy number, by restricting rRNA synthesis, constrains the translational capacity of the mutant cells, possibly explaining the slow growth observed in *orc4*^{Y232C} cells. While it remains to be seen whether these phenotypes are also common to Meier-Gorlin patient cells, my characterization of the *orc4*^{Y232C} allele in *S. cerevisiae* highlights an unsuspected pathway linking replication dysfunction and growth control.

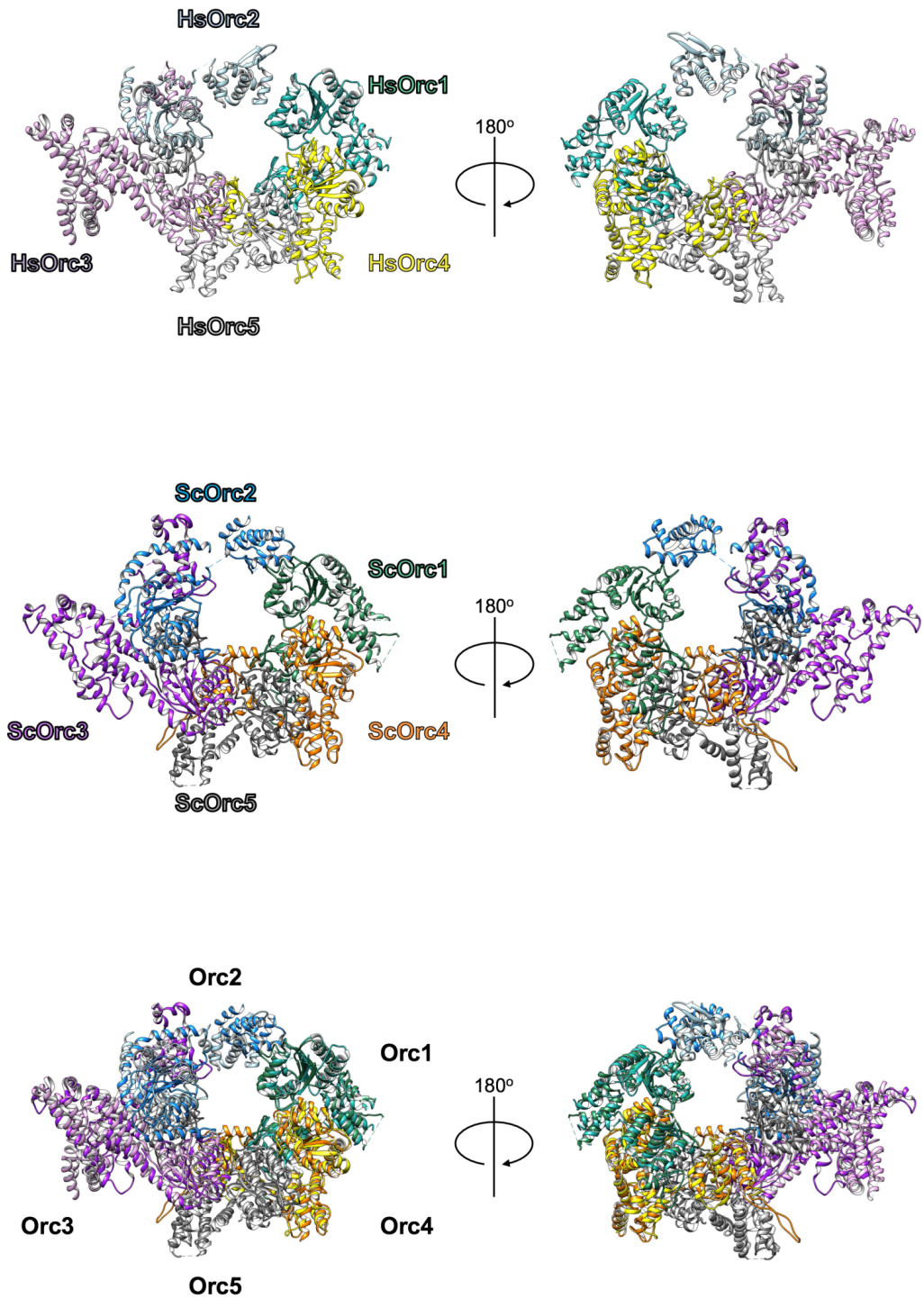

Figure 1.1: Structural comparison of the Human and *S. cerevisiae* ORC subunits. Comparison of the structural models of human (Hs; top panel) and *S. cerevisiae* (Sc; middle panel) origin recognition complex subunits (Orc1, 2, 3, 4, and 5; PDB IDs 5UJM and 5UDB, respectively). The bottom panel shows a superimposition of the Hs and Sc complexes. Data from (Tocilj et al. 2017) and (Yuan et al. 2017).

Chapter 2

Investigating the growth, cell cycle, and replication initiation phenotypes of *orc4*^{Y232C} yeast cells

2.1: Introduction

A missense mutation in *ORC4* has been shown to be causative for some instances of MGS in humans. This specific mutation results in an amino acid substitution (Tyrosine to Cysteine) at position 174 of the human Orc4 protein; the mutated residue is located within the AAA+ (ATPases Associated with diverse cellular Activities) related domain of the protein. Biochemical analysis by Tocilj et al. (2017) showed that the Y174C mutation rendered the ORC1/4/5 sub-complex hyperactive for ATPase activity; however, in the context of ORC1-5 ATPase activity is reduced compared to wild type. The Y174C mutation occurs in a region of the Orc4 protein that is highly conserved among eukaryotes (Fig 2.1). Initial work by Guernsey et al. investigating the equivalent MGS mutation (*orc4*^{Y232C}) in *S. cerevisiae* revealed a slow-growth phenotype (Guernsey et al. 2011). In that experiment, the investigators constructed a strain that had the *orc4*^{Y232C} allele on a plasmid rescuing the inviable chromosomal deletion of *ORC4*. Because the *orc4*^{Y232C} allele was not in its native location, it was not clear to what extent the slow growth was due to plasmid loss or poor expression from the plasmid versus other, more wide-spread defects in chromosome

replication or segregation. To explore in more detail the consequences of the *orc4*^{Y232C} mutation on cellular growth and chromosome replication, I replaced the wild type yeast *ORC4* allele with the MGS equivalent allele *orc4*^{Y232C} at its native chromosomal locus.

2.2: Results

The slow growth of orc4^{Y232C} yeast is due to a delay in completing S phase

Since *ORC4* is an essential gene, I introduced the *orc4*^{Y232C} allele into *S. cerevisiae* by two-step gene replacement (see Chapter 2.4: Material and Methods). Cells with the chromosomal *orc4*^{Y232C} allele grew more slowly than wild type (population doubling time of 2.7 hr. vs. 2.4 hr.; Fig 2.2). The more marked difference in growth rates reported for the strains analyzed by Guernsey et al. (2011) is probably due to loss of the plasmid bearing the sole source of Orc4p in their experiments. To explore the slow growth phenotype, I performed flow cytometry on cells synchronously proceeding through the cell cycle after having been arrested at START by treatment with alpha-factor (Fig 2.3). Initiation of S phase appears to be slightly delayed in the mutant but after replicating much of its genomic DNA the mutant shows a more pronounced delay in reaching a full G2 DNA content and progressing back into G1. I reasoned that a delay in S phase entry could result if the *orc4*^{Y232C} mutation altered early origin firing. To examine this possibility I used an assay that specifically examines early origin activation across the genome (Feng et al. 2006). This assay uses microarray hybridization to measure the levels of single stranded DNA exposed at replication forks. Both the peak position and peak amplitude of ssDNA formed at genomic loci are informative. While we do not fully understand the molecular processes

that give rise to peaks of different amplitudes—e.g., number of cells that have activated a particular origin vs. amount of ssDNA revealed at different forks—the results from different replicates of the experiment are highly reproducible. I find that origins that are known to fire early and are efficient produce the peaks of greatest magnitude, while later firing and less efficient origins produce smaller or no peaks in this assay (Feng et al. 2006).

I carried out the ssDNA assay on the wild type *ORC4* and *orc4*^{Y232C} mutant and a representative comparison of the two is shown in Fig. 2.4A (to view comparisons of all chromosomes see Fig. 2.5). I observed differences in origin usage in *ORC4* compared to *orc4*^{Y232C} and could discern three classes of origins. Some origins had comparable ssDNA peaks in both strains (cf. origins at 420 kb, 490 kb, 890 kb). Some origins that were active in *ORC4* showed significant reduction in ssDNA accumulation in *orc4*^{Y232C} (cf. 200 kb, 390 kb, 830 kb). Perhaps most surprisingly, the converse was also true: some origins that are late or inefficiently initiated in *ORC4* cells had significant ssDNA peaks in the *orc4*^{Y232C} mutant, indicating earlier or more efficient initiation than in wild type (cf. 15 kb, 170 kb, 670 kb). To assess quantitatively the magnitude of change in the early replication program of origin firing, I quantified the areas under the peaks observed in the ssDNA assays for *ORC4* and *orc4*^{Y232}. Peak areas in *ORC4* vs. *orc4*^{Y232C} were highly discordant (Fig. 2.4B; R^2 = ~0.14). These results highlight substantial differences in the early origin firing of origins in *orc4*^{Y232} cells: of the 213 origins represented in the scatter plot (Fig 2.4B), 31

are substantially depressed or delayed in activity in the *orc4*^{Y232C} mutant (x-axis: outlined in orange) while another 24 origins are now detected as firing early (y-axis: outlined in orange). However, overall, the number of early firing origins was similar between wild

type and *orc4*^{Y232} cells. While the ssDNA assay limits me to monitoring only the earliest firing origins I anticipate that even if no more origin activation occurred (as is the case for cells with a deletion of *CLB5*, the major S phase cyclin), the completion of S phase would only be delayed by an additional 15 minutes (McCune et al. 2008).

The flow cytometry data of a synchronous culture of *orc4*^{Y232C} cells showed more than a 15 minute delay in completion of S phase and cell division (Fig 2.3). For example, by 85 minutes wild type cells had divided and were undergoing a second round of DNA synthesis whereas the mutant cells do not show a comparable DNA content profile until 120 minutes after release. I hypothesized that this 35 minute delay could be due to cells encountering problems in late S phase and that the gradual shift to 2C DNA content is from slow progress in completing genomic DNA replication. Alternatively, *orc4*^{Y232C} cells may have completed genome replication on time and are continuing to replicate mitochondrial DNA but are delaying the G2/M transition for other reasons. However, the observation that cells with the *orc4*^{Y252C} mutation are unable to form colonies on plates with 200 mM hydroxyurea (HU; Fig 2.6), a drug that inhibits ribonucleotide reductase and thereby slows the progress of replication forks, supports the hypothesis that the cell cycle delay stems from a chromosome replication defect.

2.3: Discussion

What aspect of ORC function has been altered by the *orc4*^{Y232C} mutation? One possibility is that this single amino acid substitution has changed the DNA sequence recognized by the ORC complex. Origins in budding yeast share a similar core sequence called the ACS (ARS Consensus Sequence, an approximately 17 bp AT-rich sequence necessary but not sufficient for origin function) and variation in this sequence has been shown to impact origin usage (Liachko et al. 2013). Analysis of the different groups of origins did not reveal any simple pattern(s) of polymorphism within the ACS that distinguished wild type specific origins (i.e., origins that showed reduced activity in the mutant) from mutant specific origins (i.e., origins that had ssDNA peaks in the mutant but not in wild type), although I cannot rule out the possibility that such sequence differences do exist.

A second possibility is that there is some aspect of chromatin structure or nuclear architecture that is influencing origin choice in the *orc4*^{Y232C} mutant. One class of origins whose activity was influenced by the *orc4*^{Y232C} allele was those near centromeres: 11 of the 31 wild type specific origins were located within 10 kb of a centromere (Fig 2.7). To determine if this apparently skewed distribution of wild type specific origins was significantly different than would be expected to occur by chance, we performed a permutation test as follows: 31 of the of the 213 origins used to generate the scatter plots (Figure 2.4B and Fig 3.21; See Chapter 3) were randomly picked and labeled as wild type specific. We then asked whether at least 11 of those origins was within 10 kb of a centromere. In 10,000 trials of this test, we found no occurrence of 11 or more affected

origins being within 10 kb of a centromere ($p < 10^{-4}$). Relevant to this discussion is the observation that we and others have made that indicates that centromeres promote early firing time of origins in their vicinity (Blitzblau et al. 2012; Natsume et al. 2013; Pohl et al. 2012). The early firing of centromere proximal origins is thought to occur as a consequence of the kinetochore protein Ctf19 recruiting the S-phase kinase DDK to phosphorylate components of the pre-RC for replication initiation (Natsume et al. 2013). Whether the ORC complex with the *orc4*^{Y232C} variant is deficient in this interaction is unknown. Lastly, nucleosome occupancy or changing transcription factor binding around origins of replication may be preventing ORC containing Orc4^{Y232C} protein from assembling at origins (Rodriguez et al. 2017; Knott et al. 2012). Moving forward, it will be important to determine if the centromere itself, chromatin state, or specific proteins that make up the kinetochore are influencing these changes.

2.4: Material and Methods

Yeast strains and plasmids

A complete list of yeast strains and plasmids can be found in Table 1. BY4741 was used as wild type (*ORC4)* for this study and all strains were derived from this background. The MGS-like variant *orc4*^{Y323C} was introduced into BY4741 by two-step gene replacement (Duff and Huxley 1996). A plasmid containing *URA3* and the *orc4*^{Y232C} allele was integrated at the *ORC4* locus; correct integrants were confirmed by PCR and Southern analysis. I selected for loss of the integrated sequences through homologous recombination by selecting against

the *URA3* gene on plates containing 5-fluoro orotic acid. To screen for clones that had lost the wild type *ORC4* allele and had kept the *orc4*^{Y232C} allele I performed PCR using an allele specific oligonucleotide as one of the PCR primers. Unless stated otherwise, yeast cultures were grown at 30° C in synthetic complete medium supplemented with 2% glucose.

Flow cytometry for cell cycle analysis

Cell cycle progression was examined using flow cytometry. Early log phase cells (OD_{660} ~0.25) were arrested in G1 by the addition of alpha factor at a final concentration of 3 μM. When >90% of the population was un-budded (time equivalent to ~1.5 population doublings), cells were synchronously released into S-phase by the addition of Pronase (Calbiochem) at a final concentration of 0.3 mg/ml. After the release into S phase, cells were harvested at 5-minute intervals, mixed with sodium azide at a final concentration of 0.1% and fixed with 70% ethanol. Cells were prepared for flow cytometry as previously described (McCune et al. 2008). Flow cytometry was performed on a BD FACSCanto II and data were analyzed using FlowJo software.

Mapping of Single Stranded DNA

A detailed protocol for this assay has previously been published (Peng et al. 2014). Cells growing in log phase (OD_{660} ~0.25) were arrested in G1 by the addition of alpha factor and then synchronously released into S phase in the presence of 200 mM HU. Samples were collected every 15 minutes after release into S phase and cells were embedded in agarose

plugs and then spheroplasted. The ssDNA from either S phase or G1 control samples were then differentially labeled with either Cy5- or Cy3-dUTP by in-gel random-primed labeling using exo- Klenow polymerase (NEB) without denaturation of template. The differently labeled DNAs were then collected and co-hybridized to Agilent G4493A yeast 4x44K ChIP to chip DNA microarrays according to the manufacturer's recommendations. The data from scanned microarrays were extracted using Agilent's Feature Extraction software. The microarray data from the single stranded assays is available from the NCBI GEO database (accession number GSE104671).

ssDNA peak area script description

Areas under ssDNA peaks were assessed from Loess-smoothed microarray data (coordinates spaced 500 bp apart) using a custom Python script written by EX Kwan and a reference list of origins and their locations from OriDB (Siow et al. 2012) (http://cerevisiae.oridb.org/). Since most of the genome is double-stranded and therefore not a template for ssDNA labeling, the mean genome-wide signal was used as a "threshold" value for each sample. The "ssDNA peak area" for each origin was then calculated as a sum of S/G1 value at the origin's location and the sequentially-added S/G1 values from adjacent data points until three "below threshold" values were reached on each side of the origin. The script does not distinguish overlapping origin peaks and therefore overlapping early firing origins in close proximity were manually curated and excluded from the analysis.

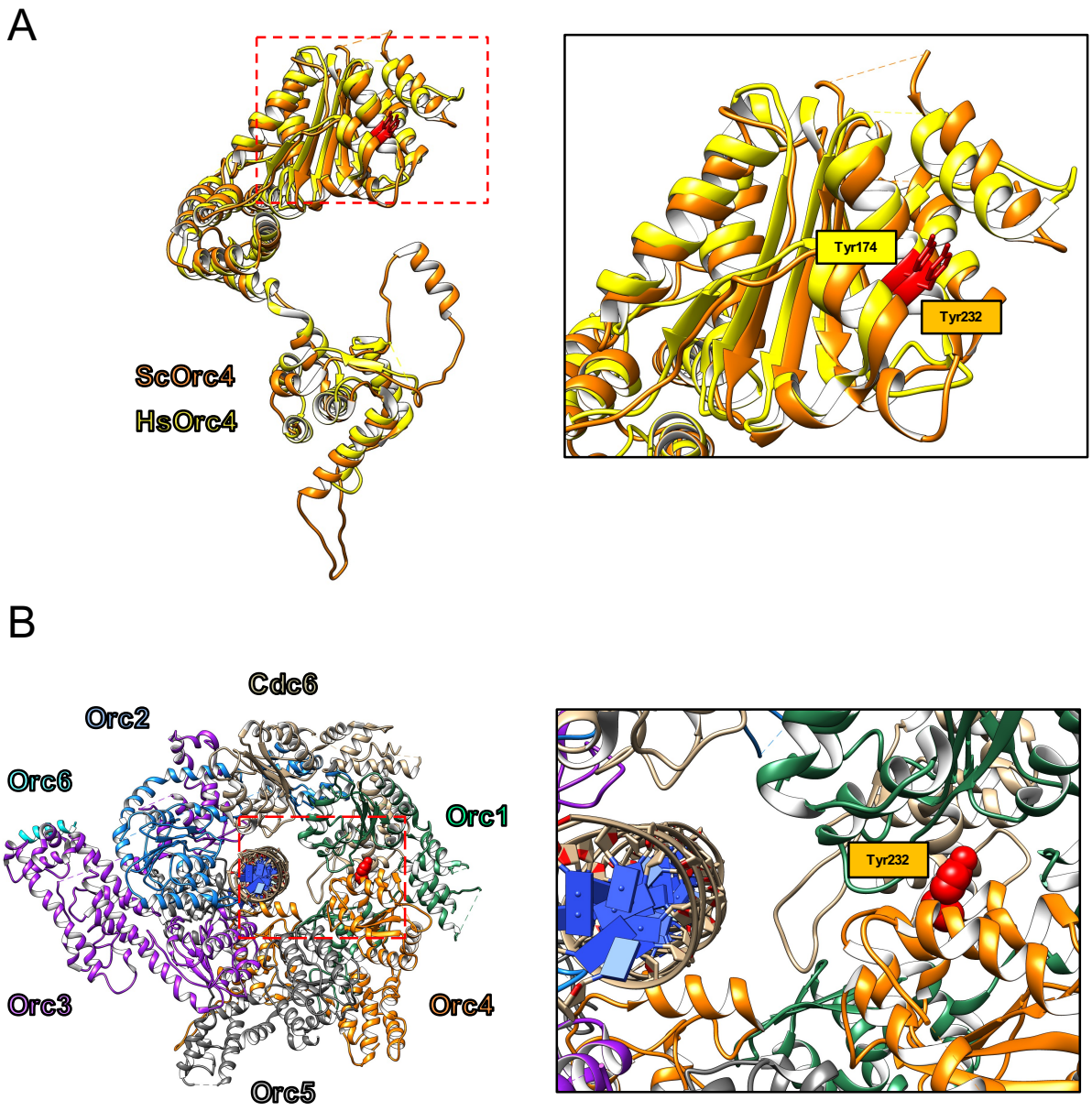

Figure 2.1: Position of the Human Orc4-Tyr174 and *S. cerevisiae* Orc4-Tyr232
(A) Superimposition of the Hs and Sc Orc4 subunits highlights the high degree of structural similarity between the proteins from the two species. The right panel focuses on the Tyrosine mutated in human MGS patients (Tyr174) and the corresponding Tyrosine in yeast (Tyr232) with the side chains of these amino acids displayed in red.
(B) Structural models of ScOrc1-6 and ScCdc6 in complex with a double stranded DNA molecule. The right panel focuses on Tyr232 of ScOrc4, with the side chain of this amino acid depicted as red spheres.

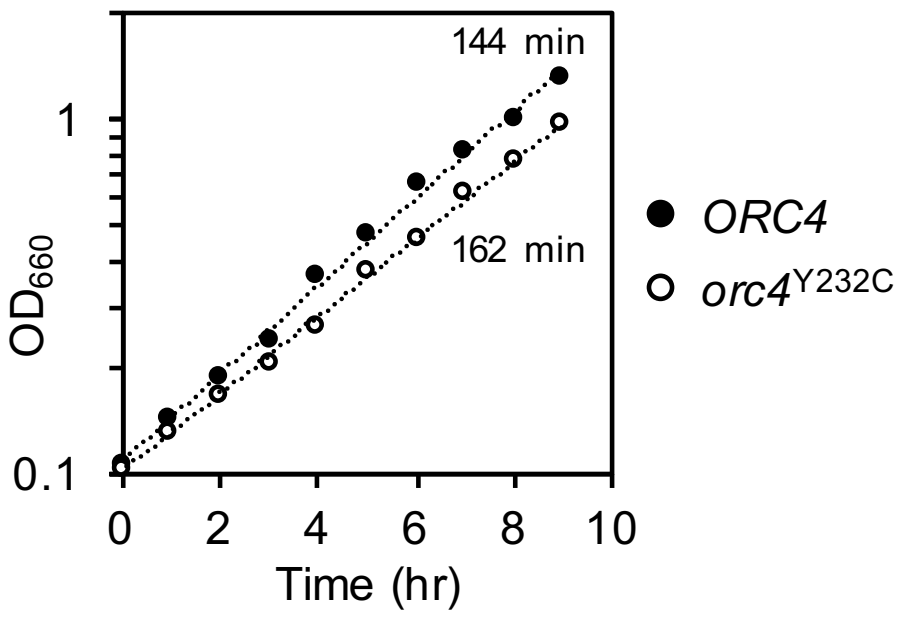

Figure 2.2: The *orc4*^{Y232C} allele confers a slow growth phenotype in budding yeast. Growth of *ORC4* and *orc4*^{Y232C} cells as measured by change in optical density (OD_{660}) of mid-log phase cultures in synthetic complete medium at 30° C. The mutant (○) shows a modest growth defect with a doubling-time 18 minutes (12%) longer than wild-type cells (●).

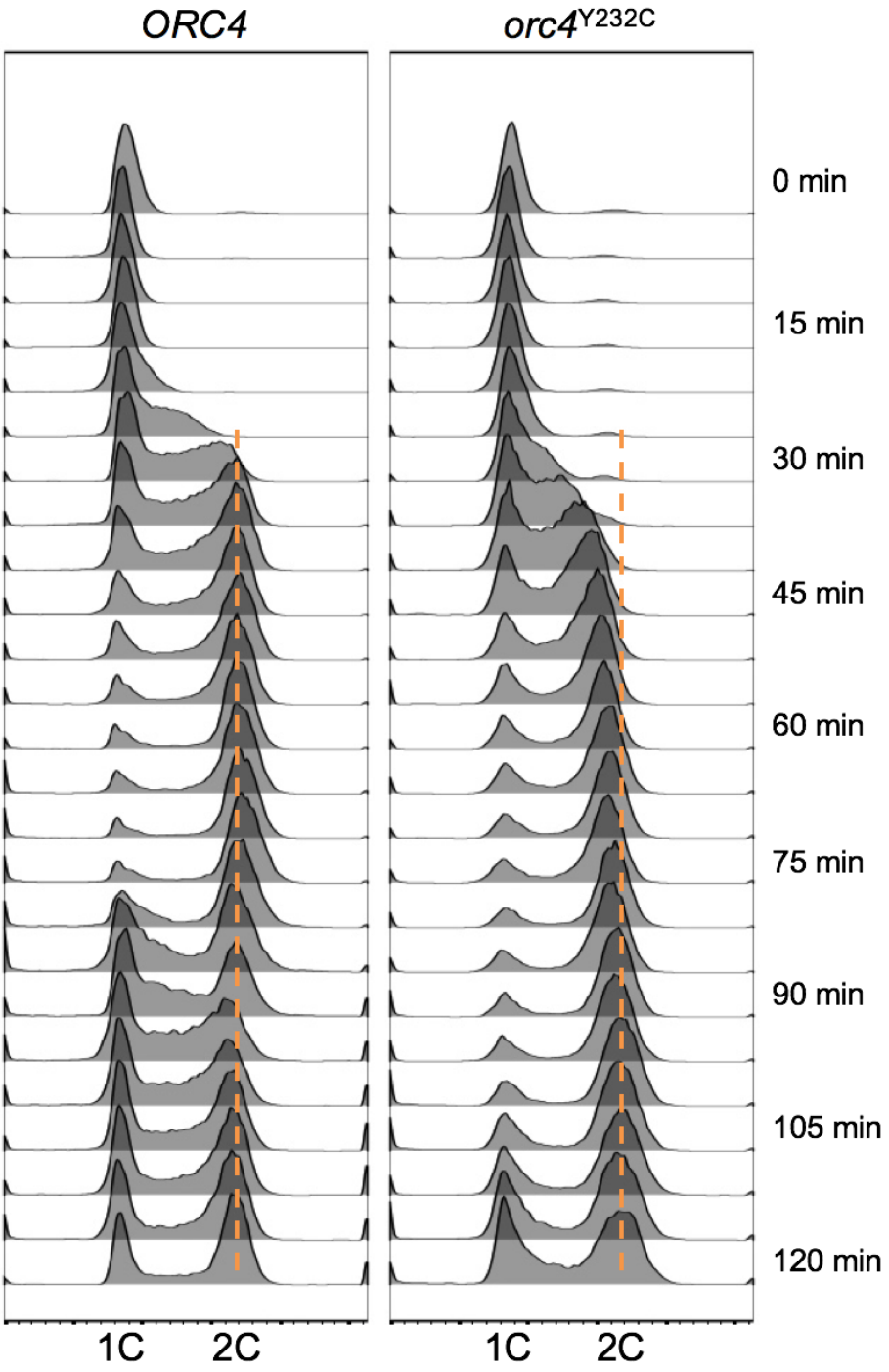

Figure 2.3: Completion of S-phase is delayed in *orc4*^{Y232C} cells.
S phase progression of *ORC4* (left) and *orc4*^{Y232C} (right) cells as measured by flow cytometry. Cells were synchronously released into S phase and cell samples were collected at 5-minute intervals. *ORC4* cells enter S phase ~20 minutes after release from alpha-factor, whereas *orc4*^{Y232C} cells entered S phase ~25 minutes after release. By 85 minutes *ORC4* cells are cycling back to begin a new cell cycle, while *orc4*^{Y232C} cells do not begin to cycle back until 120 minutes. The orange dotted line indicates the expected DNA content for cells that have completed replication.

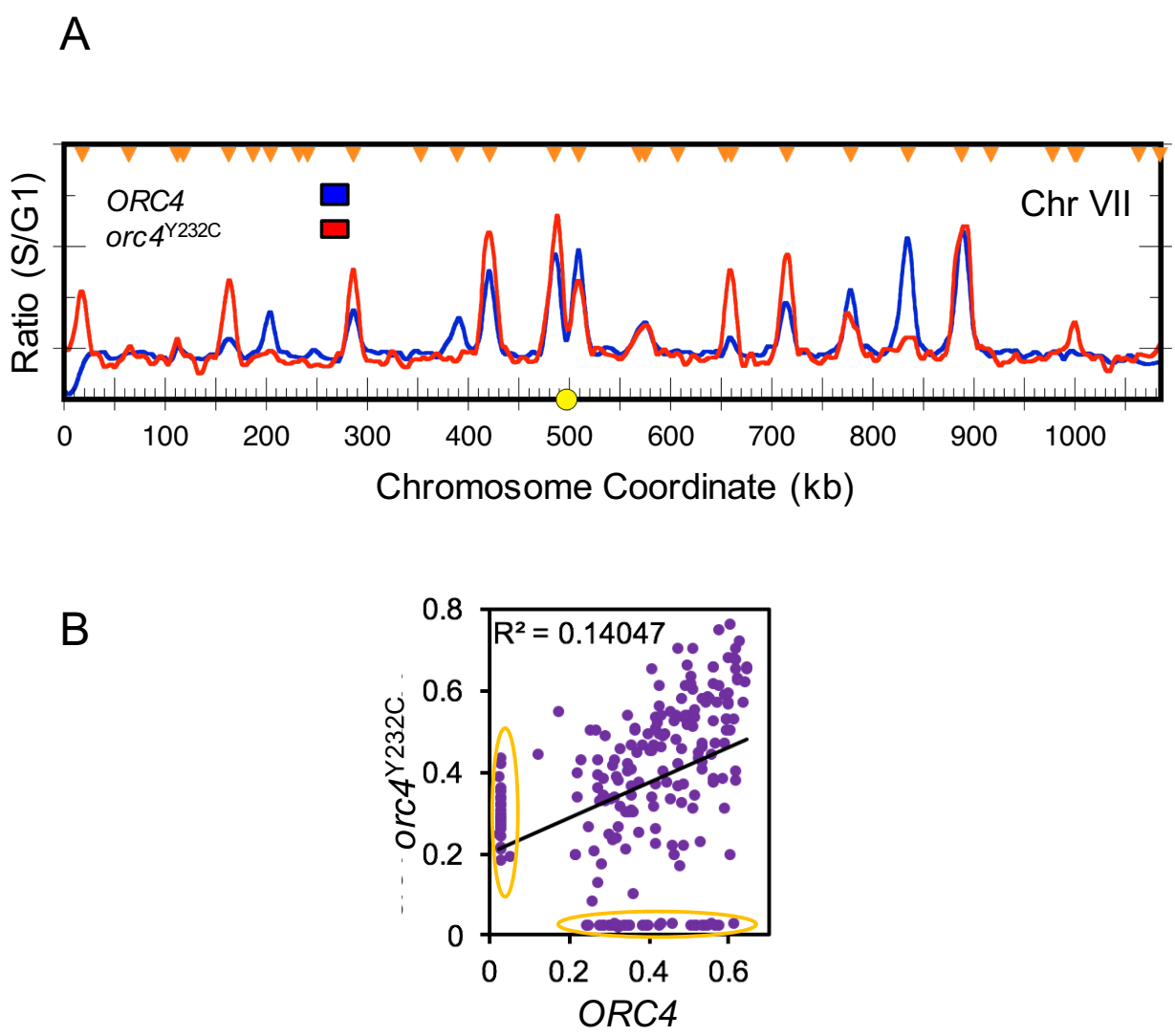

Figure 2.4: The early replication pattern is altered in *orc4*^{Y232C} cells.
(A) ssDNA profiles of early origin activity in *ORC4* (blue) compared to *orc4*^{Y232C} (red) cells are shown for Chr VII. G1 cells were synchronously released into S phase in the presence of HU to reduce movement of replisomes away from origins of replication. The y-axis values represent the relative amounts of ssDNA calculated as the ratio of fluorescent signal of S phase sample (30 min) to G1 control. Chromosome coordinates for Chr VII are displayed along the x-axis and sites of origin initiation appear as peaks along this axis. The centromere location is represented as a yellow circle on the x-axis and verified origins of replication are marked by orange triangles. See Fig. 2.5 for the full set of profiles. **(B)** Scatter plot comparing the areas under the peaks of ssDNA observed in *ORC4* vs. *orc4*^{Y232C} cells. Origins whose activity was largely restricted to one genotype or the other are encircled by the orange ovals.

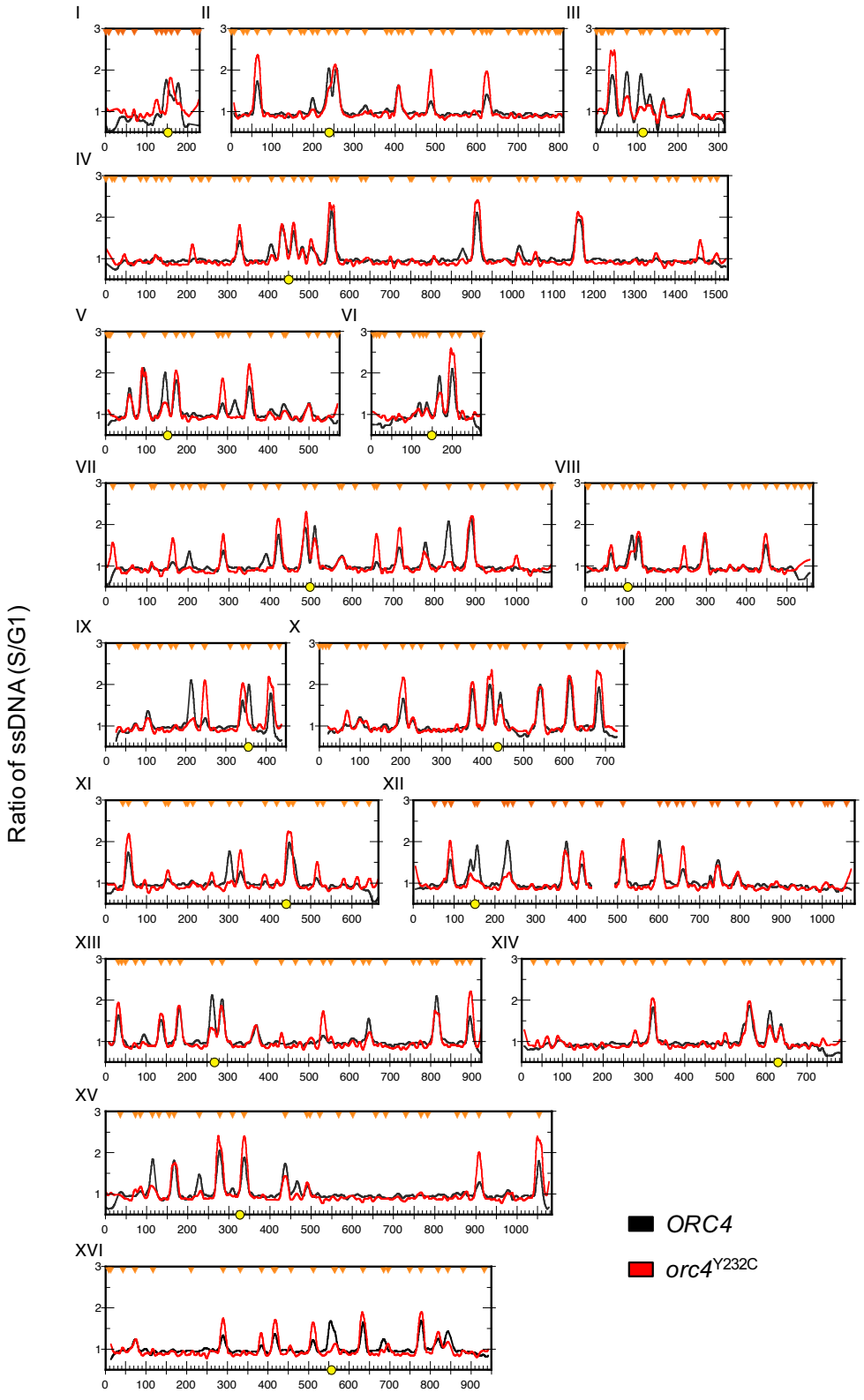
I
II
III
IV
V
VI
VII
VIII
IX
X
XI
XII
XIII
XIV
XV
XVI
Ratio of ssDNA (S/G1)
Chromosome Coordinate (kb)
ORC4
orc4Y232C

Figure 2.5: Comparison of ssDNA profiles for *ORC4* and *orc4*^{Y232C} chromosomes. Genome wide ssDNA profiles for *ORC4* (black) and *orc4*^{Y232C} (red) are shown for cells after exposure to HU for 30 min. The relative ratio of ssDNA (S/G1) is plotted against chromosome coordinates (kb). A yellow circle denotes centromere locations and the positions of verified origins of replication are marked by orange triangles. The rDNA locus and adjacent flanking sequences on Chr XII (cf. 440-490 kb) were omitted due to insufficient probe coverage on the microarray slide.

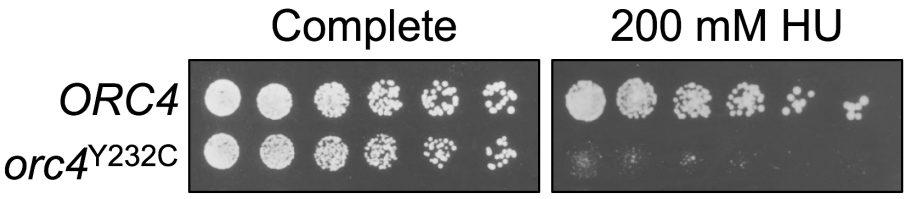

Figure 2.6: Sensitivity of *orc4*^{Y232C} cells to hydroxyurea (HU).
Serial dilutions (1:3) of cells were plated on synthetic complete medium with or without HU (200 mM) and incubated at 30° C for 3 days.

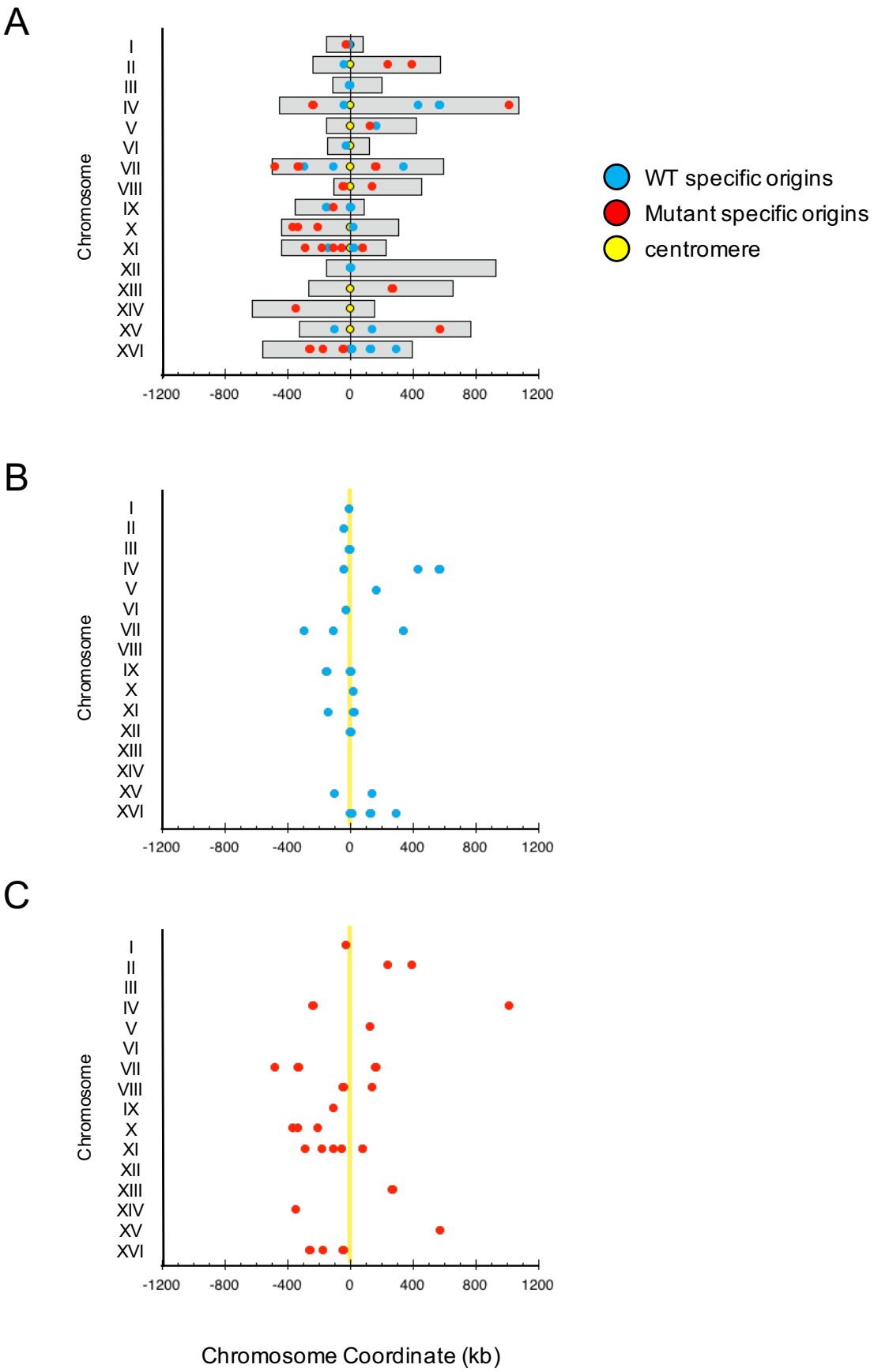
A
B
C
Chromosome
I
II
III
IV
V
VI
VII
VIII
IX
X
XI
XII
XIII
XIV
XV
XVI
-1200
-800
-400
0
400
800
1200
WT specific origins
Mutant specific origins
centromere
Chromosome Coordinate (kb)

Figure 2.7: Origins proximal to centromeres are less active in *orc4*^{Y232C} cells.
(A) The locations of *ORC4* (blue circles) and *orc4*^{Y232C} (red circles) specific origins are shown across the sixteen yeast chromosomes aligned by their centromeres at x = 0. Centromere locations are marked by a yellow circle. **(B)** The locations of only the *ORC4* specific origins are shown relative to the locations of centromeres (yellow line). **(C)** The locations of only the *orc4*^{Y232C} specific origins are shown relative to the locations of centromeres (yellow line).

Chapter 3

The *orc4*^{Y232C} allele results in reduced copy number and origin activity at the rDNA locus

3.1: Introduction

In Chapter 2, I examined how the MGS-like allele *orc4*^{Y232C} affects cellular growth and chromosome replication using budding yeast as a model system. I found that yeast cells harboring this mutation have an extended cell cycle time, due to an extended S phase. I hypothesized that perhaps the delay in late S phase was due to an overall reduction in active origins. Although the replication pattern of *orc4*^{Y232C} yeast is different than that of wild type cells, the overall number of active origin during S phase does not appear to be different. Since a similar number of origins were still able to fire in the mutant, I predicted that perhaps certain parts of the genome are more sensitive to changes in origin initiation, and might take longer to complete S phase.

In Chapter 3, I show that the rDNA locus is a part of the genome that is more sensitive to changes in origin initiation. I find that origin initiation within the rDNA locus is severely reduced in *orc4*^{Y232C} cells. Additionally, I find that reduced origin initiation within the rDNA selects for cells with a drastically shortened rDNA locus from a normal copy number of ~150 to as few as 10 repeats and that this selection for a loss of rDNA repeats is

not specific to *orc4*^{Y232C}. Yeast cells harboring a different MGS-like mutation in *CDC45* also show a loss of rDNA repeats. Variation in rDNA copy number had previously been observed in mutants compromised for DNA replication; however, a satisfying model explaining how replication stress might contribute to rDNA copy number variation had not yet been provided. I show that sufficient origin firing within the rDNA locus is necessary to maintain normal copy number of this locus and that compromised initiation creates a selection for cells with a reduced rDNA copy number. Furthermore, this model is applicable to most eukaryotic cells, including human, where the rDNA is organized as a tandem repeat with each repeat containing a potential origin of replication. Failure to maintain a sufficiently close origin spacing has long been proposed as a source of genomic instability—the "random replication gap problem". My work provides concrete evidence of chromosome breakage and instability due to a large, specific replication gap.

3.2: Results

The orc4^{Y232C} *mutation results in reduced copy number and origin activity at the rDNA locus*

When comparing the flow cytometry profiles of the *orc4*^{Y232C} cells relative to their wild type *ORC4* control cells, I noticed a consistent shift to an approximately 10% lower DNA content for the *orc4*^{Y232C} cells (Fig 3.1) regardless of their cell cycle phase. Considering that a haploid yeast genome is ~13 Mb in size, this difference in peak location means that ~1.3 Mb of sequence is missing from the mutant. Since the *ORC4* and *orc4*^{Y232C} strains analyzed in this experiment are haploid, the difference in DNA content cannot be

ascribed to chromosome aneuploidy. As an alternative possibility, I investigated whether loss of repetitive sequences could explain the shift in the mutant's flow cytometry histogram. Candidate repetitive DNA species included mitochondrial DNA (mtDNA; ~85 kb, ~50 copies per cell), the native 2-micron plasmid (6.3 kb, ~50 copies per cells), and ribosomal DNA (rDNA; 9.1 kb, 100-200 copies per cell) (Liu et al. 2014; Williamson 2002; Schweizer et al. 1969). The 2-micron plasmid and mitochondrial genomes are autonomous elements and copy number variation can occur through failure of replication and/or segregation (Chen and Butow 2005; Liu et al. 2014). In contrast, the rDNA locus is a tandemly repeated array located on chromosome XII and copy number changes occur through homologous inter- or intra-chromosome recombination (Petes 1979; Kobayashi 2006).

To determine which, if any, of these repeated sequences might account for the missing genomic DNA content of the *orc4*^{Y232C} strain I performed quantitative Southern blotting of the mutant and wild type strains. I found that the mutant cells retained most (~88%) of their mtDNA (whose replication is ORC-independent), but retained only ~21% of the 2-micron plasmid (a selfish DNA element that is dependent on ORC for maintenance (Micklem et al. 1993)) and ~23% of their rDNA copies relative to the wild type cells (Fig 3.2). The small decrease in mtDNA cannot account for the shift observed in the flow cytometry profiles; however, together the loss of 2-micron and rDNA repeats is sufficient to account for the missing DNA content. Reduction of the 2-micron plasmid would have no significant impact on the cell's health as cells completely cured of their 2-micron plasmids actually enjoy a slight selective growth advantage (Futcher and Cox 1983). However, the reduction in the rDNA locus could have a more significant impact on cell physiology.

The rDNA locus comprises over half of the physical length of chromosome XII and accounts for ~10% of the nuclear genome (Fig 3.3) (Warner 1999). Each 9.1 kb repeat contains the template for making ribosomal RNAs (rRNAs), the main structural component of ribosomes (Woolford and Baserga 2013). Based on the quantitative Southern blot analysis, I estimate that the rDNA copy number was reduced from ~150 copies in wild type cells to ~30 copies in the mutant. CHEF gel analysis of whole yeast chromosomes confirmed the expected size reduction of chromosome XII in the mutant (Fig 3.4). Thus, the deficit of ~120 copies of rDNA in the mutant would account for ~1.1 Mb of the missing sequence, with the ~40 fewer copies of 2-micron plasmid (~252 kb) accounting for the remainder of the missing ~1.3 Mb.

Since the shrinkage of chromosome XII in *orc4*^{Y232C} cells was such a striking phenomenon, I tested six additional isolates of the mutant to determine if this size reduction was a consistent phenotype of the *orc4*^{Y232C} mutation. Immediately after selection for loss of the *ORC4* allele (~20 generations), all six isolates had a smaller chromosome XII than wild type, with an rDNA locus of ~30-100 repeats (Fig 3.5). To determine the stability of the rDNA locus in the different *orc4*^{Y232C} isolates over time I monitored the size of their chromosome XII after long-term growth of the strains. I found that after ~100 generations, all six populations had arrived at the same rDNA copy number of ~30 repeats (Fig 3.6), suggesting that the *orc4*^{Y232C} mutation imposes strong selection for cells that have reduced their rDNA copy number. To determine the dynamics of rDNA repeat loss I analyzed samples collected during the ~100 generations of growth for one

isolate (e) (Fig 3.7). Rather than a steady decrease in rDNA copy number during propagation of the culture, I observed a decreasing abundance of the original chromosome XII size with concomitant increased abundance of the final size, with no obvious populations with intermediate sizes. These results support the hypothesis that a sub-population of cells with the final rDNA copy number already existed in the initial culture or appeared shortly thereafter, and had a selective advantage over cells with the longer rDNA. The descendants of the decreased-rDNA variants eventually took over the population, approaching fixation by ~80 generations of growth (Fig 3.7; indicated by the lane marked with an asterisk).

Next, I asked if the selection for the loss of rDNA repeats was a phenotype specific to the *orc4*^{Y232C} allele. To test this hypothesis, I introduced different MGS-like mutations into budding yeast, with the help from Haley Amemiya—an undergraduate researcher alumni of the Brewer/Raghuraman lab. Some cases of MGS have been reported to be caused by mutations in *CDC45*, a core component of the CMG complex, the replicative helicase that travels with the replisome during S phase (Fenwick et al. 2016; Simon et al. 2016). One such mutation, P463L, occurs at an evolutionary conserved position of the human Cdc45 protein (Fenwick et al. 2016; Fig 3.8); therefore, I introduced the equivalent MGS mutations into budding yeast (*cdc45*^{P542L}). I analyzed the chromosome XII size of five *cdc45*^{P542L} isolates immediately after selection for loss of the *CDC45* allele and found that all the isolates had shortened chromosome XII (Fig 3.9). A missense mutation (Y232S) in *ORC6* has also been shown to be responsible for some cases of MGS (Bicknell et al. 2011a; Bleichert et al. 2013). Haley introduced an equivalent MGS mutation (Y418S) into budding yeast and analyzed the size of their chromosome XII (Fig 3.10). Every *orc6*^{Y418S} isolate had

a chromosome XII that was a similar size to the chromosome XII of *ORC6* cells. The size of the chromosome XII does not appear to be immediately affected by the *orc6*^{Y418S} mutation. However, extended growth or growth at elevated temperatures may produce a more variable chromosome XII phenotype in *orc6*^{Y418S} cells. Since shrinkage of the rDNA locus is a phenotype observed in both *orc4*^{Y232C} and *cdc45*^{P542L} yeast, I sought to determine the specific event(s) responsible for this unusual phenotype.

What could account for this apparent selection for cells with reduced rDNA content? Because each rDNA repeat contains a potential origin of replication (rDNA ARS) (Brewer and Fangman 1988), I sought to determine if compromised replication initiation at the rDNA ARS could be responsible for the delay in completion of S phase and ultimately in the reduction of rDNA copy number. Replication of the rDNA locus is a bit unusual: (1) Each repeat contains a potential origin but only a subset of them—usually those rDNA ARSs downstream of transcriptionally active repeats—serve as origins in any given S phase (Muller et al. 2000). (2) Because of the high transcriptional activity, replication is almost entirely unidirectional—enforced by the replication fork barrier (RFB) that blocks forks from entering the 3' end of the 35S transcription unit in a direction that opposes transcription (Brewer and Fangman 1988). Compared to bidirectional replication elsewhere in the genome, the unidirectional replication in the rDNA would require twice the number of initiation events for the same territory to be replicated in the same amount of time. (3) The rDNA locus completes its replication late in S phase (Foss et al. 2017). I reasoned that if origin initiation at the rDNA locus were less efficient in *orc4*^{Y232C} cells it could explain the delay in completion of S phase and the reduction in rDNA copy number

because cells that had suffered a reduction in rDNA length would complete replication more quickly and their descendants would take over the culture.

To test the efficiency of rDNA origin firing, I carried out 2-dimensional (2D) gel electrophoresis of genomic DNA from cells in logarithmic growth (Brewer and Fangman 1987). By focusing on the *NheI* fragment that contains the rDNA ARS at its center I was able to detect the fraction of rDNA repeats that gives rise to bubble intermediates (active origin) relative to the fraction of repeats in which the origin region is passively replicated by a fork moving through (inactive origin) (Fig 3.11A). The wild type cells showed the expected frequency of repeats with an active origin (roughly 1 in 5 repeats has an active origin; Fig 3.11B). In contrast, *orc4*^{Y232C} cells had a greatly reduced "bubble arc" relative to the intensities of the "Y arc", the RFB pause site and the non-replicating "1N" spot. After adjusting for copy number differences in rDNA repeats between the two strains I conclude that origin activation within the rDNA array is a very rare event in the *orc4*^{Y232C} mutant cells.

What might be the cause for the reduced origin activity of rDNA origins in the mutant cells? One possibility is that the mutant allele results in a less stable protein, therefore limiting the amount of Orc4^{Y232C} protein available to form Pre-RCs on rDNA origins. Such is indeed the case in *orc2-1* mutant cells, where protein destabilization leads to reduced pre-RC formation; simply increasing the dosage of the mutant protein by providing an additional copy of the mutant gene on a plasmid alleviates the mutant phenotype (Shimada et al. 2002). Accordingly, I asked whether an additional copy of the *orc4*^{Y232C} allele on a centromere plasmid would provide any level of rescue of the rDNA

locus contraction. An *orc4*^{Y232C} clone with ~30 rDNA repeats was transformed with plasmids containing either the *ORC4* or *orc4*^{Y232C} allele and chromosome XII size was measured after ~30 generations of growth. The plasmid copy of *ORC4* resulted in a significant increase in the rDNA locus while the same plasmid with the *orc4*^{Y232C} allele provided no rescue (Fig 3.12). These results suggest that it may not be protein levels that are contributing to reduced rDNA origin firing, but rather, the rDNA origin is less efficiently activated in cells with the mutant ORC complex.

To test whether inefficient rDNA origin firing was responsible for contraction of the rDNA locus I reasoned that a compromised rDNA ARS would exacerbate the phenotype. A naturally occurring rDNA variant, obtained from the Robert Mortimer vineyard strain RM11-1a, was introduced into the laboratory background BY4741 (Kwan et al. 2013). This variant, which has a T to C transition in a highly-conserved residue of the rDNA ACS (Fig 3.13), is known to reduce but not eliminate *rARS* activity (Kwan et al. 2013). Cells with this weakened rDNA variant in an otherwise wild type background show no change in growth rate (compare Fig 2.2 and Fig 3.14). For convenience, I shall hereafter refer to the lab (BY4741) version of the rDNA as *rDNA*^{BY} and the vineyard strain (RM11-1a) variant rDNA as *rDNA*^{RM}.

Plating assays of the wild type and *orc4*^{Y232C} strains are shown in Fig 3.15. While growth of the *orc4*^{Y232C} *rDNA*^{BY} strain was comparable to that of *ORC4* strains with either rDNA version at 30°C and 37°C, growth of the *orc4*^{Y232C} *rDNA*^{RM} strain was reduced at 30˚C and was undetectable at 37˚C. Furthermore, the slow growth phenotype of the *orc4*^{Y232C} *rDNA*^{RM} strain is recapitulated in liquid medium at 30°C (Fig 3.14): relative to the wild type

strain, the growth rate of *orc4*^{Y232C} *rDNA*^{RM} is reduced by 54 minutes as compared to 18 minutes for *orc4*^{Y232C} *rDNA*^{BY}.

I analyzed the size of the rDNA locus by measuring the *BamHI* genomic fragment from chromosome XII that contains the intact rDNA locus plus adjacent single copy sequences (Fig 3.16) by CHEF gel electrophoresis and found that the rDNA locus had undergone an even greater reduction in the *orc4*^{Y232C} *rDNA*^{RM} strain compared to the *orc4*^{Y232C} *rDNA*^{BY} strain (Fig 3.17)—from 30 copies to ~10 copies. An rDNA locus of this size (91 kb) is at the upper limit of a replicon that could reasonably be expected to be replicated by a fork established at the nearest upstream origin in the flanking unique sequences (Miller et al. 1999; Rivin and Fangman 1980). 2D gel analysis (Fig 3.18) confirmed that there is no detectable origin initiation within the rDNA locus itself. Unlike the cells containing the BY version of the rDNA ARS, all the initial isolates that contained the *orc4*^{Y232C} mutation showed this drastic reduction in rDNA content and did not require an extended period of growth to achieve the steady-state reduction in rDNA copy number (Fig 3.19). Cells released from an alpha-factor arrest into a synchronous S phase showed a similar late-S/G1 delay but an additional and exaggerated delay in entry into S phase (~40 minutes in *orc4*^{Y232C} *rDNA*^{RM} compared to ~20 minutes in *ORC4 rDNA*^{RM}; Fig 3.20; compare with Fig 2.3).

If the prolonged G1 to S delay in *orc4*^{Y232C} *rDNA*^{RM} cells were caused by insufficient origin activation across the genome, I would anticipate the total number of early active origins to be lower in this strain. To test this hypothesis, I carried out the same ssDNA assay as before on both *ORC4 rDNA*^{RM} and *orc4*^{Y232C} *rDNA*^{RM} cells. The full set of

comparisons for all the chromosomes between *ORC4 rDNA*^{RM} and *orc4*^{Y232C} *rDNA*^{RM} cells are shown in Fig 3.21 and quantification of the area under peaks and pairwise comparisons between the strains are shown in Fig 3.22. Similar to my previous observation, I found differences in the activation of early origins between *ORC4 rDNA*^{RM} and *orc4*^{Y232C} *rDNA*^{RM} cells; however, the total number of active origins was similar between the two. Additionally, pairwise comparisons of the two *ORC4* or two *orc4*^{Y232C} strains with different rDNAs showed extremely good concordance, indicating that the rDNA ARS genotype does not affect early genome wide replication initiation dynamics. These observations suggest that the prolonged G1 to S transition observed in the cell cycle analysis was not due simply to inadequate genome-wide origin activation in *orc4*^{Y232C} *rDNA*^{RM} cells but suggest that some aspect of defective rDNA replication contributes to both the entry into and completion of S phase.

The initiation defect in orc4^{Y232C} rDNA^{RM} leads to chromosome XII breakage

Why are *orc4*^{Y232C} *rDNA*^{RM} cells slower to complete S phase and enter cell division? Are they experiencing difficulty in replicating their chromosome XII due to reduced origin activity at the rDNA locus, and if so, what might the consequences be? In the process of measuring rDNA copy number in the different isolates of *orc4*^{Y232C} *rDNA*^{RM} I noticed an additional minor band (Fig 3.19; indicated by an asterisk) that was present only in the *orc4*^{Y232C} *rDNA*^{RM} samples and that migrated faster than the predominant chromosome XII band. I ruled out the possibility that the presence of the additional band was due to cross hybridization of the probe I was using because I did not observe its presence in the lane loaded with DNA from *ORC4 rDNA*^{RM} cells. Therefore, I hypothesized that the additional

band might be a result of breakage of chromosome XII, specifically at the rDNA locus. As previously mentioned, I estimated that the rDNA copy number of *orc4*^{Y232C} *rDNA*^{RM} cells is ~10 copies, which should result in a reduction in the overall size of chromosome XII to ~1.13 Mb (Fig 3.23). If chromosome XII were breaking at the rDNA locus, the two resulting sizes should be ~450 kb (left of the rDNA locus) and ~590 kb (right of the rDNA locus) and I should be able to detect these two different products using probes specific to different locations along the chromosome (Fig 3.23). When hybridizing the Southern blot with a probe specific to the right of the rDNA locus (R-rDNA), in addition to the full-length chromosome XII, I also detected a band that migrated with a similar mobility to chromosomes V and VIII (~580 kb) in the lane loaded with *orc4*^{Y232C} *rDNA*^{RM} DNA (Fig 3.24). However, when probing the same Southern blot for a sequence to the left of the rDNA locus (L-rDNA), the minor band previously detected was not seen; instead, a new minor band appeared at a size of ~450 kb. Based on the locations of the probes used and the different sizes of minor bands detected, I believe that chromosome XII is breaking at the rDNA locus in a small population of *orc4*^{Y232C} *rDNA*^{RM} cells. To determine if chromosome breakage is a general feature observed at other chromosomes in *orc4*^{Y232C} *rDNA*^{RM} cells, I next probed the same Southern blot for a sequence on the second largest yeast chromosome (chromosome IV) and observed only a single band in both lanes (Fig 3.24), indicating that chromosome breakage is specific to the rDNA locus in *orc4*^{Y232C} *rDNA*^{RM} cells. Lastly, to determine if the chromosome breakage observed in *orc4*^{Y232C} *rDNA*^{RM} cells was a transient or recurrent event, I assayed for chromosome breakage again after ~60 generations of growth and observed only the major band corresponding to the intact chromosome XII (Fig 3.24). This result suggests that the locus specific breakage in

orc4^{Y232C} *rDNA*^{RM} cells occurs during a very narrow window, shortly after loss of the *ORC4* allele.

3.3: Discussion

My work demonstrates that there is a strong selection for reducing rDNA copy number when ORC function is compromised. A link between impaired ORC function and variation in rDNA copy number has been noted in previous studies. Ide et al. (2007) showed that temperature sensitive mutations in two other ORC complex proteins, Orc1 and Orc2, result in the shrinkage of the rDNA locus when cells are grown at the restrictive or semi-restrictive temperatures. In addition, they demonstrated that the shortened rDNA locus was responsible for suppressing the temperature sensitivity of these mutations. Finally, they demonstrated that replication difficulties in the rDNA triggered a Rad53 checkpoint response and that rDNA reduction attenuates this checkpoint response. Based on these observations, the authors proposed that the rDNA locus plays an important role in monitoring when origin initiation across the genome is compromised. The specific molecular event that was responsible for activation of the checkpoint response was not addressed in that study, nor was it clear why rDNA shrinkage would attenuate the checkpoint response. Furthermore, although their model assumes reduced origin firing across the genome in the *orc* mutants, origin activity was only examined for one chromosomal origin (*ARS1*) other than *rARS*. My work provides new insights into the observations made by Ide et al. and suggests an alternative interpretation of their results. In my broader assessment of origin activity, I find that *ORC4* and *orc4*^{Y232C} cells have a very

similar number of early active origins, arguing that there is unlikely to be replication defects genome-wide. Rather, it appears that the rDNA itself is the "weak link" suffering from replication gaps. My results suggest that as in the *orc4*^{Y232C} cells, chromosome breakage at the rDNA locus is likely responsible for triggering the Rad53 response observed by Ide et al.; I presume that as in the *orc4*^{Y232C} strain, the *orc1* and *orc2* cells with reduced rDNA would circumvent the rDNA replication gap problem and would therefore attenuate the checkpoint signal. Finally, although Ide, et al. demonstrated that shrinkage of the rDNA locus partially suppressed the temperature sensitive mutations in Orc1 and Orc2 they did not explore how this rDNA shrinkage might affect rRNA synthesis. As I show in the next chapter, I find that having fewer rDNA repeats may allow for complete replication of this locus in *orc4*^{Y232C} cells, but at a cost. Losing too many rDNA repeats, as in the case of *orc4*^{Y232C} *rDNA*^{RM} cells, limits the amount of rRNA that can be transcribed. Therefore, *orc4*^{Y232C} cells must walk a tightrope, as it were—too many copies of rDNA and they suffer chromosome XII instability, but too few copies and they are unable to meet the demand for protein synthesis.

A second study expanded on the idea that the ~150 rDNA origins compete for limiting replication initiation factors with the ~300 unique origins across the yeast genome (Yoshida et al. 2014). The authors of that study discovered that this competition is regulated oppositely by two histone deacetylases—Sir2 and Rpd3. When initiation in the rDNA is increased, replication at some unique genomic origins is reduced, and vice versa. In their experiments, ORC was not the limiting factor. Instead, they showed that they could increase initiation at unique origins in a *sir2Δ* strain by overexpressing three of the initiation factors known to be in limiting supply (Sld7, Sld3 and Cdc45). I initially

entertained the possibility that reduction of rDNA copy number in the *orc4*^{Y232C} mutant strain might restore a more favorable replication initiation balance between the rDNA and unique origins. However, three observations make this explanation unlikely. First, I did not find an overall reduction in unique chromosomal origin firing in the *orc4*^{Y232C} mutant—the number of early origins that failed to fire was similar to the number of new origins that appeared in the early firing class. Second, if competition between rDNA origins and unique origins were causing the growth defect in *orc4*^{Y232C}, reducing the efficiency of the *rDNA*^{BY} origin by replacing the locus with *rDNA*^{RM} should have improved growth of the *orc4*^{Y232C} strain—instead, growth was further restricted and the only detectable locus to suffer from failed replication initiation was the rDNA. Third, introducing a second copy of *orc4*^{Y232C} on a centromere plasmid did not produce any rescue in the size of the rDNA locus—suggesting that the ORC complex was not in limiting supply. Together, these observations led me to hypothesize that the *orc4*^{Y232C} mutation has altered the protein's function.

Is my proposed model for the selection of yeast cells with a reduced rDNA copy number relevant for humans with Meier-Gorlin syndrome? Just as in yeast, the structure of human rDNA is highly repetitive; however, there are some notable differences. In yeast the rDNA locus is located on a single chromosome with two transcription units separately producing the 5S rRNA transcript and 35S rRNA precursor, which is processed into the 18S, 5.8S and 25S rRNAs (Woolford and Baserga 2013). In humans, rDNA clusters are located on six different chromosomes (Stults et al. 2008). A locus near the end of the long arm of Chromosome 1 contains 50-200 copies of a 2.2 kb repeat that produces the 5S rRNA (Stults et al. 2008). Loci at the ends of the short arms of Chromosomes 13, 14, 15, 21, and 22 contain 43 kb repeats coding for a 47S transcript that gets processed into the 5.8S, 18S and

28S rRNAs (Stults et al. 2008). The number of repeats on each chromosome varies and individuals show a wide distribution of copy numbers at these five loci, ranging from between 10 to more than 100 repeats per locus (Gibbons et al. 2015). While most chromosomal origins in humans are thought not to be defined by primary DNA sequence, replication initiation events in the 43 kb rDNA repeats are confined to the non-transcribed spacer (Little et al. 1993).

What might be the consequences of impaired replication at the rDNA locus in higher eukaryotes? Bloom's syndrome (BLM) is a rare autosomal recessive disorder characterized by short stature, immunodeficiency, and predisposition for cancer (Cunniff et al. 2017). Individuals with BLM have mutations in the gene *BLM*, which encodes a member of the RecQ family of DNA helicases that acts during DNA replication (Cunniff et al. 2017). Cells derived from individuals with BLM exhibit a high frequency of sister chromatid exchange and genomic instability (Cunniff et al. 2017). Particularly, BLM cells exhibit elevated levels of instability at the rDNA locus (Killen et al. 2009); however, the exact cause for this instability is unknown. Deletion of the *BLM* orthologue *SGS1* in budding yeast also results in increased instability at the rDNA locus (Weitao et al. 2003). Additionally, cancers in both human and mouse have also been shown to exhibit elevated levels of instability at the rDNA locus (Stults et al. 2009; Pruitt et al. 2017). Stultz et al. found an increase in rDNA rearrangements in the majority of tumor samples they analyzed from lung and colorectal cancers, leading them to the conclusion that the rDNA locus is a recombination hotspot in some cancers (Stults et al. 2009). Finally, mice deficient for MCM2 (a component of the Pre-RC) develop lymphomas and exhibit elevated levels of DSBs at the 45S rDNA repeats in their genomes (Pruitt et al. 2017).

What could be the consequence(s) of increased instability at the rDNA locus in cancer? Recently, Xu et al. analyzed rDNA copy number in both human and mouse cancer genomes and contrary to their initial prediction, they found that rDNA copy number is reduced in the cancer state (Xu et al. 2017). One explanation the authors propose for this unexpected result is that having fewer rDNA repeats may allow for more efficient DNA replication and thus greater cell proliferation in cancer. Given the fact that the rDNA locus is highly sensitive to replication stress in higher eukaryotes and its copy number can change rapidly during the disease state, a similar problem with rDNA replication could lead to a reduction in rDNA copy number and could limit ribosome production in the case of MGS. However, neither the copy number of rDNA repeats nor their replication properties have been examined in cells from Meier-Gorlin patients.

3.4: Materials and Methods

Contour-clamped homogeneous electric field (CHEF) gel analysis

Stationary phase cells were embedded in agarose plugs and prepared using standard procedures (Kwan et al. 2016). CHEF gel analysis of whole yeast chromosomes was performed using a BioRad CHEF-DR® II Pulsed Field Electrophoresis System. Whole chromosomes were resolved in 0.8% LE agarose gels with a switch time ramped from 300-900 seconds at 100 volts for 68 hours in 0.5X TBE at 14° C. *BamH*I digested chromosomal DNA fragments were resolved in 1.0% LE agarose gels with a switch time ramped from 47-175 seconds at 165 volts for 62 hours in 0.5X TBE at 14˚C. Gels were stained with ethidium

bromide and photographed. Southern blotting and hybridization were performed using standard procedures.

Strain construction

The rDNA locus from the Robert Mortimer vineyard strain RM11 was introduced into the BY4741 background by standard backcrossing (10 times) to create *ORC4* rDNA^{RM} (Kwan et al. 2013). The MGS-like variant *orc4*^{Y323C} was introduced into *ORC4* rDNA^{RM} by two-step gene replacement (Duff and Huxley 1996). A plasmid containing *URA3* and the *orc4*^{Y232C} allele was integrated at the *ORC4* locus; correct integrants were confirmed by PCR and Southern analysis. I selected for loss of the integrated sequences through homologous recombination by selecting against the *URA3* gene on plates containing 5-fluoro orotic acid. To screen for clones that had lost the wild type *ORC4* allele and had kept the *orc4*^{Y232C} allele I performed PCR using an allele specific oligonucleotide as one of the PCR primers. The MGS-like allele *cdc45*^{P542L} was introduced into BY4741 using CRISPR-Cas9 following the steps described by Laughery et al. (2015).

Two-Dimensional (2D) agarose gel analysis

Mid-log phase cells were harvested and embedded in 0.5% low melt agarose (SeaPlaque) in 50 mM EDTA and prepared as previously described (Iadonato and Gnirke 1996) with slight modifications (see http://fangman-brewer.genetics.washington.edu/plug.html). DNA was subsequently digested in-gel using *NheI* (NEB). 2D gel electrophoresis was used to visualize the relative abundance of replication intermediates and was performed as

described by (Brewer and Fangman 1987). Gels were blotted and hybridized with a probe specific to the rDNA origin of replication.

Quantitative Southern blotting

DNA was harvested from stationary phase cells via the "Smash-and-grab" DNA isolation protocol (Hoffman and Winston 1987) and subsequently digested with *EcoRV* (NEB). Digested DNA was separated by electrophoresis in a 0.7% Agarose LE (GeneMate) gel and then blotted following standard Southern blotting protocols. Blots were then sequentially hybridized with probes specific to *ACT1* (single copy control), mtDNA, 2-micron plasmid, and then rDNA. The hybridization signal was analyzed using the BioRad Personal Molecular Imager and Quantity One software. Hybridization signals of repetitive sequences were first normalized to *ACT1* and then relative to wild type.

Long term growth experiments

My initial replacement of *ORC4* with the mutant *orc4*^{Y232C} allele was performed using a "pop-in/pop-out" strategy ((Duff and Huxley 1996); see Yeast strains and plasmids section above). To track long-term rDNA copy number changes following replacement of wild type with mutant *orc4*^{Y232C}, I picked fresh "pop-out" candidates and inoculated liquid cultures for growth to saturation (~30 generations). After confirming the loss of *ORC4* by allele-specific PCR, plugs for CHEF gel analysis were made for the *orc4*^{Y323C} positive isolates (a-f; Fig 3.5). From the initial overnight cultures, a 1/100 dilution was made into 5 ml of fresh

medium and allowed to grow to saturation (~7 generations). Growing of cells to saturation and then diluting back into fresh medium was performed for a total of 10 times which accounted for a total of ~100 generations of growth. In each round, cells were harvested when the culture reached saturation and embedded in agarose plugs for CHEF gel analysis.

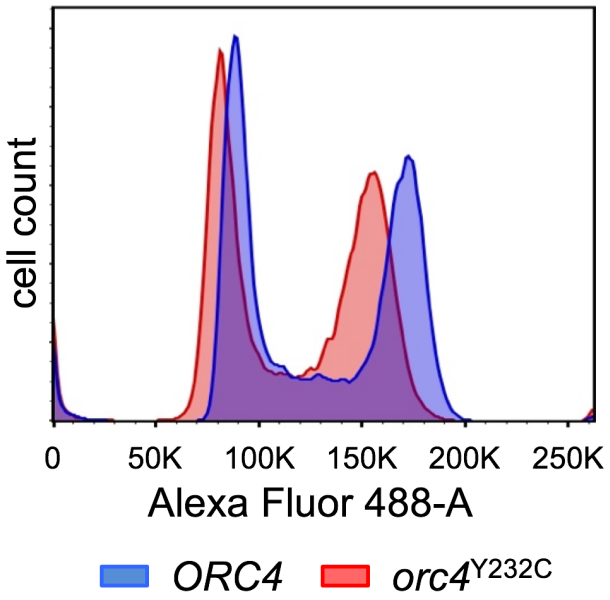

Figure 3.1: The relative DNA content of *orc4*^{Y232C} cells is less than *ORC4* cells.
Flow cytometry histograms of log-phase populations of *ORC4* (blue) and *orc4*^{Y232C} (red) cells overlaid with one another. The mutant's profile is shifted to the left indicating a loss (~10%) of cellular DNA content.

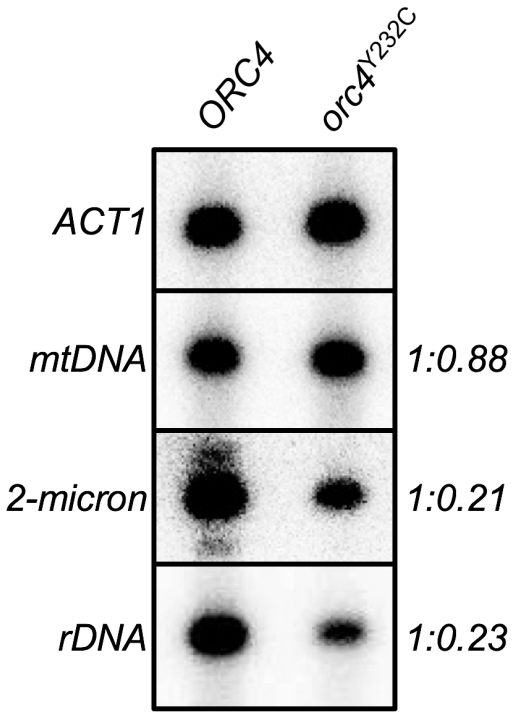

Figure 3.2: Quantitative Southern blot analysis of repetitive DNA sequences. Genomic DNA from *ORC4* and *orc4*^{Y232C} cells was digested with a restriction enzyme and separated by standard gel electrophoresis. The Southern blot of the gel was first probed with *ACT1* sequence (as a single copy control) and then subsequently probed with various repetitive DNA sequence including mitochondrial DNA, the native, nuclear 2-micron plasmid DNA, and rDNA. The bands above and below the major center band present when probed for 2-micron correspond to restriction fragments from the low levels of naturally occurring dimeric plasmid molecules between the A and B isomers of the plasmid.

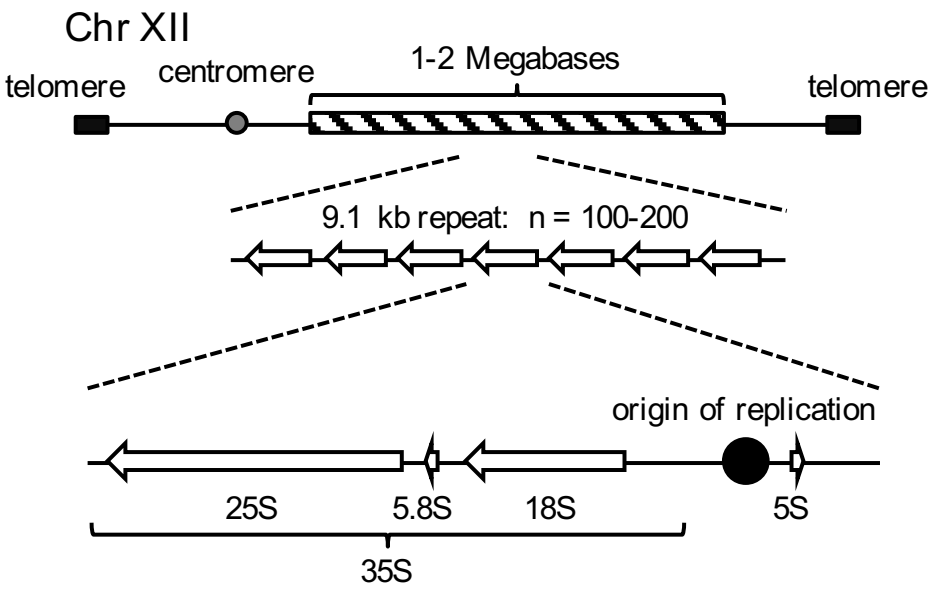

Figure 3.3: Cartoon depiction of the yeast rDNA locus.
The yeast rDNA locus consists of 100-200 copies of a 9.1 kb tandem repeat located on Chr XII. Each rDNA repeat encodes the template necessary to make ribosomal RNA (25S, 5.8S, 18S and 5S) and also contains an origin of replication.

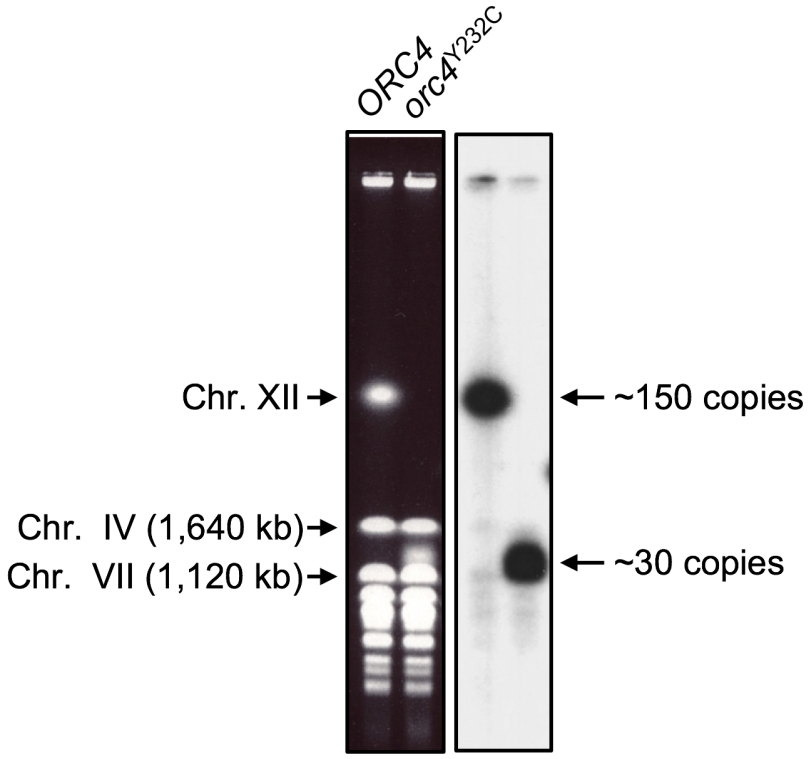

Figure 3.4: CHEF gel analysis of Chr XII size in *ORC4* and *orc4*^{Y232C} cells.
Left panel, ethidium bromide stained image; right panel, image of Southern blot following hybridization with a Chr XII-specific single-copy sequence. The faster migration of Chr XII in *orc4*^{Y232C} cells confirms the loss of chromosomal rDNA repeats from ~150 (*ORC4*) to ~30 copies (*orc4*^{Y232C}).

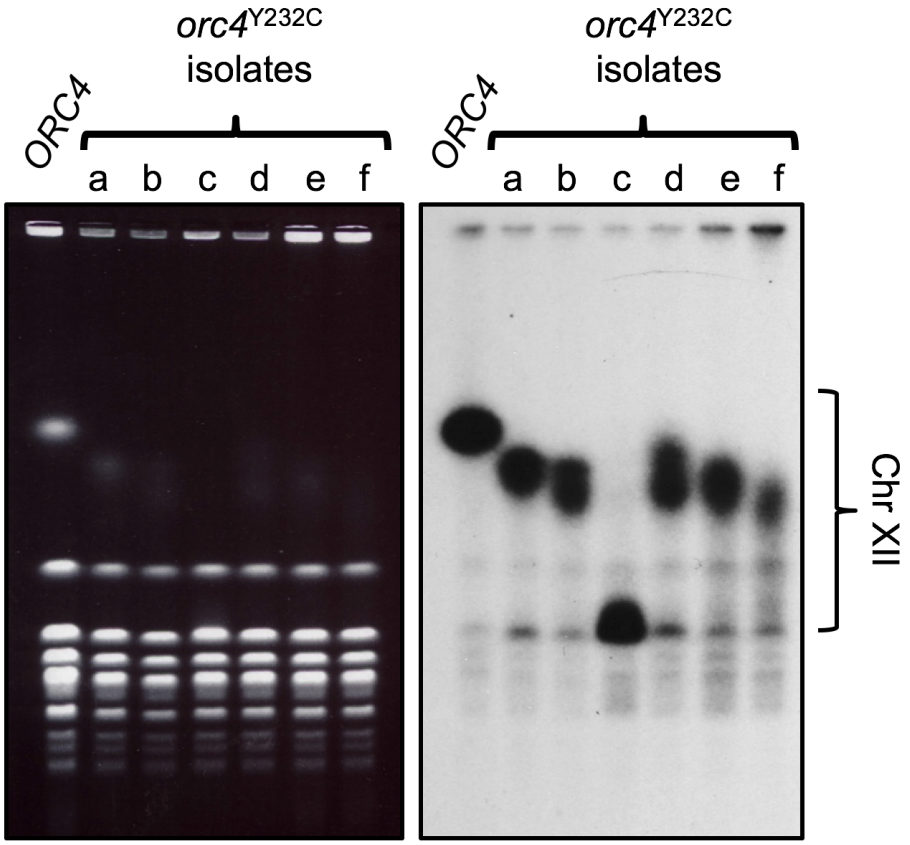

Figure 3.5: CHEF gel analysis of variation in rDNA copy number in six additional isolates (a-f) of *orc4*^{Y232C}.
Left, ethidium bromide stained image; right, Southern blot hybridization for Chr XII. Samples were prepared after ~20 generations of growth following introduction of the *orc4*^{Y232C} mutation. All six isolates had a smaller Chr XII than *ORC4* due to loss of rDNA repeats. The rDNA copy number in the isolates ranges from ~30 copies (isolate c) to ~100 copies (isolates a, b, d, and e).

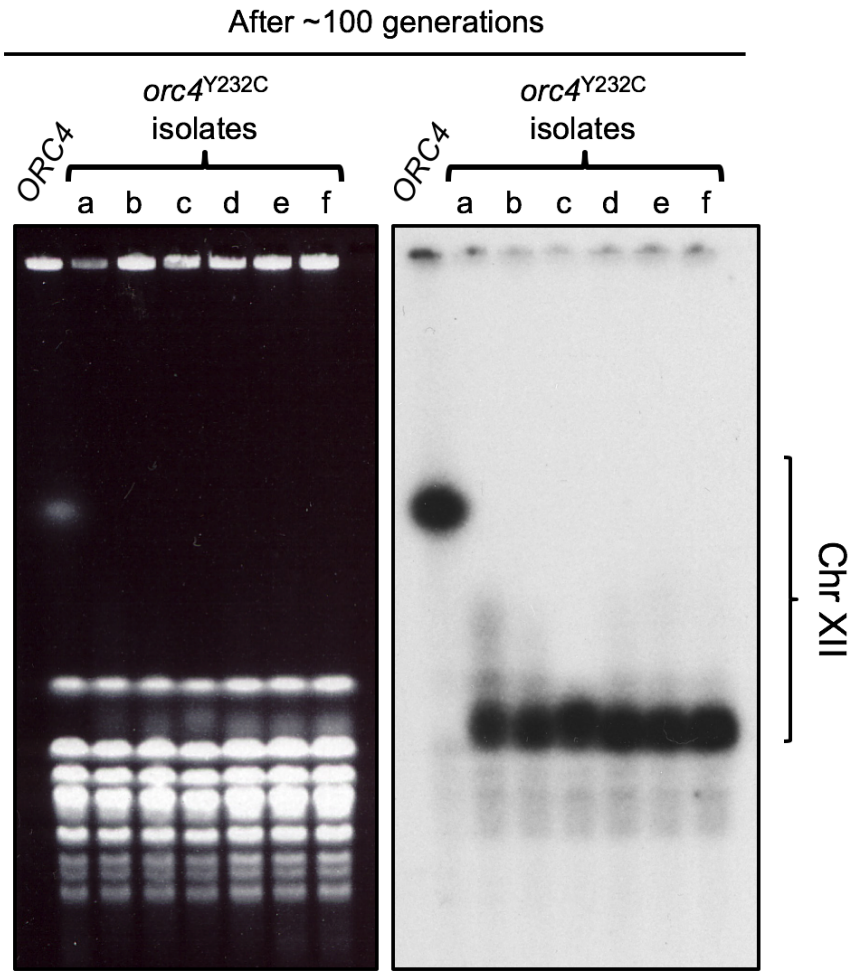

Figure 3.6: The rDNA copy number in *orc4*^{Y232C} cells stabilizes at ~30 copies. Variation in rDNA copy number was analyzed in the six isolates (a-f) of *orc4*^{Y232C} after growth for ~100 generations. Change in Chr XII size was measured by CHEF gel electrophoresis. Left, ethidium bromide stained image; right, Southern blot image following hybridization with a Chr XII-specific single-copy sequence. By ~100 generations the size of Chr XII had stabilized at ~30 copies of rDNA for most of the population in all six isolates of *orc4*^{Y232C}.

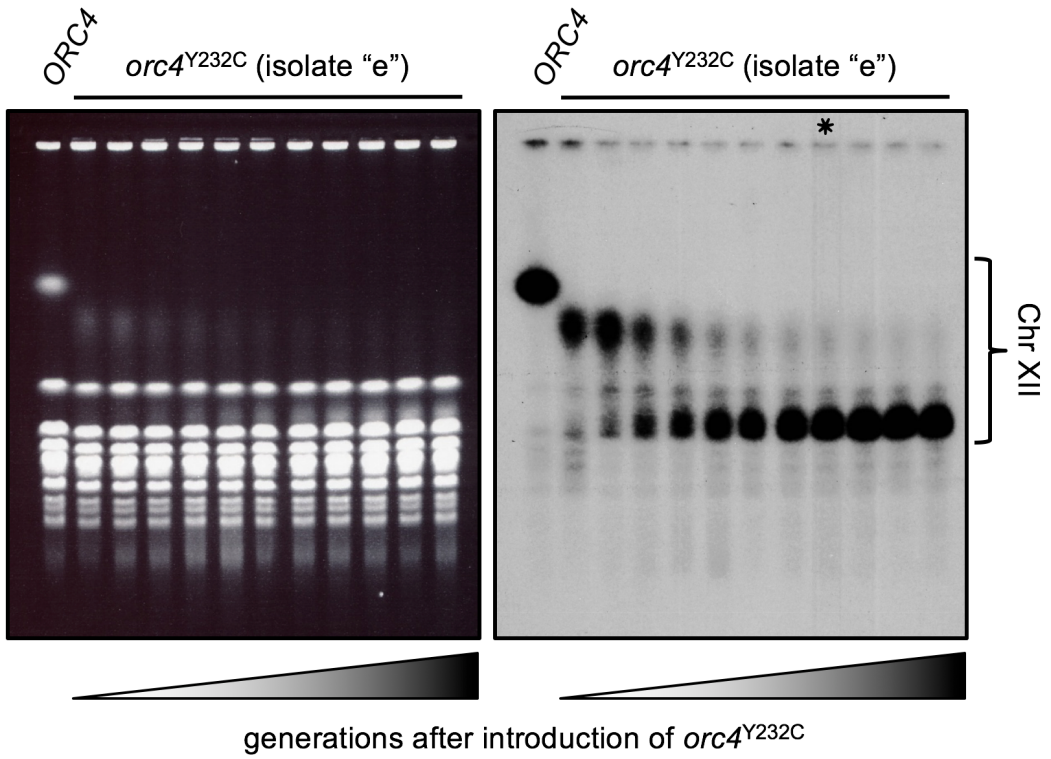

Figure 3.7: Long-term growth of isolate "e" shows rDNA copy number stabilizes at ~30 copies.
After confirming isolate "e" to have the mutant *orc4*^{Y232C} allele, cells were continuously passaged for ~100 generations in batch culture. Cells were allowed to grow to saturation after each passage. For each sample cells were collected and whole chromosomes were separated by CHEF gel electrophoresis (ethidium bromide stained image on left, Southern hybridization for Chr XII). By ~80 generations (*) the rDNA copy number stabilized at ~30 copies in the population.

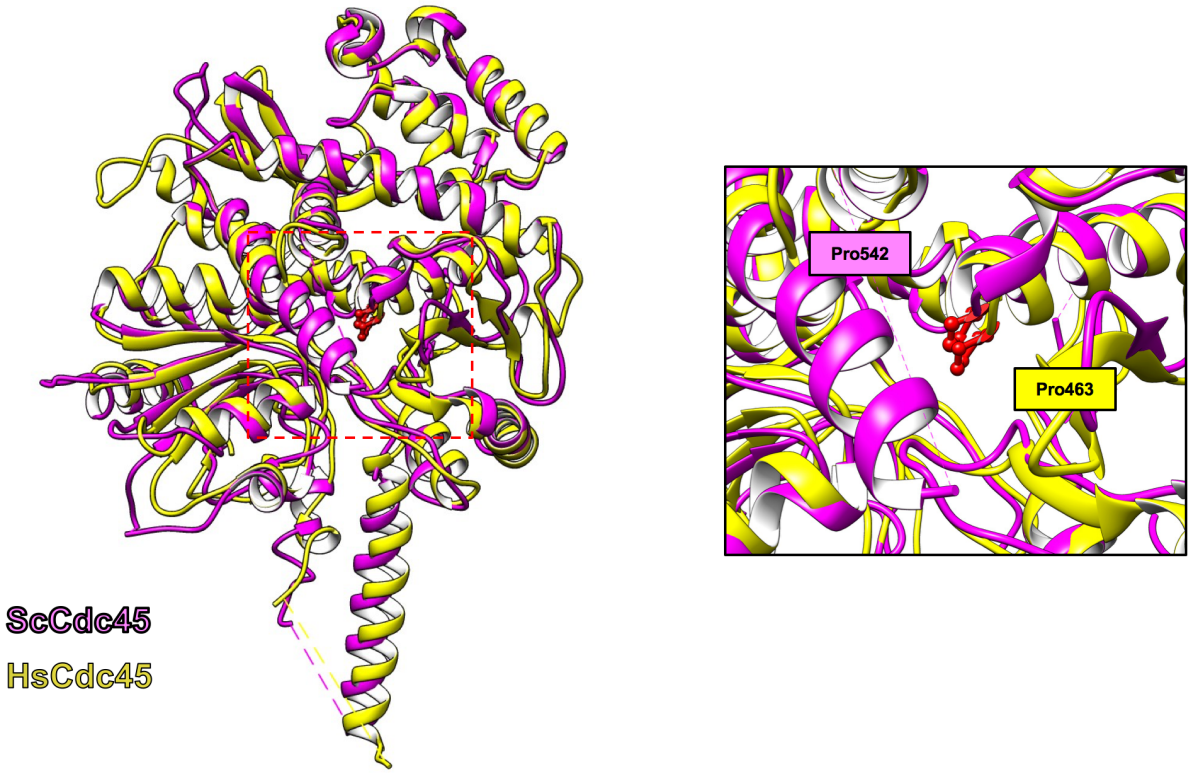

Figure 3.8: Superimposition of the Human and *S. cerevisiae* Cdc45 proteins
Superimposition of the Hs and Sc Cdc45 highlights the high degree of structural similarity between the proteins from the two species. The right panel focuses on the Proline mutated in human MGS patients (Pro463) and the corresponding Proline in yeast (Pro542) with the side chains of these amino acids displayed in red.

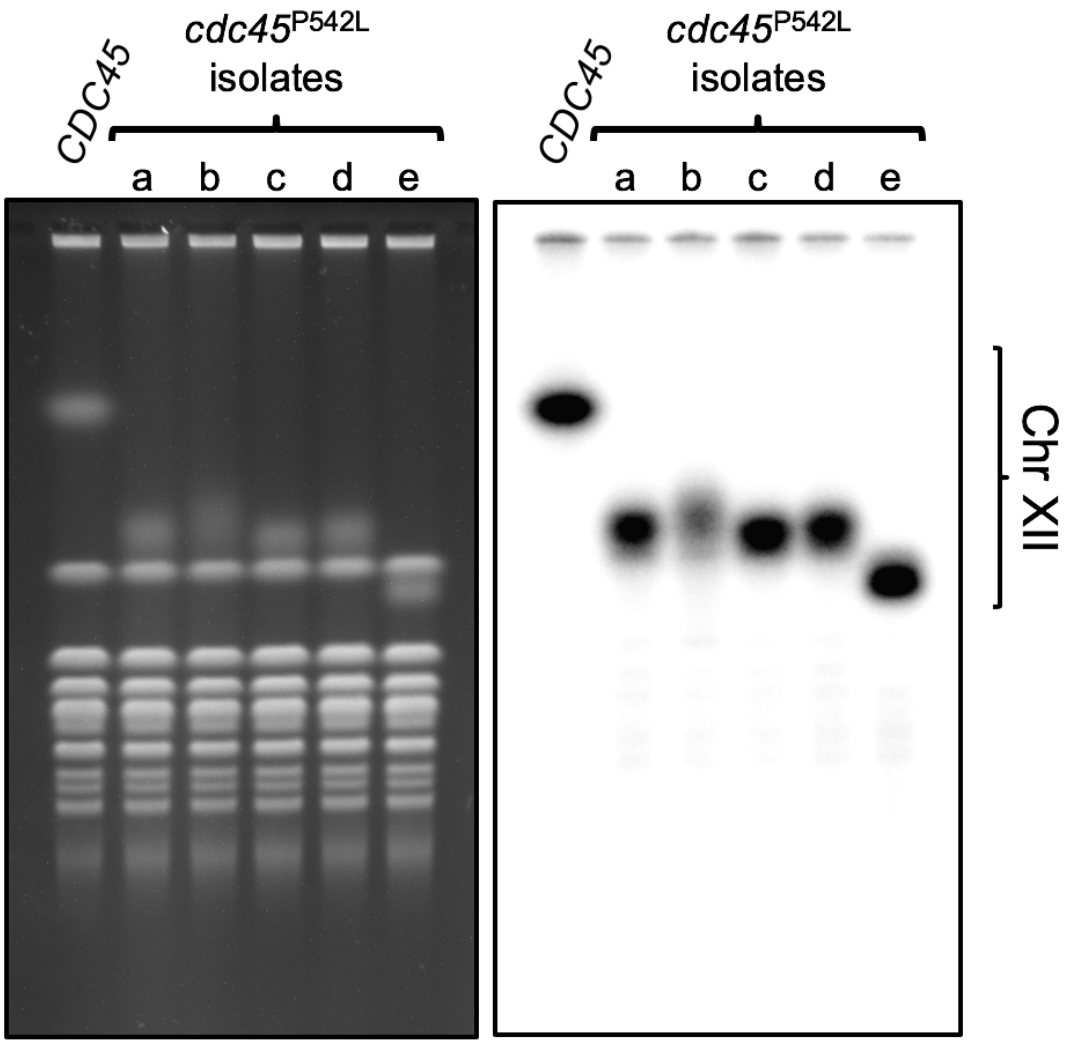

Figure 3.9: CHEF gel analysis of variation in rDNA copy number of five isolates (a-e) of *cdc45*^{P542L}.
Left, ethidium bromide stained image; right, Southern blot hybridization for Chr XII. All five isolates had a smaller Chr XII than *CDC45* due to loss of rDNA repeats.

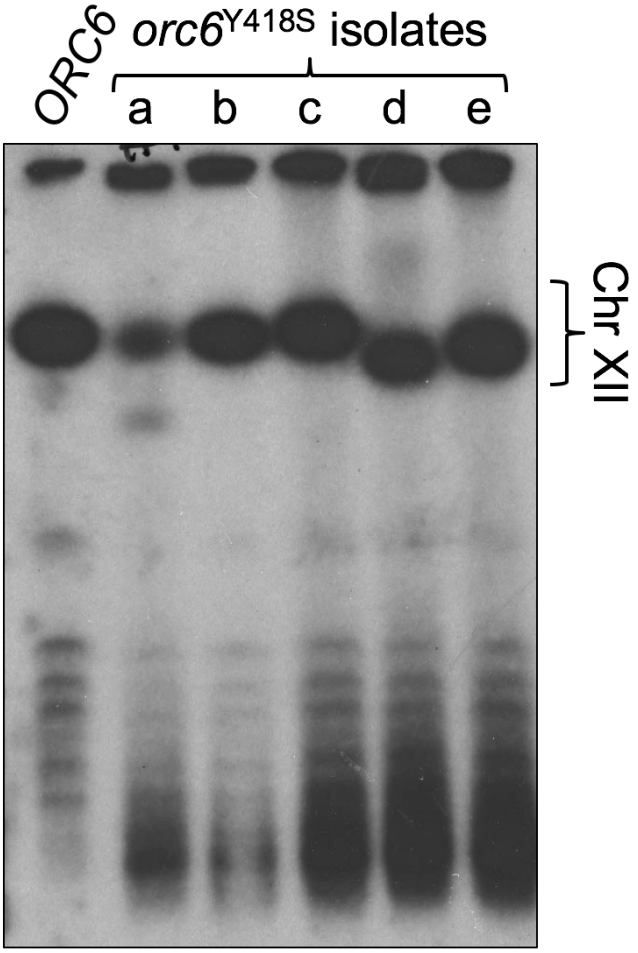

Figure 3.10: CHEF gel analysis of variation in rDNA copy number of five isolates (a-e) of *orc6*^{Y418S}.
Southern blot hybridization for Chr XII. All five *orc6*^{Y418S} isolates had a similar size Chr XII as *ORC6.*

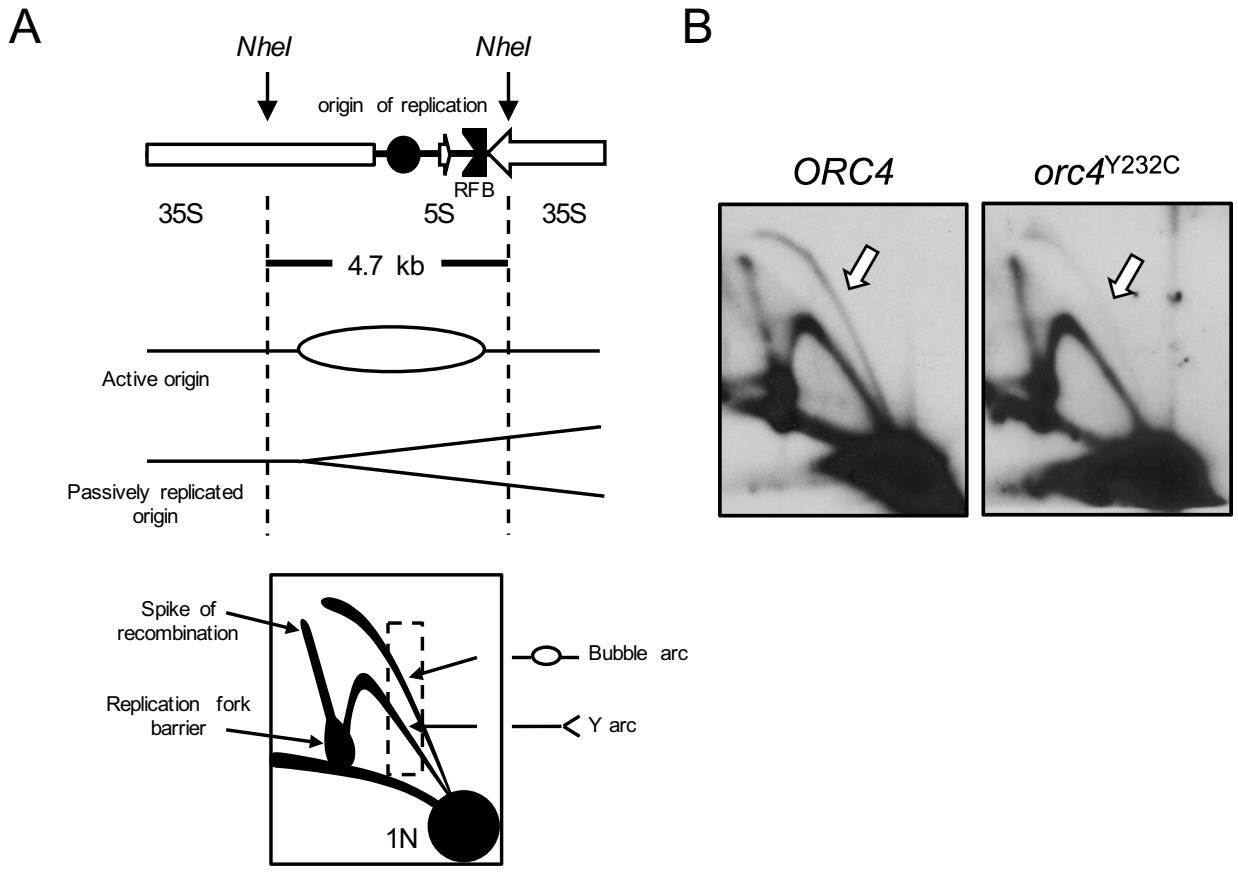

Figure 3.11: Origin initiation at the rDNA locus is reduced in orc4^{Y232C} cells
(A) (Top) Organization and *NheI* restriction map of a yeast rDNA repeat. Shown are the rDNA origin of replication (*rARS*) and replication fork barrier (RFB) located in the intergenic space between the 5S and 37S genes (white arrows). Replication intermediates present in the 4.7 kb *NheI* fragment are resolved using 2D-gel electrophoresis. (Bottom) Cartoon image of a 2D-gel illustrating how different replication intermediates are resolved. Relative origin efficiency is obtained by comparing intensities of replication intermediates with similar mass (dashed-line box). **(B)** Origin activity is reduced at the rDNA locus in *orc4*^{Y232C} cells. The 4.7 kb *NheI* fragment was excised from rDNA repeats from logarithmically growing cells and examined by 2D-gel electrophoresis. The Southern blot was probed for sequences specific to *rARS*. Bubble intermediates (white arrow) are reduced in *orc4*^{Y232C} cells compared to *ORC4* cells.

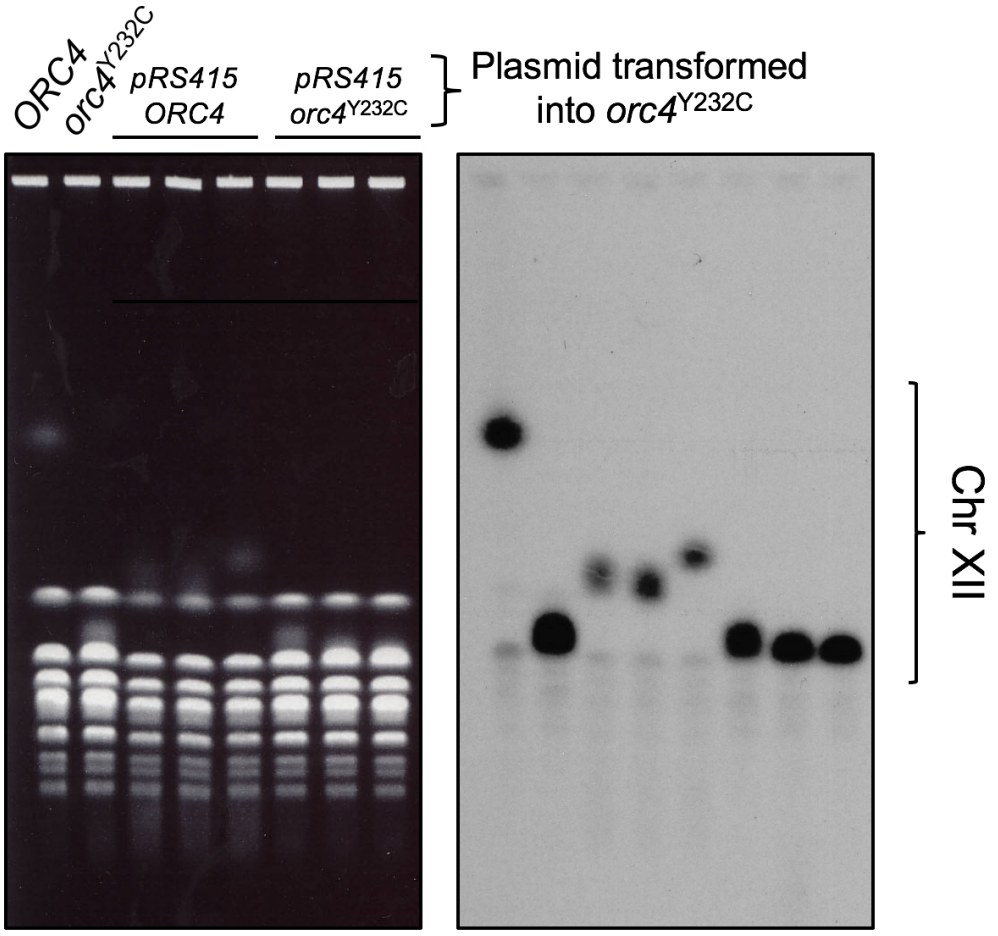

Figure 3.12: The *orc4*^{Y232C} rDNA copy number phenotype is not rescued by an additional copy of *orc4*^{Y232C}.
An isolate of *orc4*^{Y232C} with ~30 copies of rDNA (lane #2) was transformed with a centromere plasmid (*pRS415*) containing a copy of either *ORC4* or *orc4*^{Y232C}. rDNA copy number was analyzed in three isolates from each transformation. An increase in rDNA copy number was observed in cells transformed with the plasmid containing *ORC4*; however, no increase in rDNA copy number was observed in cells transformed with the plasmid containing *orc4*^{Y232C}.

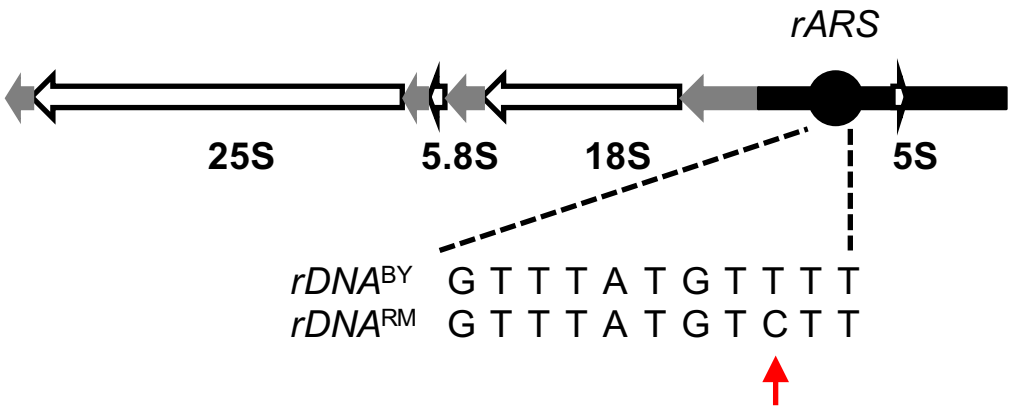

Figure 3.13: Sequence comparison of the ACS of BY4741 and RM11-1a rDNA origin, *rARS*.
Red arrow indicates the polymorphism in the ACS.

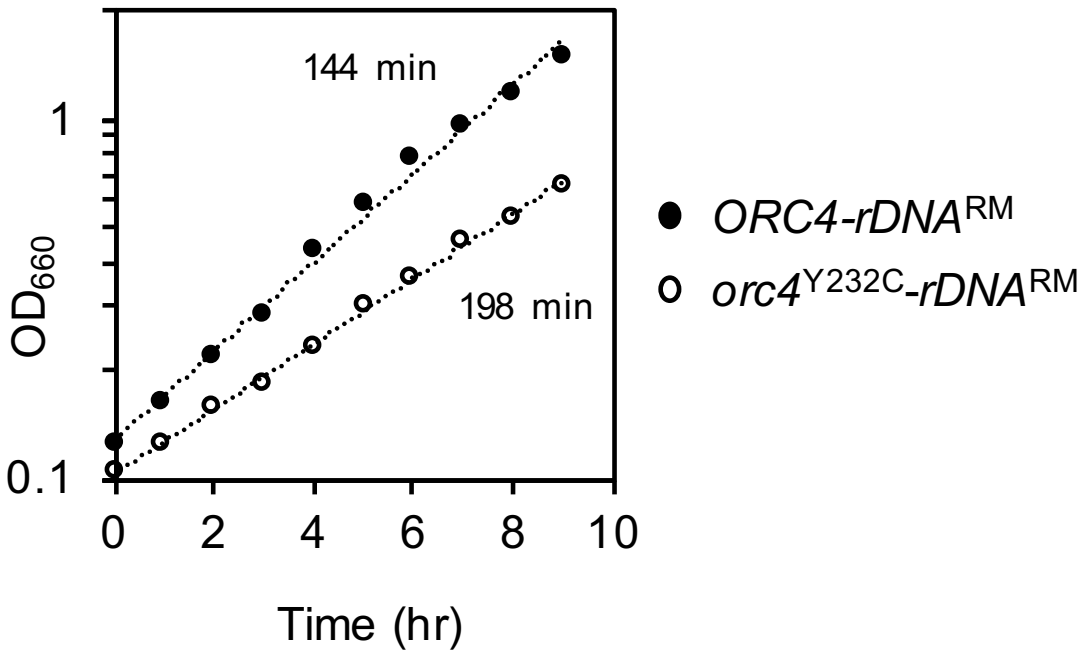

Figure 3.14: The slow growth phenotype is exacerbated in *orc4*^{Y232C}-*rDNA*^{RM} cells
Growth curves of *ORC4-rDNA*^{RM} and *orc4*^{Y232C}-*rDNA*^{RM} cells generated by measuring the optical density over time of mid-log cultures in synthetic complete medium at 30° C. The mutant (○) shows a substantial growth defect with a doubling-time 54 minutes (27%) longer than wild-type cells (●).

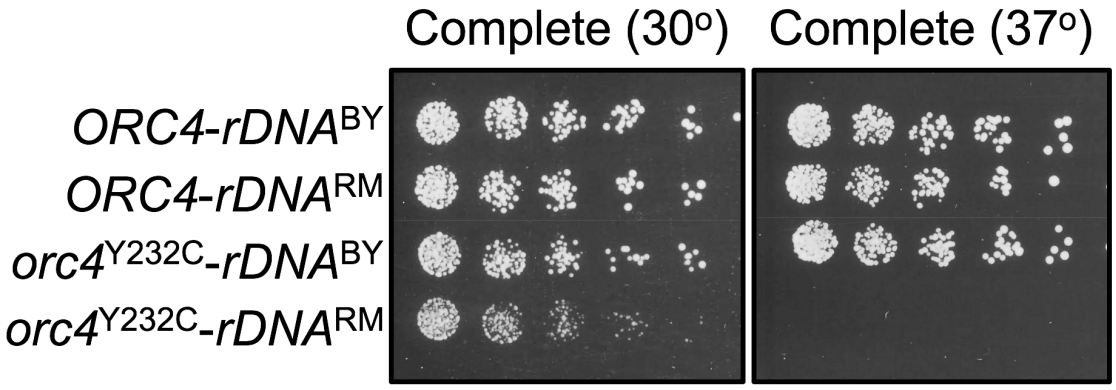

Figure 3.15: *orc4*^{Y232C}-*rDNA*^{RM} cells are unable to grow at 37° C.
Serial dilutions (1:3) of cells were plated on synthetic complete medium and incubated at either 30° or 37° C for 3 days.

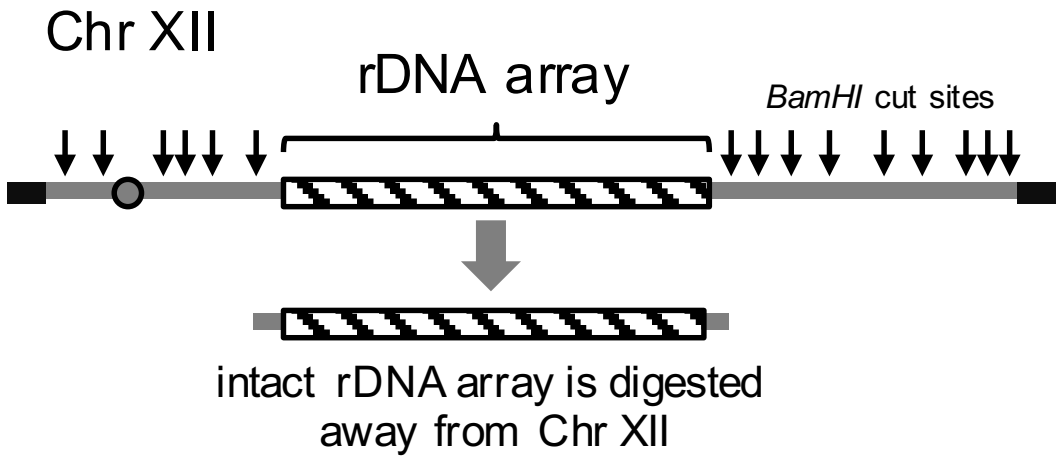

Figure 3.16: Outline of strategy used to release intact rDNA array from Chr XII by restriction enzyme digest with *BamHI*.
Several *BamHI* cut sites are present across the yeast genome except within the rDNA locus; therefore, digesting intact chromosomal DNA with *BamHI* releases the intact rDNA array away from the rest of Chr XII.

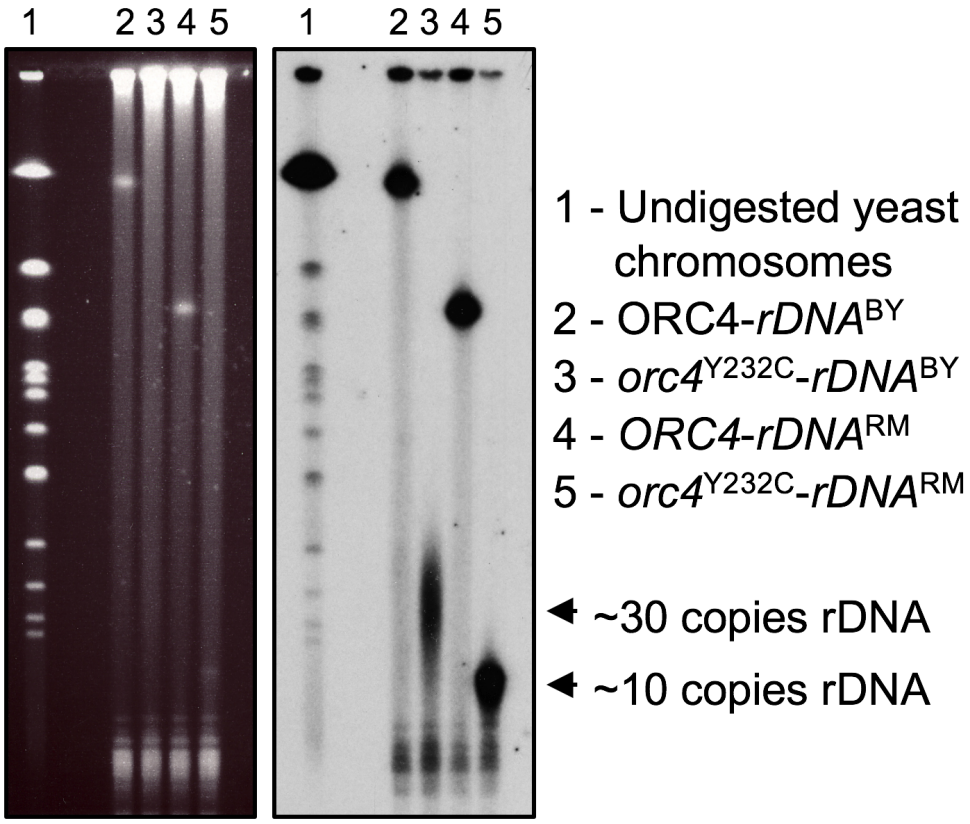

Figure 3.17: Only ~10 rDNA repeats remain in *orc4*^{Y232C}-*rDNA*^{RM} cells.
CHEF gel electrophoresis of whole yeast chromosomes digested with *BamHI* (ethidium bromide stained image on left, Southern hybridization on right). The Southern blot was probed with a single copy sequence that is within the *BamHI* rDNA fragment and adjacent to the rDNA array. The migration of this fragment relative to undigested yeast chromosomes as size standards shows that *orc4*^{Y232C}-*rDNA*^{RM} cells (lane 5) have ~10 copies of rDNA.

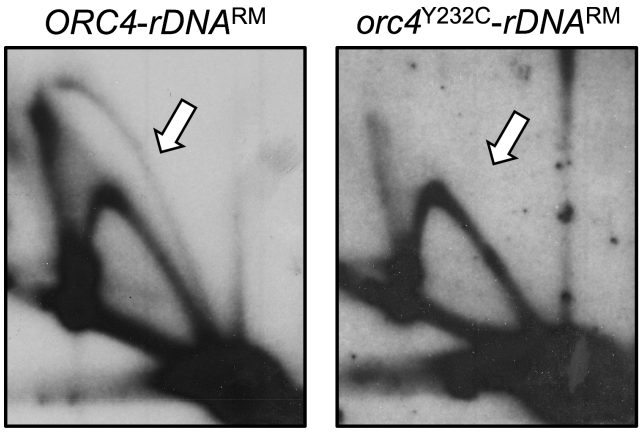

Figure 3.18: Origin activity is not detectable at the rDNA locus in *orc4*^{Y232C}-*rDNA*^{RM} cells.
Bubble intermediates (white arrow) are not detectable at the rDNA locus in *orc4*^{Y232C}-*rDNA*^{RM} cells. The 4.7 kb *NheI* fragment was excised from rDNA repeats from logarithmically growing cells and examined by 2D-gel electrophoresis. Subsequently, the Southern blot was probed for sequence specific to the *rARS*.

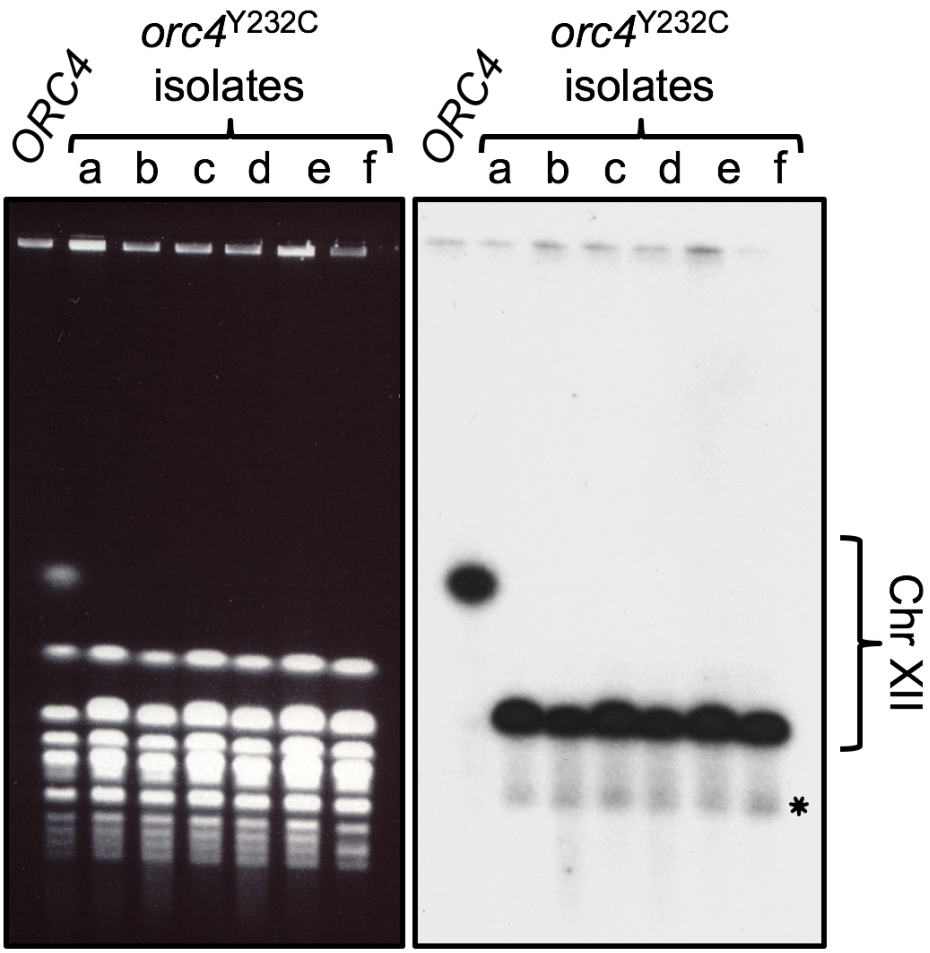

Figure 3.19: CHEF gel analysis of variation in rDNA copy number in six additional isolates (a-f) of *orc4*^{Y232C}- *rDNA*^{RM}.
Left, ethidium bromide stained image; right, Southern blot hybridization for Chr XII. Samples were prepared after ~20 generations of growth following introduction of the *orc4*^{Y232C} mutation. The rDNA copy number is estimated to be ~10 copies in all six isolates.

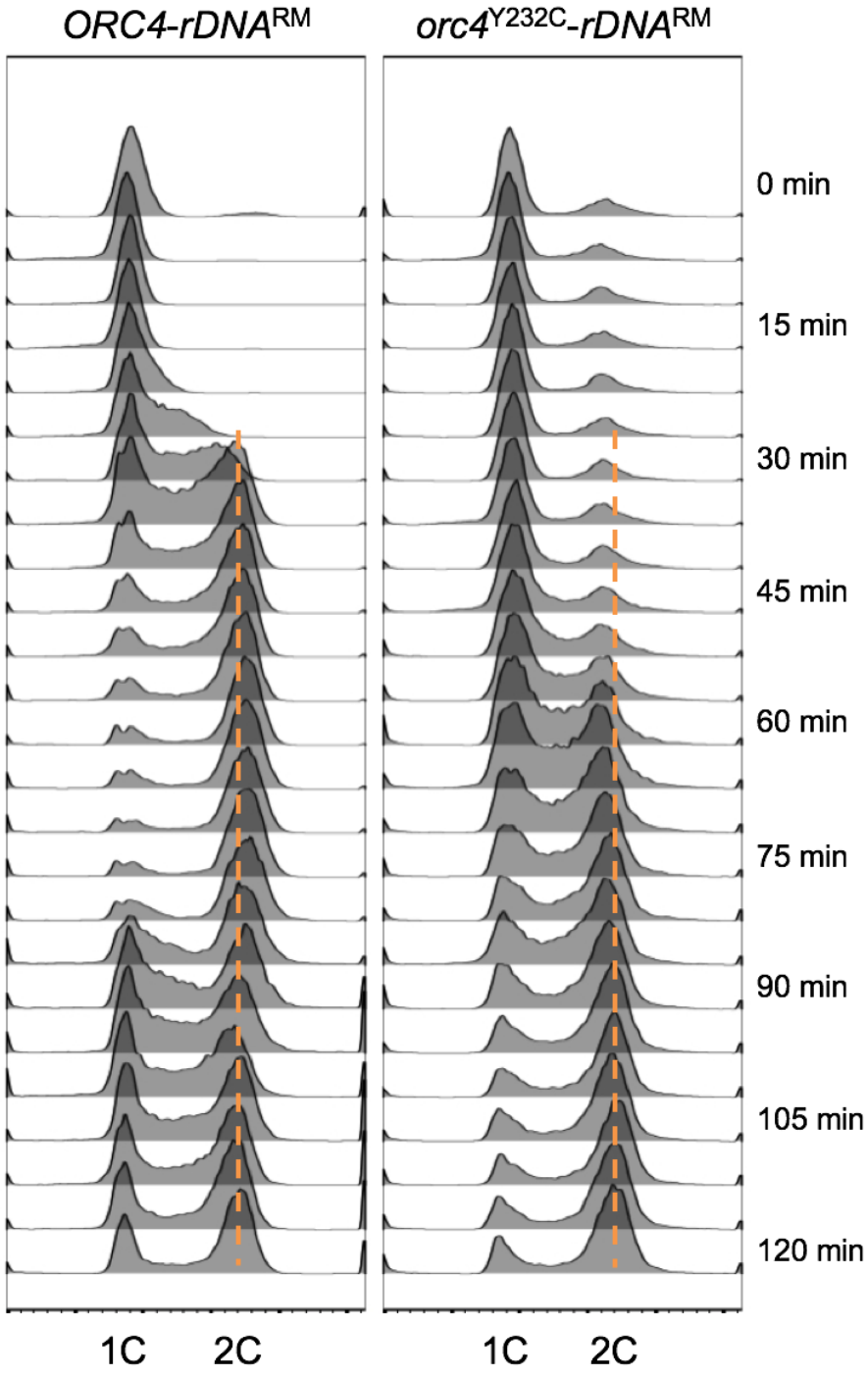

Figure 3.20: Cell-cycle defects are exacerbated in *orc4*^{Y232C}- *rDNA*^{RM} cells.
S phase progression of *ORC4-rDNA*^{RM} (left) and *orc4*^{Y232C}-*rDNA*^{RM} (right) cells measured by flow cytometry. Cells were synchronously released into S phase and samples were collected at 5-minute intervals. *ORC4-rDNA*^{RM} cells enter S phase ~20 minutes after release from alpha factor, whereas *orc4*^{Y232C}-*rDNA*^{RM} cells do not enter S phase until ~40 minutes after release. Additionally, by 85-minutes *ORC4-rDNA*^{RM} cells are cycling back to begin a new cell cycle, whereas *orc4*^{Y232C}-*rDNA*^{RM} cells have not yet completed cell division. The orange dotted line indicates the expected DNA content for cells that have completed replication.

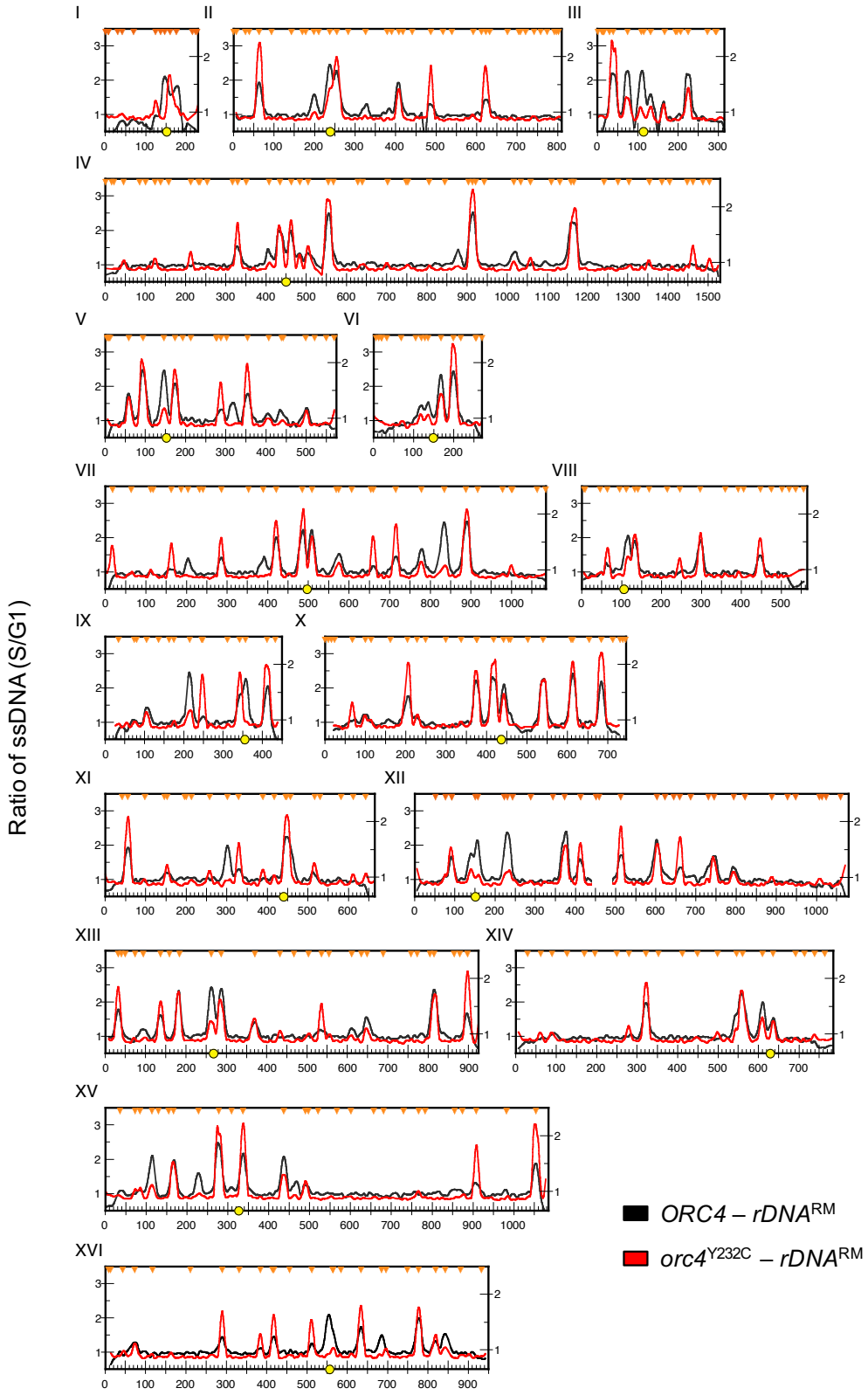
I
II
III
IV
V
VI
VII
VIII
IX
X
XI
XII
XIII
XIV
XV
XVI
Ratio of ssDNA (S/G1)
Chromosome Coordinate (kb)
ORC4 – rDNA^RM
orc4^Y232C – rDNA^RM

Figure 3.21: Comparison of ssDNA profiles for *ORC4-rDNA*^{RM} and *orc4*^{Y232C}*-rDNA*^{RM} chromosomes.
Genome wide ssDNA profiles for *ORC4-rDNA*^{RM} (black) and *orc4*^{Y232C}*-rDNA*^{RM} (red) are shown for cells after exposure to HU for 30 min. The relative ratio of ssDNA (S/G1) is plotted against chromosome coordinates (kb). A yellow circle denotes centromere locations and the positions of verified origins of replication are marked by orange triangles. The rDNA locus and adjacent flanking sequence on Chr XII (cf. 440-490 kb) were omitted due to insufficient probe coverage on the microarray slide.

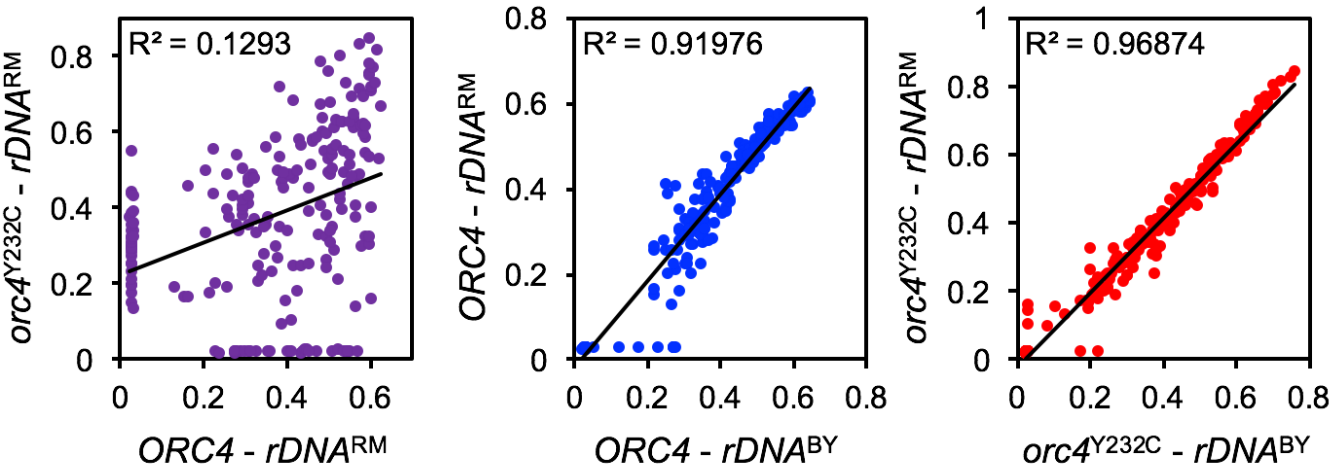

Figure 3.22: Pairwise comparisons of the relative area under the peak at each origin measured in ssDNA profiles.
The relative areas under the peaks for the four strains (*ORC4-rDNA*^{BY}, *ORC4-rDNA*^{RM}, *orc4*^{Y232C}*-rDNA*^{BY}, and *orc4*^{Y232C}*-rDNA*^{RM}) were measured and pair-wise comparisons of those values at each origin between the different strains are shown in the three scatter plots.

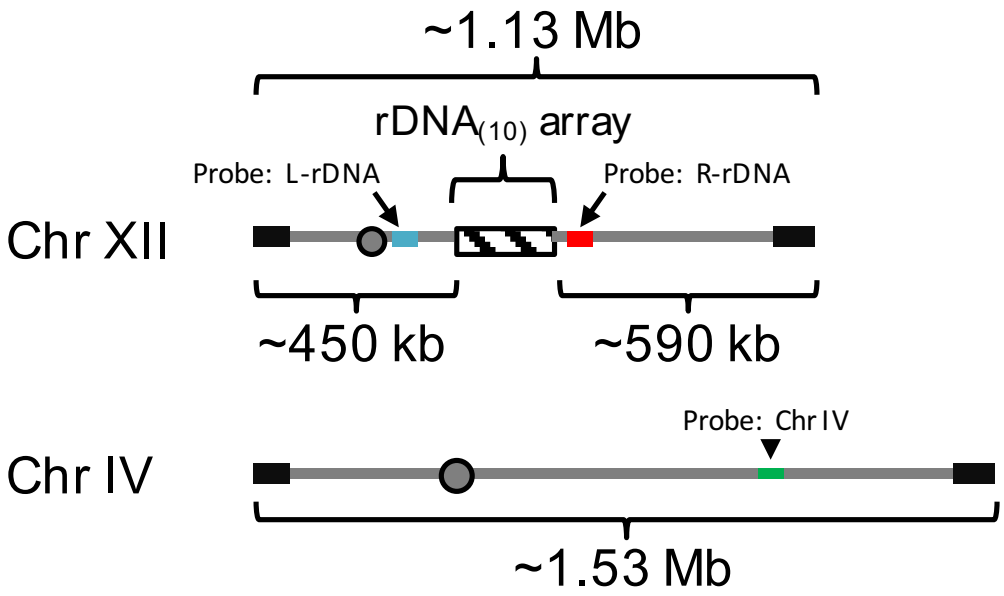

Figure 3.23: Cartoon illustration of Chr XII (containing 10 copies of rDNA ($rDNA_{10}$)) and Chr IV. Colored boxes represent the locations of different probes used in the following panel (H). The red box corresponds to a probe specific for a single copy sequence to the right of the rDNA locus (R-rDNA) and the cyan box corresponds to a single copy sequence to the left of the rDNA (L-rDNA). The green box represents a single copy sequence located on Chr IV.

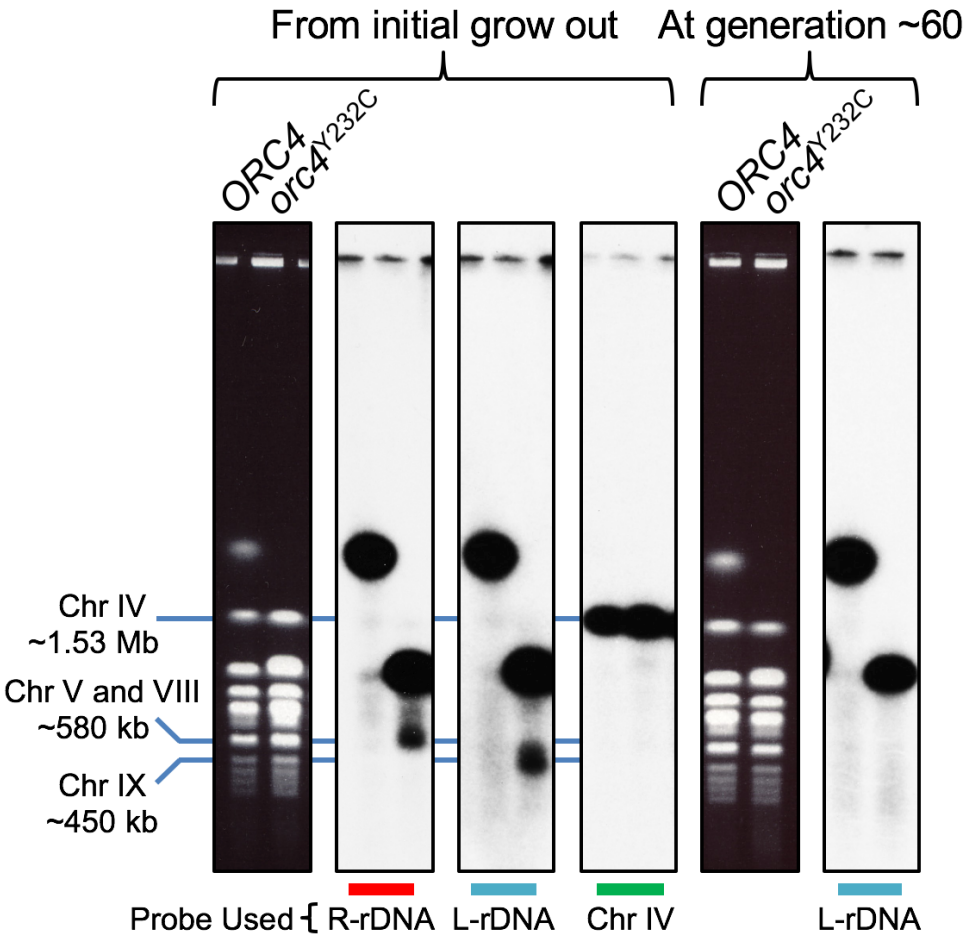

Figure 3.24: Chromosome breakage is specific to Chr XII in *orc4*^{Y232C}-*rDNA*^{RM} cells. "From initial grow out": Samples prepared after ~20 generations of growth following introduction of the *orc4*^{Y232C} mutation. Different images of the same CHEF gel are shown (ethidium bromide stain on the left and three images of the same Southern blot hybridized with different probes on the right). The blue lines mark various chromosomes and their approximate sizes: Chr IV is ~1.53 Mb and Chr IX is ~450 kb. Under these electrophoresis conditions, chromosomes V and VIII migrate closely together at a size of ~580 kb. The Southern blot image on the left was probed for a single copy sequence specific to the right of the rDNA locus (R-rDNA). Note the minor band (running at ~580 kb, below the major Chr XII band) in the *orc4*^{Y232C}-*rDNA*^{RM} sample. The middle Southern blot image was probed for a different single copy sequence specific to Chr XII left of the rDNA locus (L-rDNA). Note the shift of the minor band in the *orc4*^{Y232C}-*rDNA*^{RM} sample to a size of ~450 kb. The Southern blot image on the right was probed for a single copy sequence specific to Chr IV. "After generation ~60": The same strain was growth for an additional ~40 generations and samples were analyzed by CHEF gel electrophoresis. Left panel, image of ethidium bromide-stained gel; right panel, Southern blot probed with L-rDNA

Chapter 4

The severe loss of rDNA repeats in *orc4*^{Y232C} cells leads to a reduction in ribosome production and translational capacity

4.1: Introduction

The combination of the *orc4*^{Y232C} mutation and the *rDNA*^{RM} locus reduces the growth rate of cells further compared to that of the *orc4*^{Y232C} *rDNA*^{BY} strain. While reducing the size of the rDNA array could permit completion of genome replication, it may come at a cost—namely, in the ability to make enough ribosomes to support robust growth. Just what is the lower limit of rDNA repeat number a yeast cell can tolerate and still support a normal ribosome population? When the rDNA copy number in yeast is artificially reduced to ~40 copies there are no obvious negative effects on growth rate and the cells increase the density of Pol I RNA polymerases per rDNA repeat to produce levels of rRNA similar to cells with ~150 copies of rDNA (French et al. 2003). However, only a finite number of polymerases can be loaded onto a single rDNA repeat before space becomes limited. Based on the estimates of Pol I density and polymerization rates, yeast cells with ~30 copies of rDNA fall just short of being capable of producing levels of rRNA needed to support a normal growth rate (French et al. 2003). By these calculations, *orc4*^{Y232C} cells with only ~10 copies of *rDNA*^{RM} should be further compromised in their ability to make rRNA.

Therefore, I next tested my hypothesis that in addition to replication defects, the slow growth and prolonged G1 phase observed in *orc4*^{Y232C} strains is due to an inability to meet the demand for ribosome production.

4.2: Results

The further loss of rDNA repeats in orc4^{Y232C}-rDNA^{RM} cells leads to reduction in ribosome production and translational capacity.

Early in this study, when I was beginning to examine whether a reduction in rDNA copy number might affect ribosome production, I thought that sucrose gradients of yeast extracts would be the best way to quantify ribosomal subunits and polysomes. I performed the following experiment in yeast cells from a different strain background (BB14-3a) than what I used for experiments in the rest of this dissertation. Though performed in a different strain background, *orc4*^{Y232C} cells in the BB14-3a strain background also suffer from a loss of rDNA repeats (data not shown). I ran sucrose gradients on cell extracts from exponentially growing cells to test if *orc4*^{Y232C} cells have a decrease in ribosomal subunits, monosomes, or ploysomes (Fig 4.1). I observed prominent peaks for all the different ribosomal components for the polysome profiles from *ORC4* cells. In contrast, the polysome profile for *orc4*^{Y232C} isolate (a) were depressed, whereas the polysome profile for *orc4*^{Y232C} isolate (b) looked like those of *ORC4* cells (Fig 4.1). To determine if variation in rDNA copy number could explain the discrepancy between the two different *orc4*^{Y232C} profiles, I performed quantitative real-time PCR on the same cell extracts used to generate the polysome profiles. Performing quantitative real-time PCR revealed that *orc4*^{Y232C}

isolates (a) and (b) had ~13 and ~17 copies of rDNA, respectively. Though other factors may be responsible for the difference in profiles, it is intriguing that the isolate with fewer rDNA repeats had the polysome profile with depressed peaks, possibly indicating a ribosome deficit. While polysome profiles do provide valuable information regarding the relative abundance of ribosomal subunits to one another and polysomes in the gradient, I realized that I could not use polysome profiles to make clear conclusions about ribosomal content per cell for the following reason. When loading sucrose gradients, it is standard practice to control loading of the gradients according to total protein content. However, if MGS cells were in fact suffering from a ribosome deficiency, protein levels per cell could also be affected, thereby compromising the loading controls and possibly leading me to misinterpret the data from the polysome profiles. Realizing that polysome profiles may not provide the information regarding ribosomes per cell, I sought to find other assays that would more directly measure ribosome components per cell.

To test whether *orc4*^{Y232C} cells with a reduced rDNA copy number also have decreased levels of rRNA, I separated the total nucleic acid content from cells by gel electrophoresis (Fig 4.2) and then independently transferred to hybridization membrane the two different parts of the gel containing either genomic DNA (Southern blot) or rRNA (northern blot). I found that both *orc4*^{Y232C} mutants with a reduced rDNA copy number showed a reduction in 25S rRNA levels compared to their respective wild type counterparts (Fig 4.3). However, *orc4*^{Y232C} *rDNA*^{RM} cells were more severely affected, being able to make only approximately half as much 25S rRNA as wild type cells. Considering the drastic reduction of rRNA in *orc4*^{Y232C} *rDNA*^{RM} cells, I wanted to assess the ribosome number per cell independently of measuring rRNA.

Since the per-cell fluorescence output of GFP is directly proportional to its concentration in living cells (Lo et al. 2015), I reasoned that I could determine the relative abundance of ribosomes per cell by GFP labeling a ribosomal protein and then measuring the cells' relative fluorescence using flow cytometry. Ribosomal protein levels are tightly regulated, with excess proteins being targeted for rapid destruction (Sung et al. 2016), so the abundance of ribosomal proteins is a good proxy for the abundance of ribosomes. I constructed strains of the wild type *ORC4* and *orc4*^{Y232C} mutant in the *rDNA*^{BY} and *rDNA*^{RM} backgrounds harboring a GFP-tagged version of the single-copy ribosomal protein Rpl10 (Rpl10-GFP) and measured their relative fluorescence during exponential growth by flow cytometry. The histogram of *orc4*^{Y232C} *rDNA*^{RM} cells is shifted to the left (a decrease of nearly one log) compared to wild type (Fig 4.4). To determine if the shift were statistically significant, I recorded the fluorescence value for each of the 20,000 events recorded for each sample and performed a Wilcoxon Rank-Sum Test. The decrease in fluorescence I observed in *orc4*^{Y232C} *rDNA*^{RM} cells is statistically significant (p-value < 2.2e-16). I therefore conclude that there are fewer Rpl10-GFP molecules per cell in the *orc4*^{Y232C} *rDNA*^{RM} strain compared to wild type. The same decrease in fluorescence was not observed in *orc4*^{Y232C} *rDNA*^{BY} cells (Fig 4.5), consistent with the relatively modest reduction of 25S rRNA measured in this strain (Fig 4.3).

To investigate whether the ribosome deficiency in *orc4*^{Y232C} *rDNA*^{RM} cells might negatively impact their translation capacity, I tested their ability to grow in the presence of a low concentration of the translation inhibiting drug cycloheximide that is tolerated by wild type *ORC4* cells. I observed that *orc4*^{Y232C} *rDNA*^{RM} cells could form colonies on the plate without cycloheximide; however, their growth was severely inhibited on the plate

containing the drug (Fig 4.6). This observation supports the notion that the slower growth of *orc4*^{Y232C} *rDNA*^{RM} cells and their delay in G1 is due to a lower translation capacity, rooted in their inability to make sufficient numbers of ribosomes.

4.3: Discussion

ORC is known to play important roles in cellular processes other than DNA replication; however, its role in maintaining a healthy ribosome population has yet to be characterized. Here I show that properly functioning ORC is necessary for maintaining adequate ribosome levels through its role in rDNA replication. But when the function of Orc4 is compromised, leading to a loss of rDNA repeats and the capacity to make rRNA, how might a ribosome deficiency cause slow growth in cells? The obvious answer would be that cells cannot meet the demand for protein production—but how might certain processes such as translation and protein degradation be affected? Does the translation of certain housekeeping mRNAs take priority over non-essential ones or do cells manage to deal with a ribosome deficit by speeding up the rate of translation of all mRNAs equally? Ribosome profiling experiments to identify and quantify the mRNAs that are being actively translated by ribosomes will prove helpful in addressing these questions (Brar and Weissman 2015). Additionally, if cells are struggling to keep up with the protein synthesis demands, it is possible that they modulate their protein turnover rates in response. Coupling mass spectrometry based proteomics with metabolic pulse-labeling or cycloheximide treatment of cells will help shed light on the rate of protein turnover and the

general state of the proteome in cells with a ribosome deficiency (Larance and Lamond 2015).

Is Meier-Gorlin Syndrome a form of ribosomopathy? Meier-Gorlin syndrome phenotypes include a number of skeletal defects that have similarities to other, better-understood syndromes, all associated with deficiencies in ribosome biogenesis (Trainor and Merrill 2014). For example, Treacher Collins syndrome (TCS) can be caused by one of three different genetic mutations that are likely to affect ribosome production. One of the TCS mutations is in *TCOF1*, a gene that encodes a protein called Treacle that plays dual roles in the transcription and processing of 28S rRNA. The other two genes, *POLR1C* and *POLR1D*, are subunits of RNA Polymerases I and III. Work with mouse models of this syndrome suggest that ribosome deficiencies are reducing the migration of neural crest cells that are essential for proper craniofacial development. Whether derived from neural crest cells or mesenchymal cells, chondrocytes also have a high demand for ribosomes as they divide, enlarge and produce collagen and other bone-matrix proteins. In addition to TCS, Postaxial Acrofacial Dystosis (POADS), Diamond Blackfan Anemia (DBA), Roberts Syndrome (RBS), Schwackman Diamond Syndrome (SDS), and Cartilage-Hair Hyploplasia (CHH) are distinct ribosomopathies with a common set of skeletal malformations (Trainor and Merrill 2014). Their genetic mutations affect ribosome production in different ways—a mutation that reduces uracil biosynthesis (POADS), mutations in individual ribosomal protein genes (DBA), a mutation in a gene for cohesion (*ESCO2*) that in yeast (*ECO1*) reduces 18S and 28S production (RBS), a mutation in *SBDS* (yeast *SDO1*) that reduces maturation of the 60S ribosomal subunit (SDS), and a mutation in RMPR, the RNA component of RNase MRP, a snoRNA involved in rRNA processing (CHH). Perhaps Meier-

Gorlin syndrome is just the newest member of this interesting set of syndromes that result from a deficiency in ribosome biogenesis—in this case, from a replication defect that reduces the number of templates for rRNA transcription.

4.4: Materials and Methods

Quantitative hybrid Southern/Northern blotting

The relative abundance of 25S ribosomal RNA was measured by quantitative hybrid Southern/Northern blotting. The total nucleic acid content of cells was extracted using a version of the "Smash-and-grab" DNA isolation protocol (Hoffman and Winston 1987) with the modification that cell walls were enzymatically disrupted using Zymolyase® - 20T (Amsbio) instead of glass beads. Nucleic acids were resuspended in TE pH 8 and then separated by electrophoresis in a 1.5% LE agarose gel with ethidium bromide (0.3 μg/ml). After the ribosomal RNA was separated away from genomic DNA, the gel was photographed and then cut to separate the two portions containing genomic DNA and rRNA. Subsequently, the two different portions of the gel were blotted following standard Southern (genomic DNA) and northern (rRNA) blotting protocols. The Southern blot was probed for *ACT1* as a single copy control and the northern blot was probed for *25S rRNA* sequence. Because the amount of rRNA on the blot could be in excess of the probe, hybridization of the northern blot was limited to 2 hours to ensure that the hybridization signal was proportional to the amount of target sequence. The hybridization signals were

analyzed using a Bio-Rad Personal Molecular Imager and Quantity One software. The *25S rRNA* hybridization signal was first normalized to *ACT1* and then relative to wild type.

Flow cytometry analysis for cells expressing GFP tagged Rpl10

The GFP fluorescence of living cells was measured using flow cytometry. Strains were grown overnight in synthetic complete medium at 30° C. Fresh cultures were made by diluting these overnight cultures back to a starting OD_{660} of ~0.05. When cultures reached an OD_{660} of ~0.6, cells were diluted and sonicated, then analyzed directly using a BD Accuri C6 flow cytometer. Flow cytometry data was exported and analyzed using FloJo software.

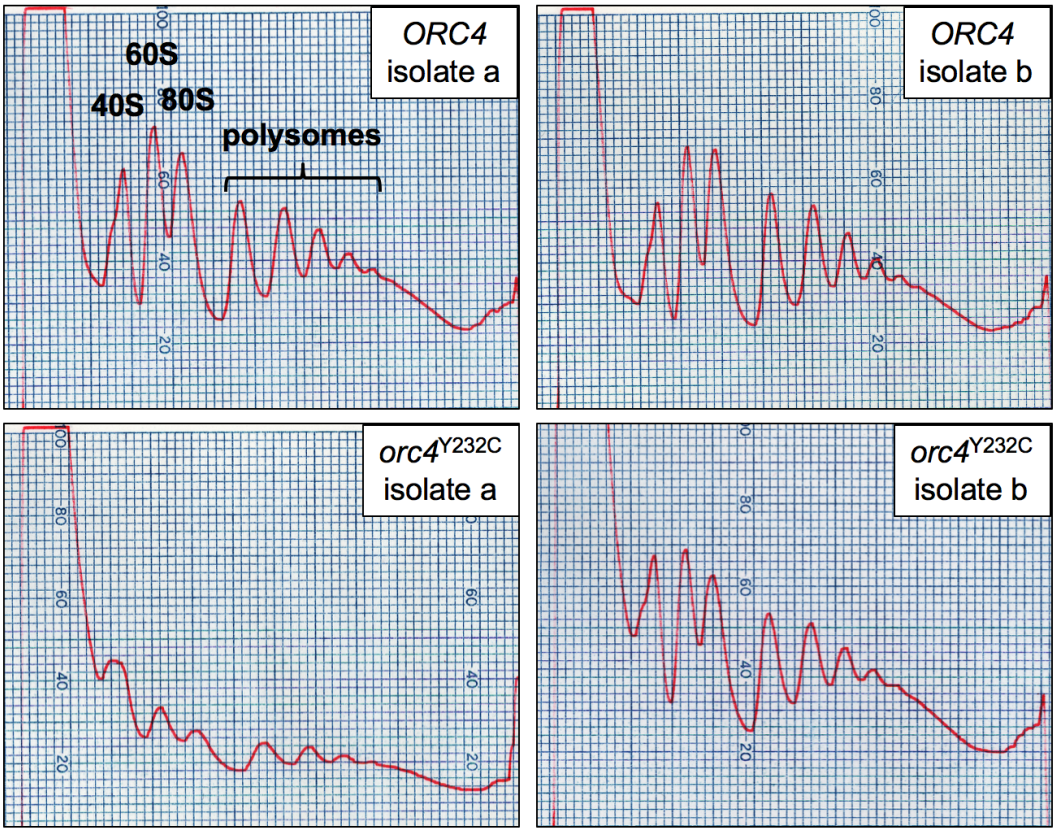

Figure 4.1: Polysome profiles from *ORC4* and *orc4*^{Y232C} yeast cells.
40S, 60S, and 80S denote the corresponding ribosomal subunits and monosome, respectively.

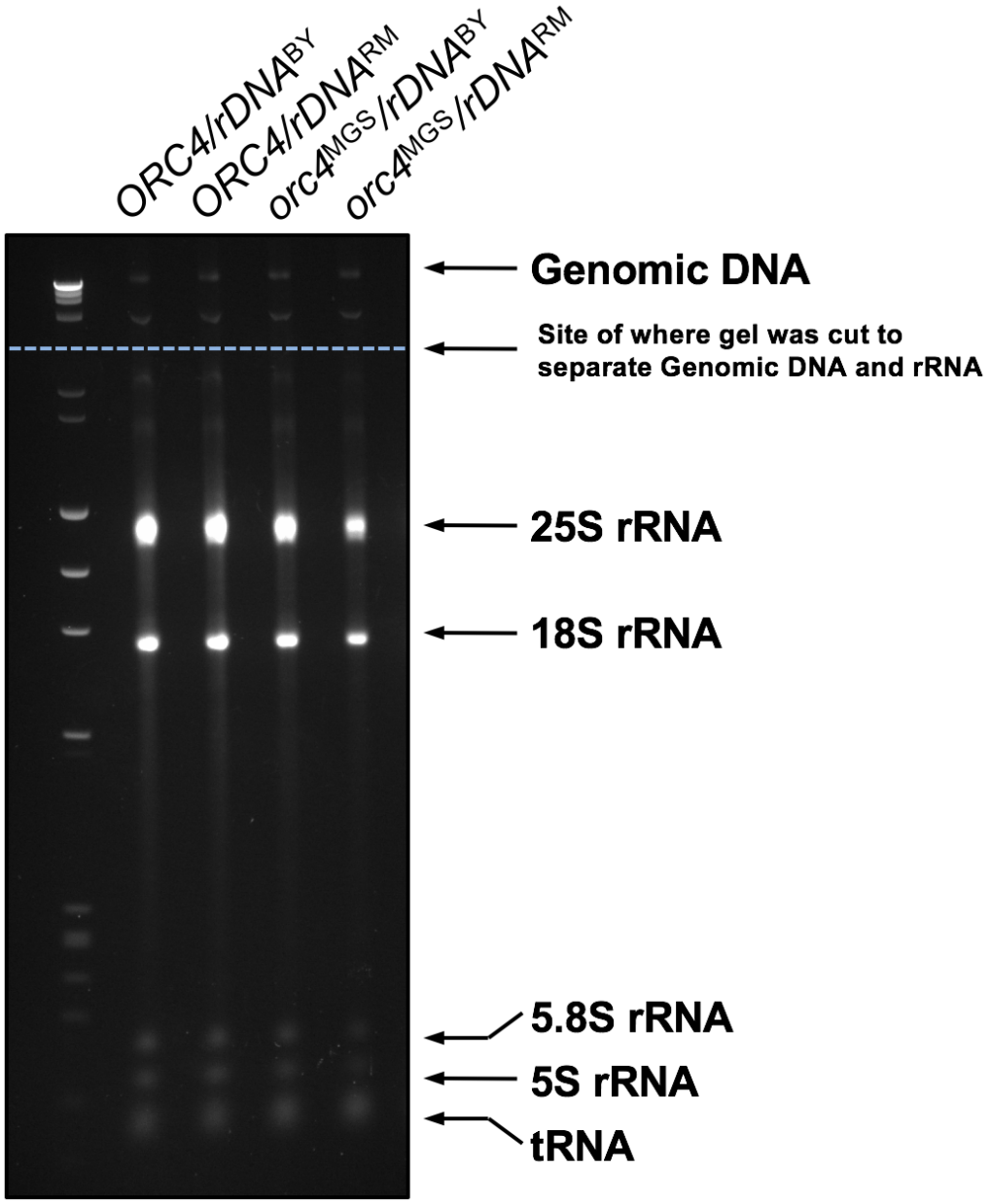

Figure 4.2: The total nucleic acid content of cells is resolved by gel electrophoresis. An ethidium bromide stained gel image of the total nucleic acid content from exponentially growing cells separated by electrophoresis. The blue dashed line indicates where the gel was cut so that the two different parts of the gel containing either genomic DNA or rRNA could be separately treated for Southern or northern transfer to hybridization membranes. The hybridization images and quantifications are shown in Fig 4.2.

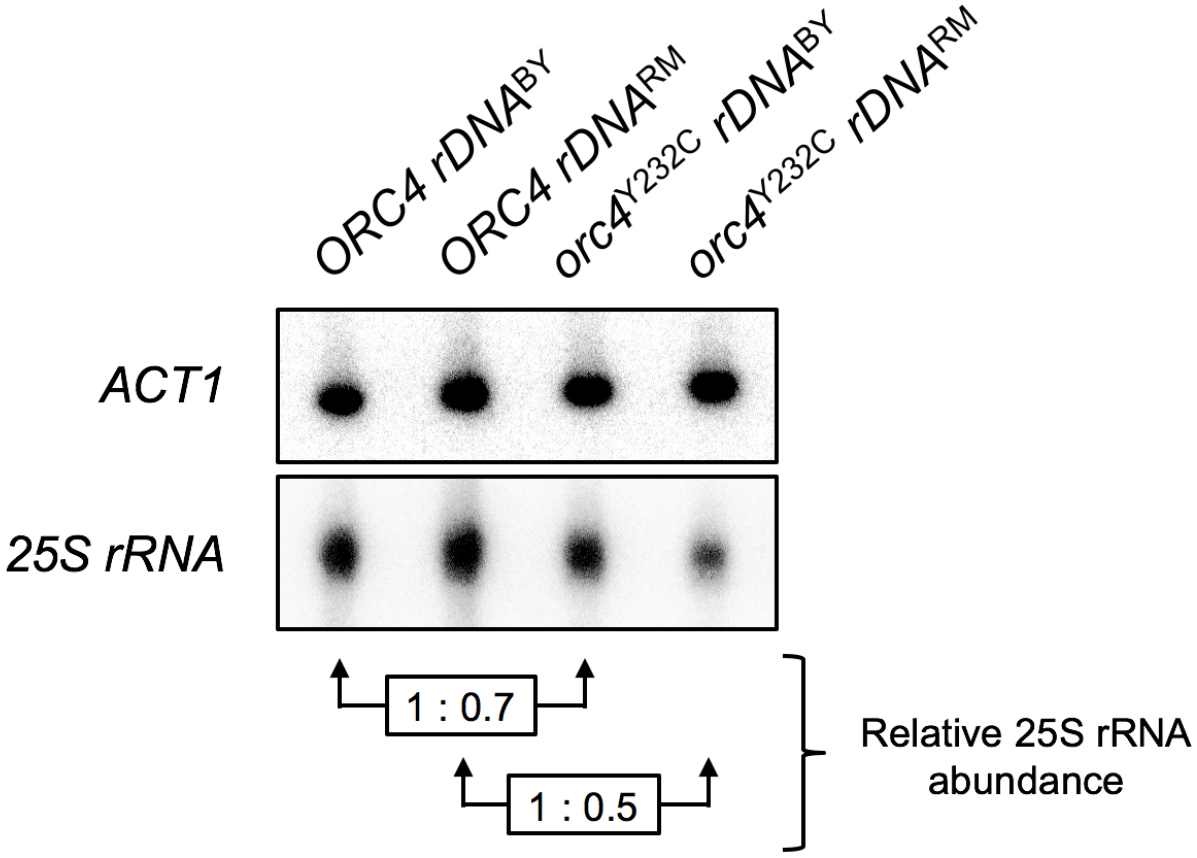

Figure 4.3: Quantitative hybrid Southern/Northern blot analysis of ribosomal RNA. Total nucleic acids (DNA+RNA) from the four strains were separated by gel electrophoresis. The top portion of the gel, containing high-molecular weight DNA, was blotted as a Southern blot and probed with *ACT1* sequence (as a single copy control). The lower portion of the gel was blotted as a Northern blot and probed with *25S rRNA* sequence to measure rRNA abundance. Values representing the relative abundance of 25S rRNA in the *orc4*^{Y232C} strains were calculated by first normalizing hybridization signals of *25S rRNA* to *ACT1* in each mutant strain and then relative to its respective wild type parent.

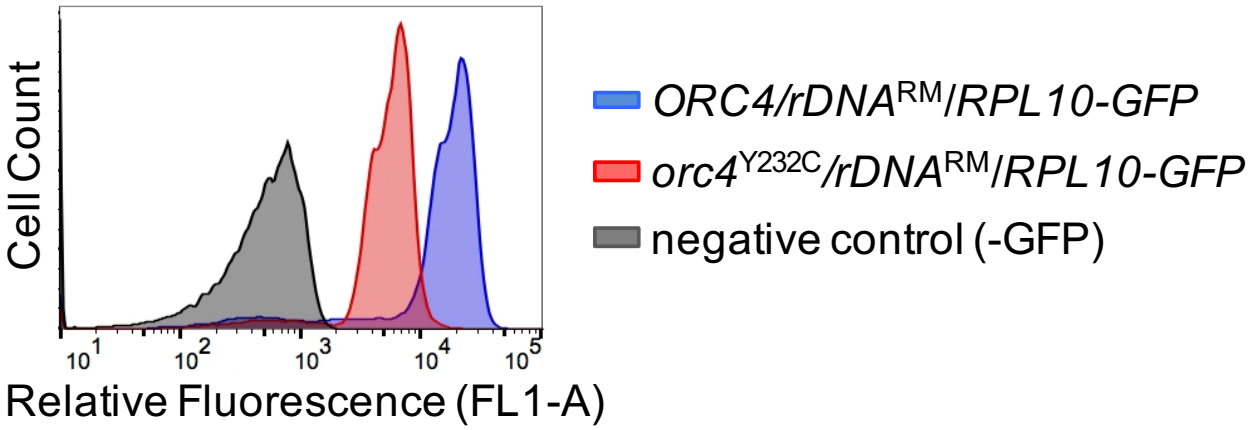

Figure 4.4: Relative fluorescence of *ORC4-rDNA*^{RM} and *orc4*^{Y232C}*-rDNA*^{RM} harboring Rpl10-GFP.
Relative fluorescence of *ORC4-rDNA*^{RM} (blue) and *orc4*^{Y232C}*-rDNA*^{RM} (red) cells harboring a GFP tagged version of the single-copy ribosomal protein Rpl10. Cells were grown to mid-log phase and relative fluorescence was measured by flow cytometry.

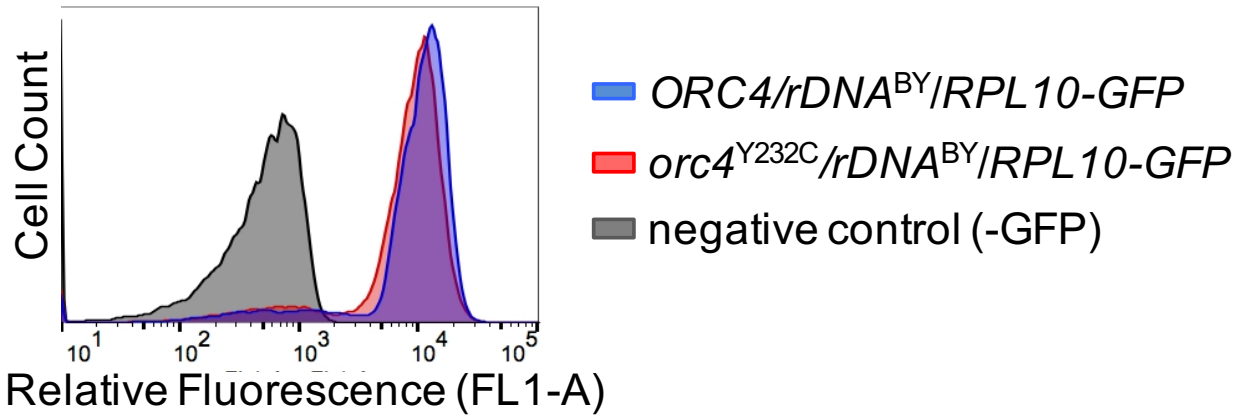

Figure 4.5: Relative fluorescence of *ORC4-rDNA*^{BY} and *orc4*^{Y232C}*-rDNA*^{BY} harboring Rpl10-GFP.
Relative fluorescence of *ORC4-rDNA*^{BY} (blue) and *orc4*^{Y232C}*-rDNA*^{BY} (red) cells harboring a GFP tagged version of the single-copy ribosomal protein Rpl10. Cells were grown to mid-log phase and relative fluorescence was measured by flow cytometry.

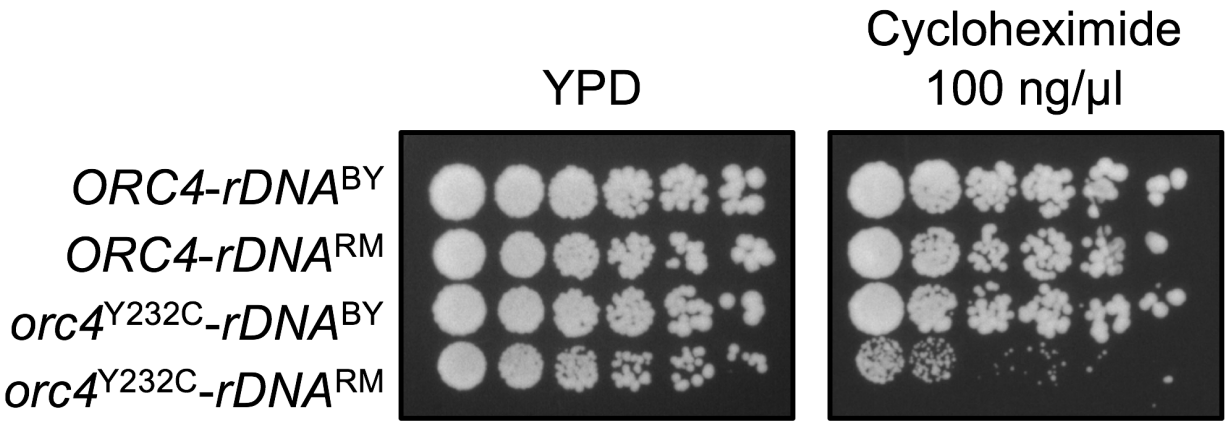

Figure 4.6: Sensitivity of *orc4*^{Y232C}-*rDNA*^{RM} cells to cycloheximide.
Serial dilutions (1:3) of cells were plated on YPD medium with or without cycloheximide (100 ng/µl) and incubated at 30° C for 3 days.

Chapter 5

Concluding remarks and remaining questions

In this dissertation, I utilized budding yeast to better understand the molecular and cellular consequences of MGS mutations. I found that yeast with an equivalent MGS mutation (*orc4*^{Y232C}) have an extended S phase and altered replication pattern. Furthermore, I found that origin activity in the rDNA repeats is severely compromised in yeast that harbor the *orc4*^{Y232C} allele. Consequently, cells that have reduced their rDNA copy number from ~150 to as low as ~10 copies overtake the culture. Although the loss of rDNA repeats helps ensure the complete replication of chromosome XII during S phase, cells with fewer rDNA repeats struggle to meet the high demand for ribosomes. The observations made in this dissertation demonstrate that the *orc4*^{Y232C} mutation in yeast indirectly affects cell growth and division by restricting ribosome production.

How does the orc4^{Y232C} mutation affect the biochemical properties of its protein product?

It is currently unclear how the *orc4*^{Y232C} mutation might affect the function of its protein product. Previous work has shown that some MGS mutations result in a less stable protein product (Fenwick et al. 2016; Bicknell et al. 2011b). Perhaps the *orc4*^{Y232C} allele

also results in a less stable protein product; however, that idea is inconsistent with my observation that introducing an additional copy of the mutant allele does not provide any rescue of the mutant rDNA phenotype (Fig. 3.11). For a more direct test of whether the mutation destabilizes the protein, quantitative western blotting could be used to measure the overall abundance of the Orc4^{Y232C} protein. Unfortunately, a primary antibody against the yeast Orc4p is not currently available, and attempts to tag the endogenous Orc4p with an epitope tag have not been successful. Therefore, different approaches such as quantitative protein mass spectrometry may be necessary to determine the relative abundance of the Orc4^{Y232C} protein. It is also possible that the *orc4*^{Y232C} allele affects properties of its protein product other than its abundance. For example, the Orc4^{Y232C} protein may be compromised in in its ability to bind DNA or interact with other proteins. Again, since a primary antibody against Orc4p is not available, performing ChIP and Co-IP experiments to address these possibilities is not currently feasible. To characterize the protein-DNA interactions in *orc4*^{Y232C} cells, it may be useful to use assays that do not require the use of an antibody, such as chromatin footprinting (Belsky et al. 2014). In addition, performing Co-IP experiments against Pre-RC proteins other than Orc4p might provide insight to whether assembly of the Pre-RC is compromised in *orc4*^{Y232C} cells.

What is the mechanism for rDNA contraction?

I found that *orc4*^{Y232C} cells suffer from a loss of rDNA repeats, and I propose that the loss of rDNA repeats allows for complete replication of the rDNA locus during S phase. However, I have as yet no direct evidence for incomplete replication of chromosome XII in

orc4^{Y232C} cells. Therefore, characterizing the initial events and repair factors necessary for the loss of rDNA repeats would help test my model that incomplete replication of chromosome XII is responsible for the loss of rDNA repeats.

Ideally, I would be able to observe the initial events occurring at the rDNA locus directly upon introduction of *orc4*^{Y232C}. However, since there is a strong selection for contraction of the rDNA locus in these cells, it is difficult to observe the initial events leading up to a loss of rDNA repeats. Since yeast cells can maintain a large rDNA array when both *ORC4* and *orc4*^{Y232C} are preset, use of a conditional degron allele of *ORC4* would possibly allow one to observe the initial events leading up to a loss of rDNA repeats. The auxin inducible degron (AID) system allows for the rapid degradation of specific proteins of interest. Therefore, the wild type Orc4p could be conditionally degraded, leaving cells to depend on the Orc4^{Y232C} protein for replication. Unfortunately, I and others have not been successful in tagging Orc4p with an AID domain; C-terminally tagging Orc4p with the AID results in cell death in yeast. However, because I find that *cdc45*^{P542L} cells also shrink their rDNA locus (Fig. 3.9), it still may be possible to observe the initial events occurring at the rDNA locus in the context of *cdc45*^{P542L} cells, as the AID system has successfully been used for the conditional degradation of Cdc45p in yeast.

In addition to characterizing the initial events leading up to the loss of rDNA repeats, knowing the proteins required for shrinkage of the rDNA locus would provide insight to which repair pathway(s) are used during this process. One could use genetics to determine the proteins that are necessary for the loss of rDNA repeats. Heterozygous *ORC4/orc4*^{Y232C} diploids maintain large rDNA arrays on both chromosome XII homologs. However, after

meiosis the rDNA locus shrinks in the segregants that receive the *orc4*^{Y232C} allele. As an initial approach, I wanted to determine how removing proteins known to be involved during DNA damage response or maintenance of rDNA copy number would affect shrinkage of the rDNA locus in the progeny that inherited the *orc4*^{Y232C} allele. Therefore, with the help of Mackenzie Croy (a former undergraduate researcher) I created two different derivatives the *ORC4/orc4*^{Y232C} diploid that had one copy of either *RAD52* or *FOB1* replaced with *KanMX*.

Rad52p stimulates strand exchange during the repair of double-strand breaks (New et al. 1998). Therefore, I predicted that any haploid segregants that inherited both *orc4*^{Y232C} and *RAD52::KanMX* would either not be able to shrink their rDNA locus or be inviable. I induced meiosis in the *ORC4/orc4*^{Y232C} *RAD52/rad52Δ::KanMX* diploid, dissected tetrads, and grew the spores on rich medium ("YPD"). In each tetrad dissected, all four of the progeny were viable. Next, I screened for variation in rDNA copy number in the progeny by CHEF gel analysis (Fig 5.1) and found that the rDNA locus was still able to shrink in the progeny that inherited *orc4*^{Y232C}, regardless of the whether they also inherited *rad52Δ::KanMX*. The observations that *orc4*^{Y232C} *rad52Δ::KanMX* cells are viable and have a shortened chromosome XII suggests that shrinkage of the rDNA locus in *orc4*^{Y232C} cells can occur through a *RAD52*-independent pathway.

Fob1p is a nucleolar protein that binds to the rDNA replication fork barrier and is important for both expansion and contraction of the rDNA (Kobayashi et al. 1998). Accordingly, I wondered if Fob1p would be necessary for the contraction of the rDNA locus in *orc4*^{Y232C} cells also. To test this prediction, I created a derivative of the *ORC4/orc4*^{Y232C}

diploid that has one of its copies of *FOB1* replaced with *KanMX* (*ORC4/orc4*^{Y232C}, *FOB1/fob1Δ::KanMX*). I sporulated this diploid, dissected tetrads, and grew the haploid spores on YPD. Next, I screened for variation in rDNA copy number in the progeny by CHEF gel analysis (Fig 5.2) and found that *orc4*^{Y232C} *fob1Δ::KanMX* segregants have a shortened chromosome XII. Therefore, perhaps the role Fob1p plays in the contraction of the rDNA locus is situation specific. Although only two genes were screened in the above experiments, expanding my list of candidate genes may provide insight to which proteins are necessary for the contraction of the rDNA locus.

Is the slow growth phenotype due primarily to the orc4^{Y232C} mutation or loss of rDNA repeats?

In Chapter 4 I demonstrated that contraction of the rDNA in *orc4*^{Y232C} cells causes a dramatic decrease in translational capacity, explaining the slow growth phenotype of the mutant cells. However, because both the allele of *ORC4* and the rDNA copy number is changing in that strain, it is difficult to ascertain exactly what are the cellular defect(s) responsible for the slow growth phenotype—it is possible that slow growth is a direct result of the *orc4*^{Y232C} mutation and not an indirect effect of rDNA size. Because a large rDNA array is unstable in *orc4*^{Y232C} cells, it is difficult to test the growth of *orc4*^{Y232C} cells with a large rDNA array. Alternatively, I could examine of growth of yeast cells with the wild type *ORC4* and a reduced rDNA copy number. This type of experiment can be accomplished in yeast cells, but is usually labor intensive and requires the deletion of *FOB1* to prevent the expansion of rDNA copy number. Furthermore, two features of the genome

would be changing—the deletion of *FOB1* and rDNA copy number. Therefore, I sought to come up with a strategy in which I could recapitulate the rDNA copy number phenotype observed in *orc4*^{Y232C} cells without introducing additional mutations outside of the rDNA locus.

In my model for shrinkage of the rDNA locus, a decrease in origin activity at this locus makes it difficult to replicate, and cells that have lost rDNA repeats have a growth advantage over ones that retain a full array. In the case of *orc4*^{Y232C} cells, decreased origin initiation at the rDNA locus is a result of the poorly functioning Orc4^{Y232C} protein. If my model is correct, then one would predict that a decrease in rDNA copy number should be observed regardless of how origin activity is decreased at the rDNA locus. Since origins of replication in yeast are defined by specific sequences, one could potentially decrease origin activity at the rDNA locus by removing the origin or replication present in each rDNA repeat. Thus, I developed a strategy to remove the origin of replication present in every rDNA repeat.

An attractive feature of CRISPR-Cas9 is its ability to introduce a specific mutation into the genome without the need to use a selectable marker (Shi et al. 2016). This strategy can be particularly useful when needing to introduce several mutations into the same strain. Therefore, I reasoned that I could use CRISPR-Cas9 to knock out the origin of replication present in each rDNA repeat. I transformed a plasmid (pML104; Laughery et al. 2015) containing the template to make Cas9p and a guide RNA that is specific to a sequence near the rDNA origin of replication. I also provided a repair template that lacked a functional origin of replication. Since double-strand breaks are toxic to cells, I predicted

that cells which incorporated the repair template that I provided would no longer be susceptible to Cas9p cutting and be viable. In addition, cells that successfully incorporated the template that I provided should not be able to initiate replication within their rDNA locus. I found that Isolates from the transformation grew slowly (Fig 5.3) and have a smaller chromosome XII (Fig 5.4) compared to their parent strain BY4741. Based on these preliminary results, I predict that the isolates from the transformation successfully incorporated the repair template that I provided and the slow growth phenotype is due to an rDNA deficiency. However, additional experiments will be required to determine how the rDNA locus has changed in these isolates regarding its structure, copy number, and origin activity. If the rDNA copy number is decreased low enough in these isolates, it may be possible to examine how a ribosome deficiency—caused by an rDNA deficiency—affects cell growth.

What are the phenotypes of an rDNA deficiency in metazoans?

There have been several reported cases of rDNA deficiencies in metazoans (Delany et al. 1994; Miller and Gurdon 1970; Terracol and Prud'homme 1986). Some of the more well-known examples are the *Drosophila* bobbed mutants, whose phenotypes include short bristles, abdominal etching, and developmental delay (Terracol and Prud'homme 1986). Bobbed mutations are partial deletions of rDNA, whose rDNA content is less than 50% of wild type. The level of rRNA synthesized in bobbed mutants does not directly correlate with rDNA copy number but rather phenotype, and bobbed mutants exhibiting more severe phenotypes synthesize less rRNA (Shermoen and Kiefer 1975). In 1971, Miller and

Knowland found that *Xenopus* embryos screened for abnormal nucleolar morphology have only 35% of the rDNA content compared to wild type. This drastic decrease in rDNA content limited the amount of rRNA that can be synthesized by cells (only 50% relative to wild type) and resulted in embryonic lethality (Miller and Knowland 1972). Lastly, work by Delany et al. examined how a reduction in rDNA copy number affects early morphogenetic processes and viability in chicken embryos. Chick embryos with only 45% of the normal rDNA complement had normal levels of rRNA during the very early stages of development; however, by the gastrula stage, rDNA deficient embryos synthesized only 58% the amount of rRNA compared to wild type and failed to differentiate past this stage of development (Delany et al. 1994). Based on the observations made in the previous studies, it is likely that minimum number of rDNA repeats is necessary for proper development in metazoans. A human disorder has not yet been shown to be caused by an rDNA deficiency; however, one might speculate the phenotypes of such a disorder. Short stature is a phenotype common to most ribosomopathies (Narla and Ebert 2010). Therefore, perhaps humans suffering from an rDNA deficiency would have a reduced stature—such a prediction was made by Bergman et al. in 1972. The authors of that study predicted that some forms of human dwarfism might be caused by an rDNA deficiency. Although their results did not support this hypothesis, it may be due to the small patient number they were sampling. Therefore, it is possible that a form of human dwarfism caused by an rDNA deficiency does exist, but has yet to be identified.

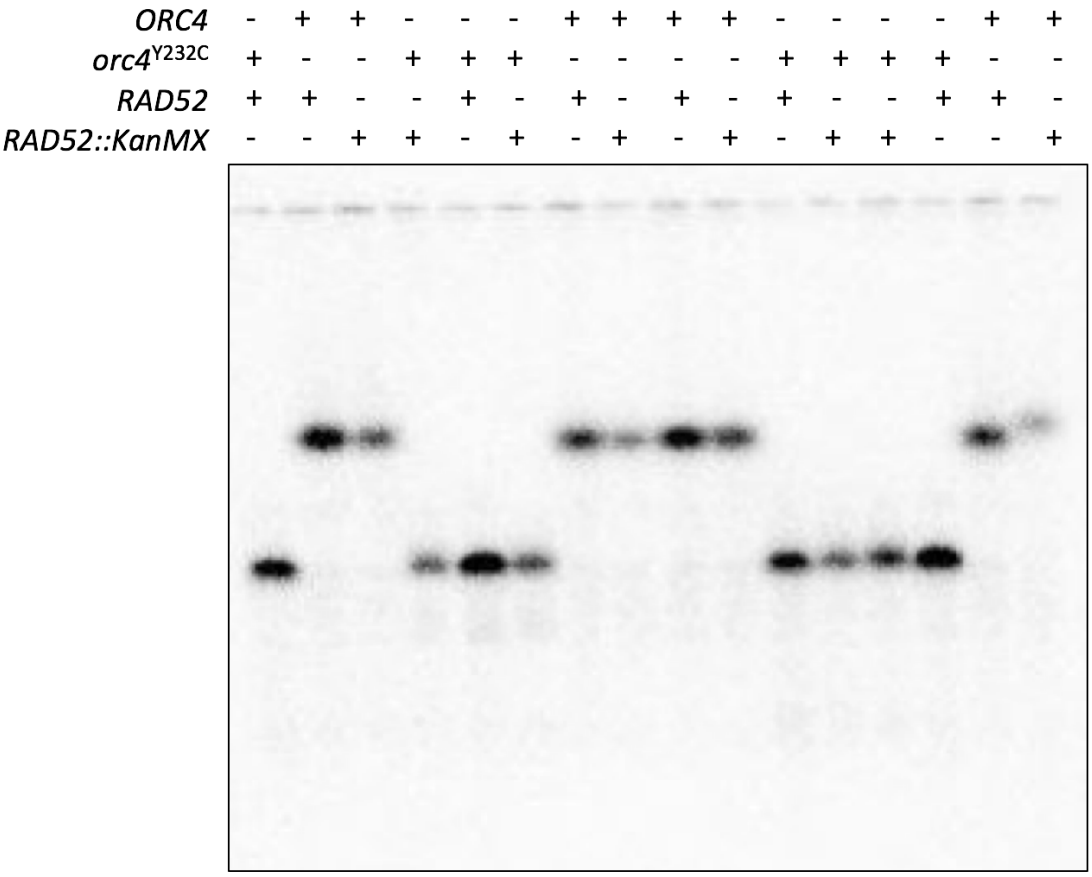

Figure 5.1: CHEF gel analysis of variation in rDNA copy in segregants from an *ORC4/orc4*^{Y232C} *RAD52/rad52Δ::KanMX* heterozygous diploid.
Southern blot following hybridization with a Chr XII-specific single-copy sequence.

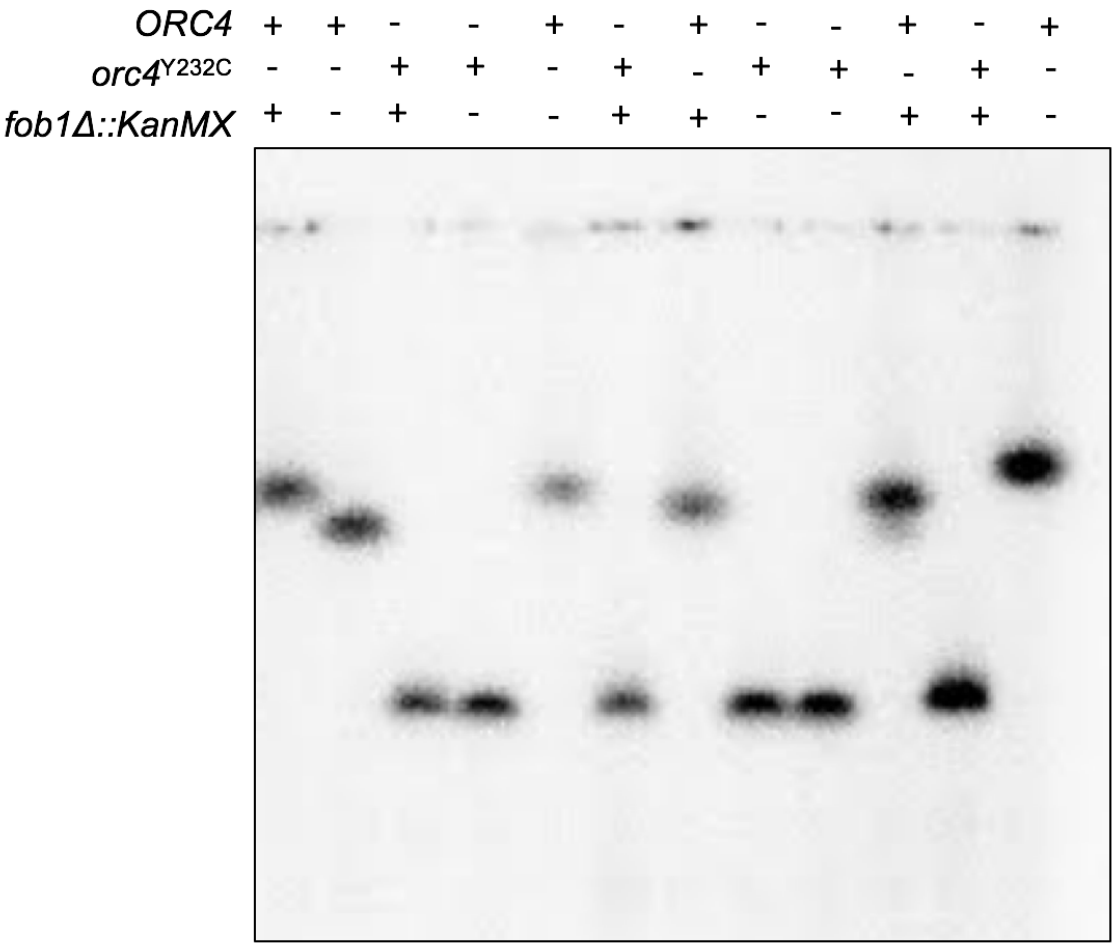

Figure 5.2: CHEF gel analysis of variation in rDNA copy in segregants from an *ORC4/orc4*^{Y232C} *FOB1/fob1Δ::KanMX* heterozygous diploid.
Southern blot following hybridization with a Chr XII-specific single-copy sequence.

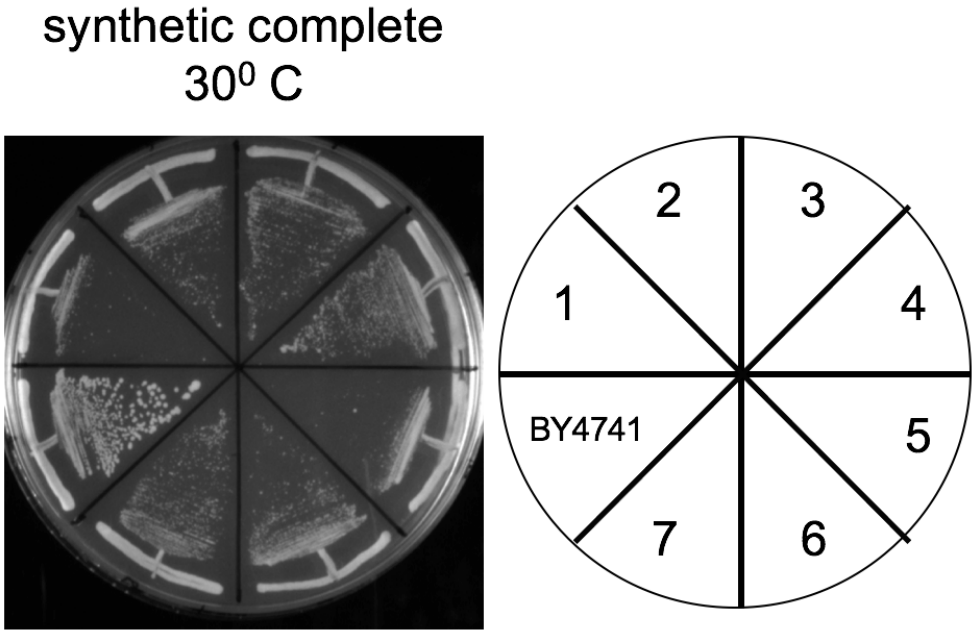

Figure 5.3: Slow growth phenotype of *rARSΔ* candidates (1-7).
Cell were streaked out for single colonies and incubated at 30° for 72 hours.

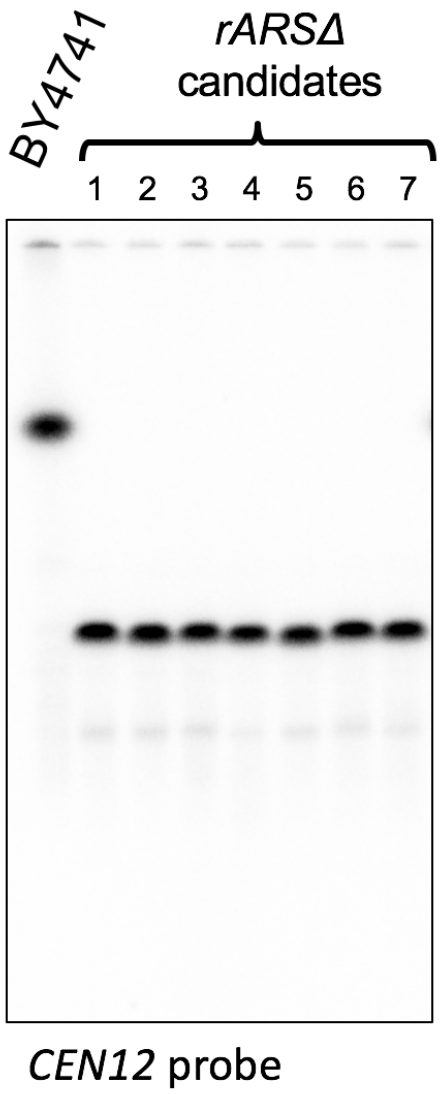

Figure 5.4: CHEF gel analysis of Chr XII size in *rARSΔ* candidates (1-7).
Southern blot following hybridization with a Chr XII-specific single-copy sequence.

Table 1: List of strains and plasmids used in this study

Name	**Genotype**	**Source**
BY4741 (*ORC4—rDNA*^{BY})	*MATa, his3Δ1, leu2Δ0, met15Δ0, ura3Δ0*	(Brachmann et al. 1998)
BY4741 w/ RM11-1a rDNA (*ORC4 —rDNA*^{RM})	*MATa, his3Δ1, leu2Δ0, lys2Δ0, ura3Δ0* The rDNA locus from RM11-1a was introduced into the BY4741 background by standard backcrossing (10 times).	(Kwan et al. 2013)
orc4^{Y232C} *—rDNA*^{BY}	*MATa, orc4*^{Y232C}, *his3Δ1, leu2Δ0, met15Δ0, ura3Δ0* The mutant *orc4*^{Y232C} allele was introduced into BY4741 using two step gene replacement (pop-in/ pop-out). See methods section.	This study
orc4^{Y232C} *—rDNA*^{RM}	*MATa, orc4*^{Y232C}, *his3Δ1, leu2Δ0, lys2Δ0, ura3Δ0* The mutant *orc4*^{Y232C} allele was introduced into BY4741 w/ RM11-1a rDNA using two step gene replacement (pop-in/pop-out). See methods section.	This study
cdc45^{P542L}	*MATa, cdc45*^{P542L}, *his3Δ1, leu2Δ0, lys2Δ0, ura3Δ0* The mutant *cdc45*^{P542L} allele was introduced into BY4741 using CRISPR-Cas9 following the steps described by Laughery et el.	This study
Plasmids	**Genotype**	**Source**
pRS415-*ORC4*	*Amp, LEU2, ORC4*	(Guernsey et al. 2011)
pRS415-*orc4*^{Y232C}	*Amp, LEU2, orc4*^{Y232C}	(Guernsey et al. 2011)
pRS406-*orc4*^{Y232C}	*Amp, URA3, orc4*^{Y232C}	This study
pML104	*Amp, URA3*	Laughery et al. (Addgene plasmid #67638)

Work Cited

Bell SP, Stillman B. 1992. ATP-dependent recognition of eukaryotic origins of DNA replication by a multiprotein complex. *Nature* **357**: 128–34.

Belsky J a, Macalpine HK, Lubelsky Y, Hartemink AJ, Macalpine DM. 2014. Genome-wide chromatin footprinting reveals dynamics of origin architecture during pre-RC assembly. *Genes Dev* **29**: 212–224.

Bicknell LS, Bongers EMHF, Leitch A, Brown S, Schoots J, Harley ME, Aftimos S, Al-Aama JY, Bober M, Brown PAJ, et al. 2011a. Mutations in the pre-replication complex cause Meier-Gorlin syndrome. *Nat Genet* **43**: 356–9.

Bicknell LS, Walker S, Klingseisen A, Stiff T, Leitch A, Kerzendorfer C, Martin C, Yeyati P, Al Sanna N, Bober M, et al. 2011b. Mutations in ORC1, encoding the largest subunit of the origin recognition complex, cause microcephalic primordial dwarfism resembling Meier-Gorlin syndrome. *Nat Genet* **43**: 350–355.

Bleichert F, Balasov M, Chesnokov I, Nogales E, Botchan MR, Berger JM. 2013. A Meier-Gorlin syndrome mutation in a conserved C-terminal helix of Orc6 impedes origin recognition complex formation. *Elife* **2**: e00882.

Blitzblau HG, Chan CS, Hochwagen A, Bell SP. 2012. Separation of DNA Replication from the Assembly of Break-Competent Meiotic Chromosomes ed. R.S. Hawley. *PLoS Genet* **8**: e1002643.

Brachmann CB, Davies A, Cost GJ, Caputo E, Li J, Hieter P, Boeke JD. 1998. Designer deletion strains derived from Saccharomyces cerevisiae S288C: a useful set of strains and

plasmids for PCR-mediated gene disruption and other applications. *Yeast* **14**: 115–32.

Brar G a, Weissman JS. 2015. Ribosome profiling reveals the what, when, where and how of protein synthesis. *Nat Rev Mol Cell Biol* **16**: 651–64.

Brewer BJ, Fangman WL. 1988. A replication fork barrier at the 3′ end of yeast ribosomal RNA genes. *Cell* **55**: 637–643.

Brewer BJ, Fangman WL. 1987. The localization of replication origins on ARS plasmids in S. cerevisiae. *Cell* **51**: 463–471.

Burrage LC, Charng WL, Eldomery MK, Willer JR, Davis EE, Lugtenberg D, Zhu W, Leduc MS, Akdemir ZC, Azamian M, et al. 2015. De Novo GMNN Mutations Cause Autosomal-Dominant Primordial Dwarfism Associated with Meier-Gorlin Syndrome. *Am J Hum Genet* **97**: 904–913.

Chen S, de Vries MA, Bell SP. 2007. Orc6 is required for dynamic recruitment of Cdt1 during repeated Mcm2-7 loading. *Genes Dev* **21**: 2897–907.

Chen XJ, Butow R a. 2005. The organization and inheritance of the mitochondrial genome. *Nat Rev Genet* **6**: 815–825.

Cocker JH, Piatti S, Santocanale C, Nasmyth K, Diffley JF. 1996. An essential role for the Cdc6 protein in forming the pre-replicative complexes of budding yeast. *Nature* **379**: 180–2.

Cunniff C, Bassetti JA, Ellis NA. 2017. Bloom's syndrome: Clinical spectrum, molecular pathogenesis, and cancer predisposition. *Mol Syndromol* **8**: 4–23.

Cvetic C, Walter JC. 2005. Eukaryotic origins of DNA replication: Could you please be more

specific? *Semin Cell Dev Biol* **16**: 343–353.

Delany ME, Muscarella DE, Bloom SE. 1994. Effects of rRNA gene copy number and nucleolar variation on early development: inhibition of gastrulation in rDNA-deficient chick embryos. *J Hered* **85**: 211–7.

Dhar MK, Sehgal S, Kaul S. 2012. Structure, replication efficiency and fragility of yeast ARS elements. *Res Microbiol* **163**: 243–53.

Diffley JF, Cocker JH, Dowell SJ, Rowley A. 1994. Two steps in the assembly of complexes at yeast replication origins in vivo. *Cell* **78**: 303–16.

Duff K, Huxley C. 1996. Targeting mutations to YACs by homologous recombination. *Methods Mol Biol* **54**: 187–98.

Feng W, Collingwood D, Boeck ME, Fox LA, Alvino GM, Fangman WL, Raghuraman MK, Brewer BJ. 2006. Genomic mapping of single-stranded DNA in hydroxyurea-challenged yeasts identifies origins of replication. *Nat Cell Biol* **8**: 148–55.

Fenwick AL, Kliszczak M, Cooper F, Murray J, Sanchez-Pulido L, Twigg SRF, Goriely A, McGowan SJ, Miller KA, Taylor IB, et al. 2016. Mutations in CDC45, Encoding an Essential Component of the Pre-initiation Complex, Cause Meier-Gorlin Syndrome and Craniosynostosis. *Am J Hum Genet* **99**: 125–138.

Foss EJ, Lao U, Dalrymple E, Adrianse RL, Loe T, Bedalov A. 2017. SIR2 suppresses replication gaps and genome instability by balancing replication between repetitive and unique sequences. *Proc Natl Acad Sci U S A* **114**: 552–557.

Fragkos M, Ganier O, Coulombe P, Méchali M. 2015. DNA replication origin activation in

space and time. *Nat Rev Mol Cell Biol* **16**: 360–74.

French SL, Osheim YN, Cioci F, Nomura M, Beyer AL. 2003. In exponentially growing Saccharomyces cerevisiae cells, rRNA synthesis is determined by the summed RNA polymerase I loading rate rather than by the number of active genes. *Mol Cell Biol* **23**: 1558–68.

Futcher AB, Cox BS. 1983. Maintenance of the 2 microns circle plasmid in populations of Saccharomyces cerevisiae. *J Bacteriol* **154**: 612–622.

Gibbons JG, Branco AT, Godinho SA, Yu S, Lemos B. 2015. Concerted copy number variation balances ribosomal DNA dosage in human and mouse genomes. *Proc Natl Acad Sci U S A* **112**: 2485–90.

Gorlin RJ, Cervenka J, Moller K, Horrobin M, Witkop CJ. 1975. Malformation syndromes. A selected miscellany. *Birth Defects Orig Artic Ser* **11**: 39–50.

Guernsey DL, Matsuoka M, Jiang H, Evans S, Macgillivray C, Nightingale M, Perry S, Ferguson M, LeBlanc M, Paquette J, et al. 2011. Mutations in origin recognition complex gene ORC4 cause Meier-Gorlin syndrome. *Nat Genet* **43**: 360–364.

Heinzel SS, Krysan PJ, Tran CT, Calos MP. 1991. Autonomous DNA replication in human cells is affected by the size and the source of the DNA. *Mol Cell Biol* **11**: 2263–72.

Hoffman CS, Winston F. 1987. A ten-minute DNA preparation from yeast efficiently releases autonomous plasmids for transformaion of Escherichia coli. *Gene* **57**: 267–272.

Hossain M, Stillman B. 2012. Meier-Gorlin syndrome mutations disrupt an Orc1 CDK inhibitory domain and cause centrosome reduplication. *Genes Dev* **26**: 1797–810.

Hughes CR, Guasti L, Meimaridou E, Chuang CH, Schimenti JC, King PJ, Costigan C, Clark AJL, Metherell LA. 2012. MCM4 mutation causes adrenal failure, short stature, and natural killer cell deficiency in humans. *J Clin Invest* **122**: 814–820.

Iadonato SP, Gnirke A. 1996. RARE-cleavage analysis of YACs. *Methods Mol Biol* **54**: 75–85.

Ilves I, Petojevic T, Pesavento JJ, Botchan MR. 2010. Activation of the MCM2-7 Helicase by Association with Cdc45 and GINS Proteins. *Mol Cell* **37**: 247–258.

Jackson AP, Laskey R a, Coleman N. 2014. Replication proteins and human disease. *Cold Spring Harb Perspect Biol* **6**: 1–16.

Killen MW, Stults DM, Adachi N, Hanakahi L, Pierce AJ. 2009. Loss of Bloom syndrome protein destabilizes human gene cluster architecture. *Hum Mol Genet* **18**: 3417–3428.

Kitsberg D, Selig S, Keshet I, Cedar H. 1993. Replication structure of the human beta-globin gene domain. *Nature* **366**: 588–90.

Knott SR V, Peace JM, Ostrow AZ, Gan Y, Rex AE, Viggiani CJ, Tavaré S, Aparicio OM. 2012. Forkhead transcription factors establish origin timing and long-range clustering in S. cerevisiae. *Cell* **148**: 99–111.

Kobayashi T. 2006. Strategies to maintain the stability of the ribosomal RNA gene repeats--collaboration of recombination, cohesion, and condensation. *Genes Genet Syst* **81**: 155–161.

Kobayashi T, Heck DJ, Nomura M, Horiuchi T. 1998. Expansion and contraction of ribosomal DNA repeats in Saccharomyces cerevisiae: Requirement of replication fork blocking (Fob1) protein and the role of RNA polymerase I. *Genes Dev* **12**: 3821–3830.

Krysan PJ, Haase SB, Calos MP. 1989. Isolation of human sequences that replicate autonomously in human cells. *Mol Cell Biol* **9**: 1026–33.

Kwan EX, Foss EJ, Tsuchiyama S, Alvino GM, Kruglyak L, Kaeberlein M, Raghuraman MK, Brewer BJ, Kennedy BK, Bedalov A. 2013. A Natural Polymorphism in rDNA Replication Origins Links Origin Activation with Calorie Restriction and Lifespan. *PLoS Genet* **9**: e1003329.

Kwan EX, Wang XS, Amemiya HM, Brewer BJ, Raghuraman MK. 2016. rDNA Copy Number Variants Are Frequent Passenger Mutations in Saccharomyces cerevisiae Deletion Collections and de Novo Transformants. *G3 (Bethesda)* **6**: 2829–38.

Larance M, Lamond AI. 2015. Multidimensional proteomics for cell biology. *Nat Rev Mol Cell Biol* **16**: 269–80.

Laughery MF, Hunter T, Brown A, Hoopes J, Ostbye T, Shumaker T, Wyrick JJ. 2015. New vectors for simple and streamlined CRISPR-Cas9 genome editing in Saccharomyces cerevisiae. *Yeast* **32**: 711–20.

Li H, Stillman B. 2012. The Origin Recognition Complex: A Biochemical and Structural View. In *Subcellular Biochemistry*, Vol. 62 of, pp. 37–58.

Liachko I, Youngblood RA, Keich U, Dunham MJ. 2013. High-resolution mapping, characterization, and optimization of autonomously replicating sequences in yeast. *Genome Res* **23**: 698–704.

Liang C, Stillman B. 1997. Persistent initiation of DNA replication and chromatin-bound MCM proteins during the cell cycle in cdc6 mutants. *Genes Dev* **11**: 3375–86.

Liang C, Weinreich M, Stillman B. 1995. ORC and Cdc6p interact and determine the frequency of initiation of DNA replication in the genome. *Cell* **81**: 667–76.

Little RD, Platt TH, Schildkraut CL. 1993. Initiation and termination of DNA replication in human rRNA genes. *Mol Cell Biol* **13**: 6600–13.

Liu Y-T, Fan H-F, Kachroo AH, Jayaram M, Rowley PA, Sau S, Chang K-M, Ma C-H. 2014. The Partitioning and Copy Number Control Systems of the Selfish Yeast Plasmid: An Optimized Molecular Design for Stable Persistence in Host Cells. *Microbiol Spectr* **2**: 1–32.

Lo C-A, Kays I, Emran F, Lin T-J, Cvetkovska V, Chen BE. 2015. Quantification of Protein Levels in Single Living Cells. *Cell Rep* **13**: 2634–44.

McCune HJ, Danielson LS, Alvino GM, Collingwood D, Delrow JJ, Fangman WL, Brewer BJ, Raghuraman MK. 2008. The temporal program of chromosome replication: genomewide replication in clb5Δ Saccharomyces cerevisiae. *Genetics* **180**: 1833–47.

Meier Z, Poschiavo, Rothschild M. 1959. Case of arthrogryposis multiplex congenita with mandibulofacial dysostosis (Franceschetti syndrome). *Helv Paediatr Acta* **14**: 213–6.

Micklem G, Rowley A, Harwood J, Nasmyth K, Diffley JF. 1993. Yeast origin recognition complex is involved in DNA replication and transcriptional silencing. *Nature* **366**: 87–89.

Miller CA, Umek RM, Kowalski D. 1999. The inefficient replication origin from yeast ribosomal DNA is naturally impaired in the ARS consensus sequence and in DNA unwinding. *Nucleic Acids Res* **27**: 3921–3930.

Miller L, Gurdon JB. 1970. Mutations affecting the size of the nucleolus in Xenopus laevis. *Nature* **227**: 1108–10.

Miller L, Knowland J. 1972. The number and activity of ribosomal RNA genes in Xenopus laevis embryos carrying partial deletions in both nucleolar organizers. *Biochem Genet* **6**: 65–73.

Muller M, Lucchini R, Sogo JM. 2000. Replication of yeast rDNA initiates downstream of transcriptionally active genes. *Mol Cell* **5**: 767–777.

Narla A, Ebert BL. 2010. Ribosomopathies : human disorders of ribosome dysfunction. *Blood* **115**: 3196–3205.

Natsume T, Müller CA, Katou Y, Retkute R, Gierliński M, Araki H, Blow JJ, Shirahige K, Nieduszynski CA, Tanaka TU. 2013. Kinetochores coordinate pericentromeric cohesion and early DNA replication by Cdc7-Dbf4 kinase recruitment. *Mol Cell* **50**: 661–74.

New JH, Sugiyama T, Zaitseva E, Kowalczykowski SC. 1998. Rad52 protein stimulates DNA strand exchange by Rad51 and replication protein A. *Nature* **391**: 407–10.

Paixão S, Colaluca IN, Cubells M, Peverali F a, Destro A, Giadrossi S, Giacca M, Falaschi A, Riva S, Biamonti G. 2004. Modular structure of the human lamin B2 replicator. *Mol Cell Biol* **24**: 2958–67.

Peng J, Raghuraman MK, Feng W. 2014. Analysis of ssDNA Gaps and DSBs in Genetically Unstable Yeast Cultures. *Methods Mol Biol* **1170**: 501–515.

Petes TD. 1979. Yeast ribosomal DNA genes are located on chromosome XII. *Proc Natl Acad Sci U S A* **76**: 410–4.

Pohl TJ, Brewer BJ, Raghuraman MK. 2012. Functional Centromeres Determine the Activation Time of Pericentric Origins of DNA Replication in Saccharomyces cerevisiae ed. C.S. Newlon. *PLoS Genet* **8**: e1002677.

Pruitt SC, Bailey KJ, Freeland A. 2007. Reduced Mcm2 expression results in severe stem/progenitor cell deficiency and cancer. *Stem Cells* **25**: 3121–32.

Pruitt SC, Qin M, Wang J, Kunnev D, Freeland A. 2017. A Signature of Genomic Instability Resulting from Deficient Replication Licensing ed. L.S. Symington. *PLOS Genet* **13**: e1006547.

Randell JCW, Bowers JL, Rodríguez HK, Bell SP. 2006. Sequential ATP hydrolysis by Cdc6 and ORC directs loading of the Mcm2-7 helicase. *Mol Cell* **21**: 29–39.

Rivin CJ, Fangman WL. 1980. Replication fork rate and origin activation during the S phase of Saccharomyces cerevisiae. *J Cell Biol* **85**: 108–15.

Rodriguez J, Lee L, Lynch B, Tsukiyama T. 2017. Nucleosome occupancy as a novel chromatin parameter for replication origin functions. *Genome Res* **27**: 269–277.

Schweizer E, MacKechnie C, Halvorson HO. 1969. The redundancy of ribosomal and transfer RNA genes in Saccharomyces cerevisiae. *J Mol Biol* **40**: 261–277.

Sclafani RA, Holzen TM. 2007. Cell cycle regulation of DNA replication. *Annu Rev Genet* **41**: 237–80.

Shermoen AW, Kiefer BI. 1975. Regulation in rDNA-deficient Drosophila melanogaster. *Cell* **4**: 275–80.

Shi S, Liang Y, Zhang MM, Ang EL, Zhao H. 2016. A highly efficient single-step, markerless strategy for multi-copy chromosomal integration of large biochemical pathways in Saccharomyces cerevisiae. *Metab Eng* **33**: 19–27.

Shima N, Alcaraz A, Liachko I, Buske TR, Andrews C a, Munroe RJ, Hartford S a, Tye BK, Schimenti JC. 2007. A viable allele of Mcm4 causes chromosome instability and mammary adenocarcinomas in mice. *Nat Genet* **39**: 93–8.

Shimada K, Pasero P, Gasser SM. 2002. ORC and the intra-S-phase checkpoint: A threshold regulates Rad53p activation in S phase. *Genes Dev* **16**: 3236–3252.

Simon AC, Sannino V, Costanzo V, Pellegrini L. 2016. Structure of human Cdc45 and implications for CMG helicase function. *Nat Commun* **7**: 11638.

Siow CC, Nieduszynska SR, Müller CA, Nieduszynski CA. 2012. OriDB, the DNA replication origin database updated and extended. *Nucleic Acids Res* **40**: D682-6.

Speck C, Chen Z, Li H, Stillman B. 2005. ATPase-dependent cooperative binding of ORC and Cdc6 to origin DNA. *Nat Struct Mol Biol* **12**: 965–71.

Stiff T, Alagoz M, Alcantara D, Outwin E, Brunner HG, Bongers EMHF, O'Driscoll M, Jeggo PA. 2013. Deficiency in origin licensing proteins impairs cilia formation: implications for the aetiology of Meier-Gorlin syndrome. *PLoS Genet* **9**: e1003360.

Stillman B. 2005. Origin recognition and the chromosome cycle. *FEBS Lett* **579**: 877–84.

Stinchcomb DT, Struhl K, Davis RW. 1979. Isolation and characterisation of a yeast chromosomal replicator. *Nature* **282**: 39–43.

Stults DM, Killen MW, Pierce HH, Pierce AJ. 2008. Genomic architecture and inheritance of human ribosomal RNA gene clusters. *Genome Res* **18**: 13–18.

Stults DM, Killen MW, Williamson EP, Hourigan JS, Vargas HD, Arnold SM, Moscow JA, Pierce AJ. 2009. Human rRNA gene clusters are recombinational hotspots in cancer.

Sung M-K, Reitsma JM, Sweredoski MJ, Hess S, Deshaies RJ. 2016. Ribosomal proteins produced in excess are degraded by the ubiquitin-proteasome system. *Mol Biol Cell* **27**: 2642–52.

Tanaka S, Diffley JFX. 2002. Interdependent nuclear accumulation of budding yeast Cdt1 and Mcm2-7 during G1 phase. *Nat Cell Biol* **4**: 198–207.

Tatsumi R, Ishimi Y. 2017. An MCM4 mutation detected in cancer cells affects MCM4/6/7 complex formation. *J Biochem* **161**: 259–268.

Terracol R, Prud'homme N. 1986. Differential elimination of rDNA genes in bobbed mutants of Drosophila melanogaster. *Mol Cell Biol* **6**: 1023–31.

Tocilj A, On KF, Yuan Z, Sun J, Elkayam E, Li H, Stillman B, Joshua-Tor L. 2017. Structure of the active form of human origin recognition complex and its ATPase motor module. *Elife* **6**: e20818.

Trainor PA, Merrill AE. 2014. Ribosome biogenesis in skeletal development and the pathogenesis of skeletal disorders. *Biochim Biophys Acta* **1842**: 769–78.

Vetro A, Savasta S, Russo Raucci A, Cerqua C, Sartori G, Limongelli I, Forlino A, Maruelli S, Perucca P, Vergani D, et al. 2017. MCM5: a new actor in the link between DNA replication and Meier-Gorlin syndrome. *Eur J Hum Genet* 1–5.

Wang L, Lin C-M, Brooks S, Cimbora D, Groudine M, Aladjem MI. 2004. The human beta-globin replication initiation region consists of two modular independent replicators. *Mol Cell Biol* **24**: 3373–86.

Warner JR. 1999. The economics of ribosome biosynthesis in yeast. *Trends Biochem Sci* **24**: 437–440.

Weitao T, Budd M, Campbell JL. 2003. Evidence that yeast SGS1, DNA2, SRS2, and FOB1 interact to maintain rDNA stability. *Mutat Res* **532**: 157–72.

Williamson D. 2002. The curious history of yeast mitochondrial DNA. *Nat Rev Genet* **3**: 475–81.

Woolford JL, Baserga SJ. 2013. Ribosome biogenesis in the yeast Saccharomyces cerevisiae. *Genetics* **195**: 643–681.

Xu B, Li H, Perry JM, Singh VP, Unruh J, Yu Z, Zakari M, McDowell W, Li L, Gerton JL, et al. 2017. Ribosomal DNA copy number loss and sequence variation in cancer ed. C. Eng. *PLOS Genet* **13**: e1006771.

Yoshida K, Bacal J, Desmarais D, Padioleau I, Tsaponina O, Chabes A, Pantesco V, Dubois E, Parrinello H, Skrzypczak M, et al. 2014. The Histone Deacetylases Sir2 and Rpd3 Act on Ribosomal DNA to Control the Replication Program in Budding Yeast. *Mol Cell* **54**: 691–697.

Yuan Z, Riera A, Bai L, Sun J, Nandi S, Spanos C, Chen ZA, Barbon M, Rappsilber J, Stillman B, et al. 2017. Structural basis of Mcm2-7 replicative helicase loading by ORC-Cdc6 and Cdt1. *Nat Struct Mol Biol*.

VITA

Joseph C. Sanchez was born in Farmington, New Mexico on March 28th, 1986. In 2008, he entered the University of New Mexico's Initiates for Maximizing Student Development Program directed by Dr. Maggie Werner-Washburne where he began conducting research under the guidance of Mary Ann Osley investigating chromatin remodeling during double strand break repair. Joseph graduated from the University of New Mexico in 2011 with a Bachelor of Science in Biology. In 2011, Joseph began his graduate work at the University of Washington in the laboratory of Dr. Bonita J. Brewer and Dr. M.K. Raghuraman. During graduate school, Joseph utilized the model organism *Saccharomyces cerevisiae* to study a rare form of dwarfism called Meier-Gorlin syndrome. In 2017, he graduated from the University of Washington with a Doctor of Philosophy in Molecular and Cellular Biology.